Universidade de Aveiro

2021

ARIANA DOS SANTOS CARVALHO

Novel tools to study the interplay between peroxisomes and lipid droplets in hepatitis C virus infection

Novas estratégias para o estudo da interação entre peroxissomas e *lipid droplets* em infeção pelo vírus da hepatite C

Universidade de Aveiro

2021

ARIANA DOS SANTOS CARVALHO

Novel tools to study the interplay between peroxisomes and lipid droplets in hepatitis C virus infection

Novas estratégias para o estudo da interação entre peroxissomas e *lipid droplets* em infeção pelo vírus da hepatite C

Thesis submitted to the University of Aveiro to fulfil the requirements to obtain the Master degree in Molecular Biomedicine, held under the scientific guidance of Dr. Daniela Maria Oliveira Gandra Ribeiro, Assistant Researcher at the Department of Medical Sciences and Principal Investigator of the "Virus Host-Cell Interactions Laboratory" at the Institute of Biomedicine (iBiMED), Department of Medical Sciences, University of Aveiro, and Dr. Ana Rita Filgueiras Ferreira, Junior Investigator at the Department of Medical Sciences and at the Institute of Biomedicine (iBiMED), University of Aveiro.

Tese submetida à Universidade de Aveiro para cumprimento dos requisitos necessários à obtenção do grau de Mestre em Biomedicina Molecular, realizada sob a orientação científica da Doutora Daniela Maria Oliveira Gandra Ribeiro, Investigadora Auxiliar do Departamento de Ciências Médicas e Investigadora Principal do "Virus Host-Cell Interactions Laboratory" do Instituto de Biomedicina (iBiMED), Departamento de Ciências Médicas, Universidade de Aveiro e da Doutora Ana Rita Filgueiras Ferreira, Investigadora Júnior do Departamento de Ciências Médicas e do Instituto de Biomedicina (iBiMED), Universidade de Aveiro.

This work was supported by the Portuguese Foundation for Science and Technology (FCT): PTDC/BIACEL/31378/2017 (POCI-01-0145-FEDER-031378), CEECIND/03747/2017, UID/BIM/04501/2013, POCI-01-0145-FEDER-007628 under the scope of the Operational Program "Competitiveness and internationalization", in its FEDER/FNR component. It was also supported by the European Union through the Horizon 2020 program: H2020-WIDESPREAD-2020-5 ID-952373.

Image acquisition was performed in the LiM facility of iBiMED, a node of PPBI (Portuguese Platform of BioImaging): POCI-01-0145-FEDER-022122.

Este trabalho contou com o apoio financeiro da Fundação para a Ciência e a Tecnologia (FCT): PTDC/BIACEL/31378/2017 (POCI-01-0145-FEDER-031378), CEECIND/03747/2017, UID/BIM/04501/2013, POCI-01-0145-FEDER-007628, no âmbito do Programa Operacional "Competitividade e Internacionalização", componente FEDER/FNR. Foi também apoiado pela União Europeia através do programa "Horizonte 2020": H2020-WIDESPREAD-2020-5 ID-952373.

A aquisição de imagens foi realizada nas instalações LiM do iBiMED, parte integrante do PPBI *(Portuguese Platform of BioImaging*): POCI-01-0145-FEDER-022122.

o júri

presidente

Professor Doutor Bruno Miguel Alves Fernandes do Gago
Professor Auxiliar do Departamento de Ciências Médicas da Universidade de Aveiro

Doutora Tânia Filipa Arsénio Geraldes Francisco
Investigadora do Instituto de Investigação e Inovação em Saúde (I3s) da Universidade do Porto

Professora Doutora Daniela Maria Oliveira Gandra Ribeiro
Investigadora Auxiliar do Departamento de Ciências Médicas da Universidade de Aveiro

Acknowledgements

To Dr. Daniela Ribeiro, my supervisor, not only for accepting me in her laboratory to develop this project, but also for making it possible to include an experience abroad in this journey, as I so desired from the beginning. Her passion for this topic of investigation has been a true inspiration.

To (Dr.) Rita, my co-supervisor, for all the help and guidance with the practical and in silico work during this entire journey, especially during the final stretch of the thesis' writing. Her questioning on how and why things happen the way they happen played a major role in stimulating my critical spirit since my very first day at the laboratory. To the rest of the team members, I am truly grateful for all the help, the motivating talks, the sharing of frustration, and all the funny moments and coffee breaks we have collected over the past year and a half - they will be missed a lot! So, to Jessica and Daniel, with whom I shared this last step of achieving a Master's degree, Mariana, Bruno, Vanessa (my HCV partner), and Alex, thank you so much for everything!

To Dr. Eva Herker, for accepting to receive me for a few months in her laboratory and for all the amazing tips that, in the end, have allowed experiments to work out in such a short time. Also, to each one of the people I have met in Marburg, inside and outside the lab, who made me feel so welcomed and happy there, even with all the pandemic restrictions. To Dr. Anja Schöbel, in particular, with whom I have worked in closer proximity, for sharing her knowledge and for all the support and patience, even after I left Marburg.

Aos meus pais, claro, que me acompanham de perto desde sempre, por nunca terem hesitado em aceitar e apoiar as minhas decisões e por terem também tornado possível não só os meus estudos em Aveiro, como sempre desejei, mas também a experiência Erasmus em Marburg, onde eles foram, uma vez mais, uma companhia constante. Sou-vos eternamente grata por estarem sempre lá para mim e por me ajudarem a levantar nos momentos mais complicados!

A toda a minha família, amigos e amigos que são família que estiveram sempre dispostos a ouvir os meus desabafos e celebraram a meu lado todas as minhas conquistas ao longo destes 5 anos e meio. A todos vocês, que sempre foram tão compreensivos nas fases em que eu não consegui estar tão presente quanto gostaria, obrigado por todo o carinho, paciência e presença!

Ao Armando, que foi, sem dúvida, quem mais teve de me aturar diariamente a falar sobre coisas que ele nem tinha de perceber. Obrigado por, mesmo assim, me teres ouvido, por teres sempre feito o esforço para compreender tudo e por toda a paciência que tiveste de ter para ouvires falar do mesmo tantas e tantas vezes. Obrigado por teres sido, sem exceção, a minha companhia, de uma ou de outra forma, das idas tardias ao Instituto e das noitadas de trabalho. E, acima de tudo, obrigado por teres sido o abraço que tanto me tranquilizou em tantos momentos de necessidade ao longo desta jornada.

Keywords

Peroxisomes, Lipid Droplets, Hepatitis C virus (HCV), Interorganellar interaction, Lentivirus, Cloning

Abstract

Hepatitis C represents a serious public health burden, with a high incidence rate worldwide. Infection normally progresses to cirrhosis and liver cancer, and while antiviral treatments are effective, access to diagnosis and treatment is still limited, with no vaccine yet developed.

Hepatitis C virus (HCV) takes advantage of several host cell mechanisms through the manipulation of cellular organelles' functions. HCV specifically modulates lipid droplets (LDs) and critically depends on the cellular lipid metabolism. Peroxisomes are also essential organelles in lipid metabolism and coordinate some of their functions with LDs, though their role as a metabolic organelle in HCV infection is still unknown.

With this work, we aimed to create tools to study the effect of HCV infection on peroxisome morphology, cellular distribution, and their interplay with LDs. Moreover, these tools would also allow to understand the importance of this crosstalk for the HCV life cycle. We successfully created plasmids and lentiviruses expressing peroxisome-targeted fluorescent fusion proteins. We have also generated a plasmid expressing an LD-targeted fluorescent protein. Preliminary studies on the influence of HCV core protein overexpression on peroxisome morphology and subcellular localisation have revealed no clear alterations.

Further studies are required to improve the LD-targeting fluorescent fusion protein-expressing lentiviruses, which will then allow the generation of stable cell lines with fluorescently stained LDs and peroxisomes. Furthermore, additional morphology and subcellular localisation analyses of peroxisomes throughout infection must be conducted to better understand the role of this organelle in HCV infection. These studies may unravel new roles of peroxisomes in HCV infection which can ultimately lead to the discovery of novel targets for antiviral therapeutics' development.

Palavras-chave

Peroxissomas, *Lipid Droplets*, Vírus da Hepatite C (VHC), Interação entre organelos, Lentivírus, Clonagem

Resumo

A hepatite C representa um grave problema de saúde pública, apresentando uma alta taxa de incidência em todo o mundo. A infeção normalmente progride para cirrose e cancro no fígado e, embora os tratamentos antivirais existentes sejam eficazes, o acesso ao diagnóstico e ao tratamento é limitado, não existindo ainda uma vacina disponível.

O vírus da hepatite C (VHC) tira proveito de vários mecanismos da célula hospedeira, manipulando as funções dos organelos celulares. O VHC modula especificamente as *lipid droplets* (LDs) e é altamente dependente do metabolismo lipídico celular. Os peroxissomas são também organelos essenciais no metabolismo lipídico e coordenam algumas das suas funções a par com as LDs, todavia o seu papel na infeção por VHC é ainda desconhecido.

Com este trabalho, era pretendido desenvolver novas estratégias para estudar o efeito da infeção por VHC na morfologia e distribuição celular dos peroxissomas, bem como na sua interação com as LDs. Além disso, tais estratégias também permitiriam entender a importância dessa interação para o ciclo de vida do VHC. Construímos com sucesso plasmídeos e lentivírus que codificam proteínas de fusão fluorescentes direcionadas para os peroxissomas. Gerámos também um plasmídeo que expressa uma proteína fluorescente localizada nas LDs. Para além disso, estudos preliminares da influência da proteína *core* do VHC na morfologia e localização subcelular dos peroxissomas não revelaram alterações claras.

Mais estudos são necessários para melhorar os lentivírus que expressam a proteína de fusão fluorescente direcionada para as LDs, o que virá a permitir o desenvolvimento de linhas celulares estáveis com expressão de LDs e peroxissomas fluorescentes. Por outro lado, análises adicionais de morfologia e localização subcelular dos peroxissomas durante a infeção deverão ser realizados para melhor compreender o papel deste organelo na infeção por VHC. Estes estudos poderão desvendar novas funções dos peroxissomas na infeção por VHC, podendo até, eventualmente, levar à descoberta de novos alvos para o desenvolvimento de terapêuticas antivirais.

List of abbreviations

(+)ssRNA	Positive single-stranded RNA
AA	Arachidonic acid
ABCD	ATP-binding cassette transporter D subfamily
ACSL	Long-chain acyl-coenzyme A synthetase
Acyl-CoA	Acyl-Coenzime A
ADHAPR	Acyl/Alkyl dihydroxyacetone phosphate reductase
ADHAPS	Alkyl dihydroxyacetone phosphate synthase
ADRP	Adipocyte differentiation-related protein
AGP	1-*O*-Alkyl G3P
AGPAT	1-Acylglycerol-3-phosphate O-acyltransferase
ALDP	Adrenoleukodystrophy protein
ARD	Adult Refsum disease
ATGL	Adipose triglyceride lipase
ATP	Adenosine triphosphate
BCFA	Branched-chain fatty acids
bGHpA	Bovine growth hormone poly A
CGI-58	Comparative gene identification-58
CIDE	Cell death-inducing DNA fragmentation factor 45-like effector
DENV	Dengue virus
DGAT	Acyl-CoA:diacylglycerol acyltransferase
DHCA	3α-, 7α-dihydroxy-5β-cholestanoic acid
DHAP	Dihydroxyacetone phosphate
DHAPAT	Dihydroxyacetone-phosphate acyltransferase
DLP1	Dynamin-like protein 1
DMEM	Dulbecco's Modified Eagle Medium
EGFP	Enhanced green fluorescent protein
eIF	Eukaryotic initiation factor
ER	Endoplasmic reticulum
ESCRT	Endosomal sorting complex required for transport
FA	Fatty acids
FAR1	Fatty acyl-CoA reductase 1

FIS1	Mitochondrial fission 1 protein
GBF1	Golgi-specific brefeldin A-resistance guanine nucleotide exchange factor 1
H_2O_2	Hydrogen peroxide
HCV	Hepatitis C virus
HCVcc	Cell culture-derived hepatitis C virus
HIV	Human immunodeficiency virus
IFN	Interferon
IFNAR	Interferon-alpha/beta receptor
IFNLR	Interferon-lambda receptor
IRES	Internal ribosome entry site
IRF	Interferon regulatory factor
iRFP	Near-infrared fluorescent protein
ISG	Interferon-stimulated gene
JAK/STAT	Janus kinase/Signal transducer and activator of transcription
LCFA	Long-chain fatty acids
LCFA-CoA	Long-chain fatty acyl-coenzyme A
LD	Lipid droplet
LOX	Lipoxygenase
LPA	Lysophosphatidic acid
LTR	Long terminal repeat
MAVS	Mitochondrial antiviral signalling
MCS	Multiple Cloning Site
MFF	Mitochondria Fusion Factor
mPTS	Membrane peroxisomal targeting signal
NLSD	Neutral lipid storage disease
NS	Non-structural
O_2	Oxygen
PBD	Peroxisome biogenesis disorder
PCR	Polymerase chain reaction
PEX	Peroxin
PLIN	Perilipin
PMP	Peroxisomal membrane protein
ppV	Pre-peroxisomal vesicles

PQ	Perylenequinones
PTS	Peroxisomal targeting sequence
RCDP	Rhizomelic chondrodysplasia punctata
RdRp	RNA-dependent RNA polymerase
rER	Rough endoplasmic reticulum
RIG-I	Retinoic-inducible gene-I
RLR	Retinoic-inducible gene-I-like receptor
RNS	Reactive nitrogen species
ROS	Reactive oxygen species
RRE	Rev response element
SE	Sterol esters
TG	Triglycerides
THCA	3α-, 7α-, 12α-trihydroxy-5β-cholestanoic acid
TIP47	Tail-interacting protein of 47 kDa
UPR	Unfolded protein response
UTR	Untranslated region
Viperin	Virus inhibitory protein ER-associated interferon inducible
VLCFA	Very long-chain fatty acids
VLDL	Very low-density lipoprotein
VSV	Vesicular stomatitis virus
WNV	West Nile virus
X-ALD	X-linked adrenoleukodystrophy
ZIKV	Zika virus

Index

List of figures

List of tables

I. INTRODUCTION

1.1 Hepatitis C Virus

1.1.1 Epidemiology of hepatitis C

Hepatitis C is a liver inflammatory disease caused by the hepatitis C virus (HCV). It can vary in severity from a mild illness, lasting a few weeks (acute infection), to a more serious lifelong illness (chronic infection), which can evolve to liver fibrosis and cirrhosis and ultimately to hepatocellular carcinoma (WHO, 2021).

According to World Health Organization, each year 1.5 million new infections occur, and 70% of these infected patients develop chronic disease. The global estimation predicts that there are 58 million chronically infected people, and a significant number of them progresses to cirrhosis or liver cancer (WHO, 2021).

Since acute and even chronic infection can remain asymptomatic until the development of secondary liver damage, many people are undiagnosed for this disease. Recommended treatment normally consists of pan-genotypic direct-acting antivirals which display an efficacy of more than 95%, thereby reducing the mortality rate. However, access to diagnosis and treatment has been limited, and furthermore, no effective vaccine against HCV infection is available (WHO, 2021).

1.1.2 Virus classification and genome

HCV was first discovered in 1989 (Choo *et al.*, 1989) and since then, seven different genotypes have been identified, which are further subdivided into sixty-seven confirmed subtypes, reflecting the high genetic diversity of this virus. Genotypes are denoted by Arabic numerals, whereas subtypes are represented by lower-case letters (Dustin *et al.*, 2016). These genotypes differ from each other in at least 30% at the genomic level as well as in geographic distribution, specific symptoms, and antiviral therapy response (Dustin *et al.*, 2016; Aziz, 2018). Due to this huge genetic variability, HCV can be seen as a large group of genetically related but not identical viruses, being referred as quasispecies. The capacity of this virus to persist for many decades in its host, is thought to be linked to its genetic variability (Payne, 2017).

The *Flaviviridae* family, to which this virus belongs, is constituted of enveloped and positive single-stranded RNA ((+)ssRNA) viruses. HCV is part of the *Hepacivirus* genus, being the only human member of this category (Payne, 2017).

HCV's RNA genome is a 9.6 kb long molecule that contains a single open reading frame coding a 3000 amino acids long polyprotein flanked by 5' and 3' non-coding sequences, or untranslated regions (UTRs) (Chevaliez and Pawlotsky, 2006; Dustin *et al.*, 2016) (**Figure 1**). The 5' UTR contains an internal ribosome entry site (IRES), essential for viral translation (explained in the next section) (Chevaliez and Pawlotsky, 2006). On the other hand, the 3' UTR signal is required for an efficient replication of the viral RNA (Yi and Lemon, 2003; Chevaliez and Pawlotsky, 2006; Anjum *et al.*, 2013). The polypeptide consists of ten proteins that can be categorised in structural or non-structural (NS). The structural proteins are located at N-terminus of the polypeptide and include the core protein and envelope glycoproteins, E1 and E2. Non-structural proteins lie at the C-terminus and consist of the small integral membrane protein, p7, as well as the NS2, NS3, NS4A NS4B, NS5A and NS5B proteins (Popescu *et al.*, 2014).

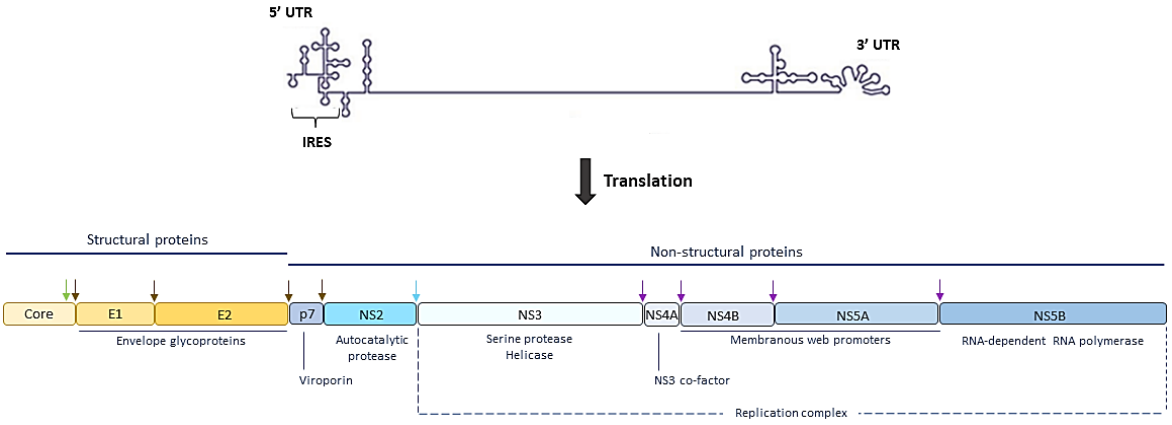

Figure 1. **HCV genome translation and polyprotein post-translation processing.** The HCV genome consists of a single open reading frame flanked by 5' and 3' UTRs. The 5' UTR contains an IRES. Upon translation, the HCV polyprotein is cleaved by host signal peptidase (brown arrows) and by the viral proteases NS2 (blue arrow) and NS3/4A (purple arrows). Furthermore, the carboxy-terminal region of the core protein is further cleaved by cellular signal peptide peptidase (green arrow).

1.1.3 Structure of the hepatitis C virus particle

Several advances in research tools and techniques allowed to overcome the initial obstacles of studying HCV *in vitro*, such as low viral titres and poor virion stability (Catanese *et al.*, 2013). For this, cDNA clones, subgenomic replicons, and cell culture-derived HCV (HCVcc) particles were critical (Yanagi *et al.*, 1997; Zhong *et al.*, 2005). The development of HCV cDNA clones (Yanagi *et al.*, 1997) made possible to first molecularly characterise the virus, while HCV subgenomic replicons promoted the study of the molecular intracellular steps of viral RNA replication without producing infectious viral particles (Tariq *et al.*, 2012). Contrastingly, HCVcc, which consist in the production of viral particles using reverse-genetics systems, promoted the study of HCV by allowing robust amplification and production of infectious particles in cell culture (Zhong *et al.*, 2005; Tariq *et al.*, 2012). HCV morphological characterisation revealed that this virus differs from the other *Flaviviridae* members as it presents a spherical form instead of an icosahedral structure (Merz *et al.*, 2011; Catanese *et al.*, 2013). HCV particles' diameter can vary between 50 to 80 nm and their density ranges from 1.03 to 1.20g/cm^3 (Popescu *et al.*, 2014). While cell culture-generated virions or particles isolated from infected patients present variable size and density, HCV particles present a classical structure, containing a genome, a nucleocapsid, and an outer envelope (**Figure 2**). HCV (+)ssRNA genome interacts with the core protein to form the nucleocapsid which, in turn, is surrounded by a lipid membrane to which some glycoproteins are anchored, constituting the viral envelope (Bartenschlager *et al.*, 2011; Popescu *et al.*, 2014).

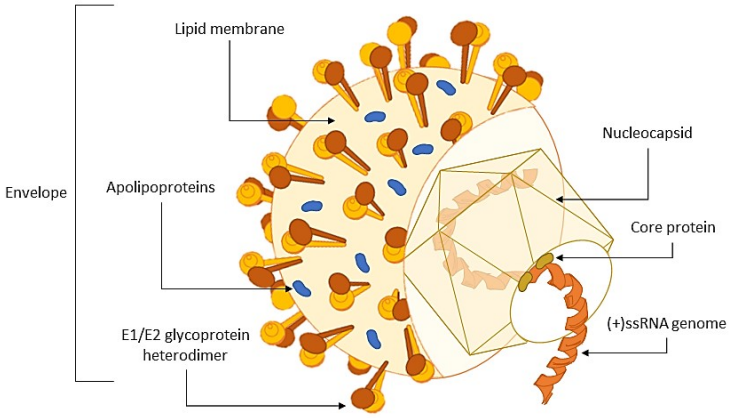

Figure 2. **Schematic representation of the structure of the HCV particle.**

1.1.4 Hepatitis C virus life cycle

Entry and uncoating

The circulating HCV virions are transported in the bloodstream either free or surrounded by host low-density lipoproteins until becoming attached to the target cell membrane via sequential binding to several proteins (Dustin *et al.*, 2016) (**Figure 3**). HCV primarily infects hepatocytes, but it can also be found in other cells, such as B cells, and dendritic cells (Moradpour, Penin and Rice, 2007). Several host receptors and binding factors have been reported to be necessary for HCV entry in the host cells (Cocquerel, Voisset and Dubuisson, 2006; Popescu *et al.*, 2014; Zhu *et al.*, 2014). Clathrin-dependent endocytosis is the primary process for internalization of this virus, although alternative entry routes have also been reported in Huh7 cells, where after viral envelope fusion with cellular membrane, the viral particle reaches Rab5a positive early endosomes through actin stress fibres (Coller *et al.*, 2009).

Once inside the cell, endosomal environment acidification induces the fusion of the viral envelope with the endosomal membrane and consequent release of the viral RNA genome to the cytosol (uncoating) (**Figure 3**). The molecular processes that govern this low pH-induced fusion are not clear yet, but it is believed that, through conformational rearrangements, E1 and E2 may form a fusion complex. The release of viral RNA to the cytoplasm allows viral translation and replication (Moradpour, Penin and Rice, 2007; Popescu *et al.*, 2014; Zhu *et al.*, 2014).

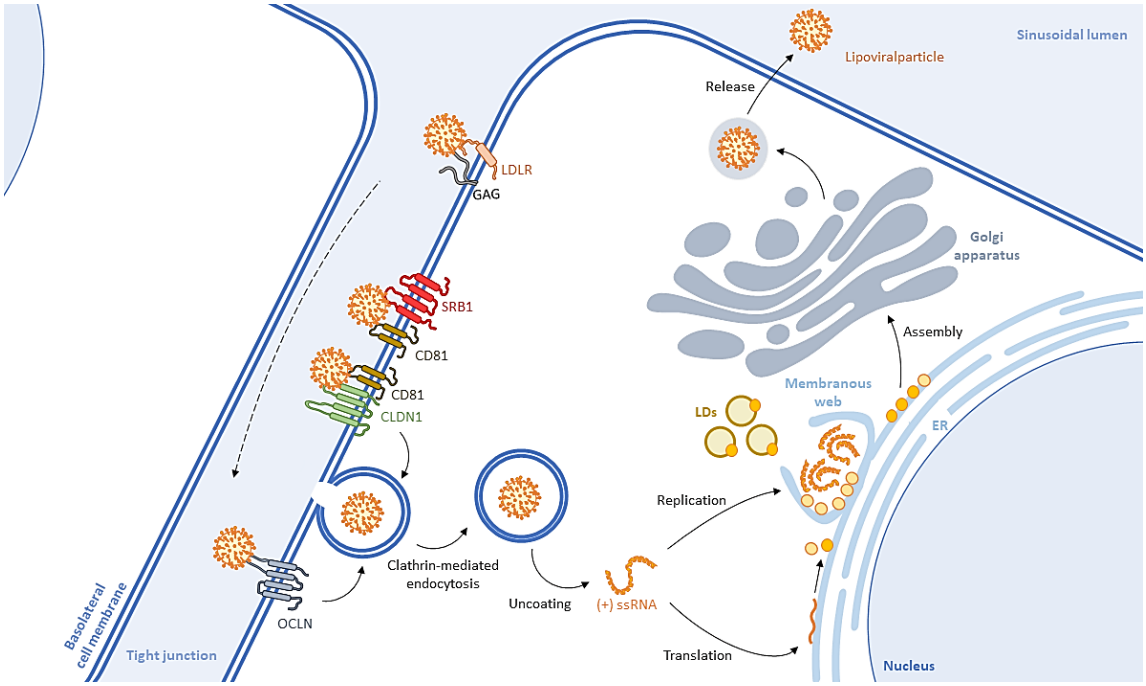

Figure 3. **HCV life cycle.** HCV reaches the cell surface as a lipoviralparticle, i.e., conjugated with lipoproteins, and it is consecutively recognised by several host proteins until its internalisation via clathrin-mediated endocytosis. Cellular and viral membranes fuse and the nucleocapsid is degraded, thus releasing the viral RNA into the cytosol (uncoating). At the rough endoplasmic reticulum (rER), HCV genome is translated into a polyprotein that is further processed by host and viral proteases releasing the ten single mature viral proteins. The membranous web is formed through ER membrane rearrangements to accommodate the viral genome replication. The assembly of new virions is dependent of the host lipid metabolism and occurs upon a strong interaction between lipid droplets (LDs), membranous web and endoplasmic reticulum. Finally, new virions suffer maturation, hence becoming associated with lipoproteins (lipoviralparticles) and being then released by exocytosis. *LDLR*: low-density lipoprotein receptor; *GAG*: glycosaminoglycan; *SRB1*: scavenger receptor class B type I; *CD81*: Cluster of Differentiation 81; *CLDN1*: claudin-1; *OCLN*: occludin.

Genome translation and replication

In HCV infection, both translation and replication events must be closely coordinated since both reactions have the viral (+)ssRNA genome as template. While HCV replication implies the conversion of the (+)ssRNA into a complementary (-)ssRNA, which occurs from 3' to 5', translation uses the same (+)ssRNA for polyprotein synthesis from 5' to 3' (Shi and Lai, 2006). It was shown that HCV translation is dependent of HCV replication, and when RNA synthesis is blocked viral protein synthesis significantly decreases (H. M. Liu *et al.*, 2012). Both viral and host proteins have been identified as regulators of both processes.

After uncoating, viral genome translation initiates at rough endoplasmic reticulum (rER), where (+)ssRNA serves as template for HCV polyprotein synthesis (**Figure 3**). As introduced previously, the 5´UTR contains an IRES, which is critical for the formation of a stable pre-initiation complex. IRES binds to the 40S ribosomal subunit that then recruits the eukaryotic initiation factor (eIF) 3 and the ternary complex eIF2-GTP-Met-tRNAi, forming the 48S like complex. Afterwards, eIF2-GDP and eIF3 are hydrolysed and released, allowing 60S ribosomal subunit binding, hence forming the 80S complex. This complex is responsible for the elongation and termination of the

viral polyprotein translation (Shi and Lai, 2006; Hoffman and Liu, 2011), and, interestingly, exerts regulatory feedback since translation has been suggested to be influenced not only by cellular factors, but also by the 3'UTR and some viral proteins, like NS4A, NS5B, and core (Chevaliez and Pawlotsky, 2006; Moradpour, Penin and Rice, 2007).

The polyprotein resulting from HCV RNA translation is co- and post-translationally processed to originate the ten mature individual viral proteins, whose functions in viral life cycle are described in **Table 1**. For this, two cellular signal peptidases and two viral proteases are required. Host cellular enzymes act mostly in the structural region of the polyprotein, whereas viral NS2 autocatalytic cysteine protease and NS3/4A serine protease are responsible for cleaving the NS region proteins (Lindenbach and Rice, 2005; Popescu *et al.*, 2014) (**Figure 1**).

Table 1. **Functions of hepatitis c virus proteins in viral life cycle**

HCV protein	Viral Life Cycle Step	Function
E1	Entry	Viral envelope functional unit (heterodimer); Fusion domain for uncoating
E2	Entry	Viral envelope functional unit (heterodimer); Fusion domain for uncoating; Receptor binding domains (to SRB1 and CD81)
Core	Assembly	Complex with viral genome (nucleocapsid)
p7	Assembly Release	Forms a calcium ion channel (viroporin)
NS2	Polyprotein processing Assembly	Autocatalytic cysteine protease; Complex with E1, E2, p7 and NS3 for assembly
NS3	Polyprotein processing Replication	N-terminal: Serine protease (NS3/4A complex); C-terminal: helicase responsible for binding and unwinding the viral RNA or displacing RNA-binding proteins; complement in membranous web induction
NS4A	Replication	Protease cofactor (NS3/4A complex); Stabilises NS3; Targets NS3/4A complex to membranes
NS4B	Replication	Induces membranous web formation
NS5A	Replication Assembly	Binding to host proteins involved in replication; Promotes double-membrane vesicles formation; Enables viral RNA interaction with the core protein
NS5B	Replication	RNA-dependent RNA polymerase; Complex with NS3, NS4A, NS4B and NS5A (replication complex)

HCV genome replication depends on NS4B-induced rER membrane alterations that form 'sponge-like inclusions', multi-vesicular structures highly mobile and dispersed throughout the cytoplasm that consist of both double- and single-membrane vesicles devoid of ribosomes, designated as membranous web (Egger *et al.*, 2002; Gosert *et al.*, 2003; Popescu *et al.*, 2014) (**Figure 3**). The membranes of these HCV replication sites are enriched in cholesterol and sphingolipids, residual components of the endoplasmic reticulum (ER) membrane, which suggested that, even though derived from ER membrane, biochemical modifications are also necessary to create a specific lipid

detergent-resistant environment. Membranous webs are very advantageous for the virus since they allow compartmentalisation and local concentration of viral products and replication complexes and provide physical support and lipids essential for viral RNA tethering during unwinding and replication. Moreover, they provide protection to viral RNA from host antiviral factors (Gosert *et al.*, 2003; Penin *et al.*, 2004). Besides NS4B, NS3/4A is also a critical regulator of HCV replication, by being involved in viral RNA unwinding and viral RNA binding proteins displacement, as well as for the membranous web formation (Moradpour, Penin and Rice, 2007; Scheel and Rice, 2013). NS5A also regulates HCV RNA replication by regulating host proteins and it also promotes the formation of double-membrane vesicles (Tang and Grisé, 2009).

Viral replication is accomplished by the RNA-dependent RNA polymerase (RdRp), NS5B protein, which is responsible for the synthesis of complementary viral RNA that serves as template for the formation of new copies of the HCV genome (Bartenschlager and Lohmann, 2000). A replication complex is formed by NS5B, NS3/4A, NS4B and NS5A (Moradpour, Penin and Rice, 2007). An important characteristic of NS5B is that it lacks proofreading activity which explains the high mutation rate of HCV, and the rapid generation of new viral variants (Bartenschlager and Lohmann, 2000). As result, infected patients usually exhibit several heterogeneous microvariants of a predominant viral sequence, which is linked to distinct biological properties and phenotypes, as carcinogenicity or tissue tropism, as well as therapy response in different patients (Enomoto and Sato, 1995; Bartenschlager and Lohmann, 2000).

As for translation, several host factors have been proposed as important regulators of HCV replication, including the phosphatidylinositol-4 kinase-III, Golgi-specific brefeldin A-resistance guanine nucleotide exchange factor 1 (GBF1), and the availability of fatty acids, especially phospholipids for membrane generation along with the enzymes involved in their synthesis (Su *et al.*, 2002; Kapadia and Chisari, 2005; Moriishi and Matsuura, 2007; Yang *et al.*, 2009; Nasheri *et al.*, 2013; Nguyen *et al.*, 2014).

Assembly and release

Assembly and release of new virions are dependent on the viral interplay with cellular lipid metabolism, as well as spatial and temporal synchronisation between structural proteins and replication complexes (Bartenschlager *et al.*, 2011; Popescu *et al.*, 2014). Additionally, these events mainly depend on lipid droplets (LDs) and HCV core protein (Popescu *et al.*, 2014) (**Figure 3**).

HCV core protein is composed of two distinct domains: a hydrophilic domain at the N-terminus, responsible for interaction with viral genomic RNA, and a double amphipathic-helix hydrophobic domain crucial for attachment to ER cytosolic leaflet and further recruitment to LDs (Boulant *et al.*, 2005, 2006). The attachment of this viral protein to LDs dislocates the adipocyte differentiation-related proteins (ADRPs), which results in alterations in both size and subcellular distribution of the organelle (Boulant *et al.*, 2006, 2008). Hence, LDs become closer to the ER and the membranous web, where replication is occurring (Boulant *et al.*, 2008). This core-LDs association is critical for the recruitment of other viral proteins and host factors, such as acyl-CoA:diacylglycerol acyltransferase (DGAT) 1, enzyme involved in triacylglycerol synthesis and LD biogenesis, to assembly sites (Miyanari *et al.*, 2007; Herker *et al.*, 2010). However, subcellular

localization of core at LDs inversely correlates with the efficacy of viral assembly, suggesting core protein may shuttle between LDs and budding site, which may correspond either to the ER or the LD-ER interface (Boson *et al.*, 2011; Counihan, Rawlinson and Lindenbach, 2011; Coller *et al.*, 2012). Interestingly, core has been shown to be lately recruited into LD-independent small mobile structures which should correspond to viral particles (Popescu *et al.*, 2014).

HCV nucleocapsid is formed when viral RNA-associated NS5A protein becomes close enough to the core protein, allowing their interaction. Beyond its role in replication, NS5A hyperphosphorylation enables this interaction, thus inducing an extensive relocation of the replication complexes to the proximity of LDs (Masaki *et al.*, 2008, 2014). Some host factors have been suggested to regulate the replication complexes recruitment and redistribution, as Rab18 and DGAT1 (Camus *et al.*, 2013; Salloum *et al.*, 2013). Moreover, NS5A also recruits the GTPase Rab1 and the GTPase activator protein TBC1 Domain Family Member 20 (TBC1D20), and it was suggested that their interaction with the apolipoprotein E (apoE) may be critical for the recruitment of this apolipoprotein to assembly sites (Benga *et al.*, 2010; Cun, Jiang and Luo, 2010; Nevo-Yassaf *et al.*, 2012).

Afterwards, the newly formed nucleocapsids are encapsulated by an envelope before being released from cells. NS2, a HCV transmembrane protein that localizes at the ER, interacts with E1, E2, p7 and NS3 forming a complex that is translocated to virus-induced structures located near LDs (Jirasko *et al.*, 2010; Popescu *et al.*, 2011). It is believed that newly formed nucleocapsids are then incorporated in the ER lumen, entering in the very low-density lipoprotein (VLDL) pathway, to acquire the lipid envelope (Bartenschlager *et al.*, 2011). Viral envelope glycoproteins E1 and E2 are known to become conjugated in non-covalent heterodimers after being translated, which are then retained in the ER luminal region until HCV assembly (Lindenbach and Rice, 2013). These proteins are believed to be incorporated in the forming virion during its envelopment in the ER lumen (Jones and McLauchlan, 2010; Bartenschlager *et al.*, 2011; Lindenbach and Rice, 2013).

Finally, new viral particles are released via the endosome secretory pathway, which is controlled by the host endosomal sorting complex required for transport (ESCRT) pathway, without inducing cell lysis (Jones and McLauchlan, 2010; Lindenbach and Rice, 2013). Through this pathway, the nascent virions mature to become low-density particles and the viral glycoproteins form large covalent complexes, resulting in a new infectious viral particle (Gastaminza *et al.*, 2008; Tews, Popescu and Dubuisson, 2010).

1.2 Lipid droplets

As previously mentioned, LDs, specialized intracellular compartments responsible for lipid storage, play a very important role in HCV life cycle. LD's core stores different species of neutral lipids, such as triglycerides (TG) and sterol esters (SE), which are enclosed within a polar phospholipid monolayer that anchors several proteins. Depending on the type of tissue or cells, LD can vary greatly in size, measuring in the majority of cells less than 1 mm in diameter, but can go up to 100 mm. For example, in mature white adipocytes the large unilocular LD occupy most of the cytosol, while in brown adipocytes, they are small and multilocular (Reue, 2011; Welte and Gould, 2017).

1.2.1 Biogenesis

LDs derive from the ER and several models to explain their biogenesis have been proposed. The most widely accepted model defends neutral lipids are synthesized and incorporated as discs in the interspace of the bilayer leaflets of the ER membrane, where various neutral lipid synthesis enzymes are located. As the accumulation of these lipids continues, the discs enlarge into spheres, increasing the space between the opposed monolayers of the ER membrane. When a threshold for lipid accumulation is reached, the outer leaflet of the ER membrane puffs out into the cytosol, and a new LD buds off from the ER (Brown, 2001; Farese and Walther, 2009) (**Figure 4**). Thereby, the new LD is surrounded by a phospholipid monolayer that derives from the ER membrane, however the process behind still needs to be clarified. At the cytoplasm, LDs increase their volume through local *de novo* lipogenesis, import of extracellular lipids, or fusion with other LDs (Olzmann and Carvalho, 2019).

Although the interior of LDs consists solely of neutral lipids, several proteins can be found on their surface, and these play key roles in organelle's structure and function (Brown, 2001). The PAT protein family, which comprises the proteins perilipins (PLINs), ADRPs, and tail-interacting protein of 47 kDa (TIP47), represents the majority of proteins found in the LDs of mammalian cells. They are thought to derive from a common ancestral gene since they share sequence similarity, besides their capacity to bind LDs (Bickel, Tansey and Welte, 2009). PLINs are the best characterized member of the PAT family, being the main LD protein family in adipocytes. They include PLIN1, 2, and 3, which coat LDs surface partly or even entirely. They have a crucial role in LD dynamics since they affect the access of cytosolic lipases, such as the hormone-sensitive lipase (HSL), to the organelle's surface and, consequently, the neutral lipid core. Hence, they are important for lipid homeostasis (Tansey *et al.*, 2001; Itabe *et al.*, 2017). Also, many other proteins related to lipid homeostasis can be found in this organelle. Some are involved in lipid biogenesis, as long-chain fatty acyl-coenzyme A (LCFA-CoA) ligases, lanosterol synthase, and squalene epoxidase; others are linked to lipid metabolism maintenance, like LCFA-CoA ligases; and others relate to lipid degradation, e.g., the comparative gene identification-58 (CGI-58) protein (Hodges and Wu, 2010). Additionally, LDs also carry the so-called 'refugee proteins', which are believed to not be related to LDs functions, but instead they are subdivided into four functional groups: signalling proteins, membrane-trafficking proteins, chaperons, and organelles-associated proteins. The identification of membrane-trafficking proteins on LDs surface and interorganellar interactions were crucial for LDs to stop being considered simple static lipid storage depots to begin to be accepted as important distributors of lipids to various cellular membrane-bound organelles (Onal *et al.*, 2017). Among several other proteins, this category comprises the small GTPases driving vesicle formation and motility, the soluble NSF attachment receptor (SNARE) proteins that regulate membrane docking and fusion on LDs, the motor proteins (as kinesin and myosin) that mediate LDs transport throughout the cytoskeleton, and vesicular traffic proteins, that control cargo sorting and vesicle budding (Zehmer *et al.*, 2009). Another characteristic group of proteins found in LDs are caveolins, more specifically caveolin-1 and caveolin-2, which are resident proteins of the organelle that can act as regulators of some signalling proteins (Fujimoto *et al.*, 2001; Van Meer, 2001).

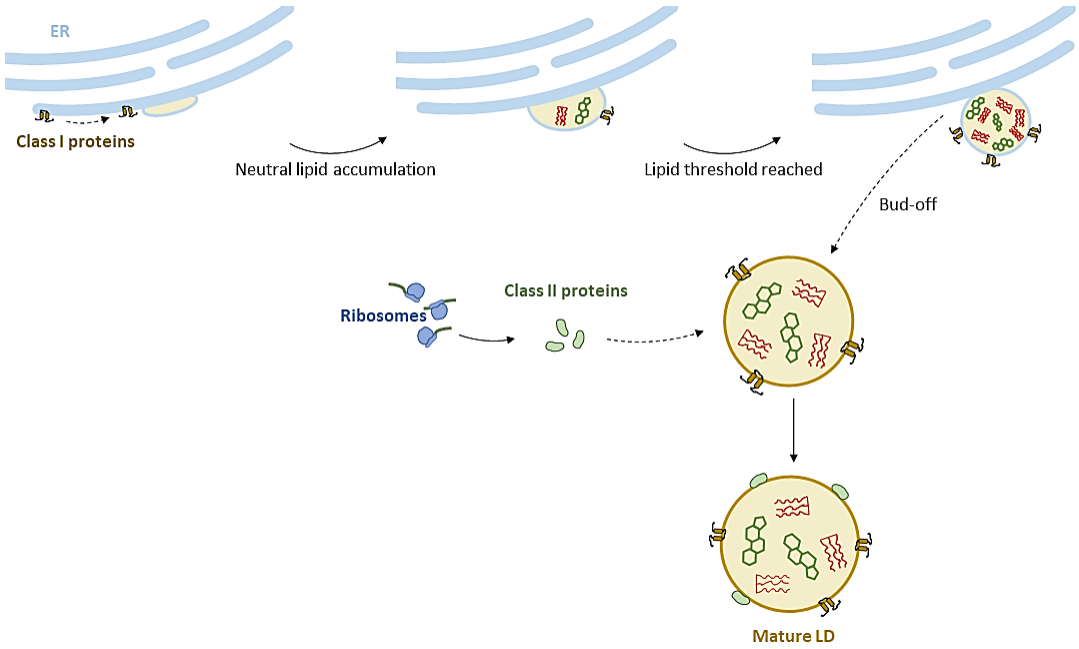

Figure 4. **LD biogenesis.** LDs are formed *de novo* from the accumulation of newly synthesised neutral lipids as discs between the ER membrane leaflets membrane. Upon neutral lipid accumulation, the discs enlarge until they become spheres that bud off from the ER along with the outer leaflet and membrane-spanning domain-containing (class I) proteins such as caveolins that, after being synthesised, diffuse between the ER and the nascent LD membrane. In opposition, transmembrane ER proteins are excluded during LD formation. Finally, class II LD proteins, as PLINs and HSL, are translated on free cytosolic ribosomes and then recruited to the organelle.

A lot of debate still exists regarding how proteins are targeted to LDs since, even though some sequences that could work as targeting signals had been proposed (Londos *et al.*, 1999; Murphy and Vance, 1999; Hope and McLauchlan, 2000), no consensus has been yet achieved. More recently, however, a new hypothesis has emerged, defending that LD proteins can be subdivided into two categories, class I and class II proteins, which would be targeted to this organelle via two general mechanisms (Kory, Farese and Walther, 2016) (**Figure 4**). Accordingly, class I proteins contain hydrophobic hairpin structures, i.e., v-shaped (often due to proline residues present at the middle of the hydrophobic sequence) α-helical domains which are able of embedding into membranes. These proteins localize to LD surface monolayer from the ER bilayer since they lack ER luminal domains and their transfer may occur during LD formation or even after budding via membrane bridges (Kory, Farese and Walther, 2016). Class II proteins, on the other hand, carry amphipathic helices or short hydrophobic-rich sequences that are responsible for their targeting to the organelle. However, these proteins are translated in the cytosol, where these amphipathic sequences are unfolded until binding to the membrane surface, after which they fold into helix (Seelig, 2004; Kory, Farese and Walther, 2016).

1.2.2 Fusion and fission

This organelle can undergo both fusion and fission. LD fusion is explained by two possible mechanisms: (1) the Ostwald ripening or (2) coalescence (Cohen, 2018).

The Ostwald ripening involves the diffusion of lipids from the smaller to larger LDs in close apposition via the cell death-inducing DNA fragmentation factor 45-like effector (CIDE) family of proteins. This results in a larger LD with more efficient storage due to the minimized ratio of surface area to volume of lipids (Gong *et al.*, 2011; Jambunathan *et al.*, 2011; Thiam, Farese and Walther, 2013). In contrast, the coalescence mechanism consists in the fusion of two LDs, but without a specific direction of lipid transfer (Thiam, Farese and Walther, 2013). Nevertheless, it is uncertain whether this process occurs under normal physiological conditions because the surfactant properties of the LD surface phospholipids usually inhibit fusion (Guo *et al.*, 2008; Krahmer *et al.*, 2011; Cohen, 2018).

Under certain circumstances of altered phospholipid composition and decreased surface tension, LDs are known to spontaneously fuse, which may have a role in certain pathophysiological conditions (Cohen, 2018). Moreover, this also occurs in response to some pharmacological agents (Murphy, Martin and Parton, 2010).

LD fission or fragmentation was first stated in studies with yeast that inclusively reported a transition state in which LDs present a “dumbbell”-shaped form (Long *et al.*, 2012). In mammalian cells, however, it is not clear if this process occurs (Marcinkiewicz *et al.*, 2006; Hashimoto *et al.*, 2012; Paar *et al.*, 2012; Chitraju *et al.*, 2017; Cohen, 2018).

1.2.3 Catabolism

LDs are degraded to release fatty acids (FA) and glycerol in response to energetic demands of the cell. This may occur via two different pathways, lipolysis or lipophagy (**Figure 5**), although further investigation on which factors drive cells to perform one or the other is still required (Cohen, 2018). While lipolysis involves changes in the LD-associated lipases’ activity for local hydrolysis of neutral lipids, lipophagy leads to the release of FA through intervention of lytic compartments and autophagic machinery.

The biological significance of LD catabolism goes far beyond energy supply. FA have been shown to play diverse cellular signalling roles, they may act as ligands for transcription factors, allosteric modulators, and even substrates to produce other signalling molecules, e.g., eicosanoids and sphingolipids (Schulze, Sathyanarayan and Mashek, 2017). Moreover, not only LD catabolism is also critical to prevent lipotoxicity, but a controlled regulation of lipid synthesis, lipolysis and lipophagy is also essential to maintain cellular homeostasis.

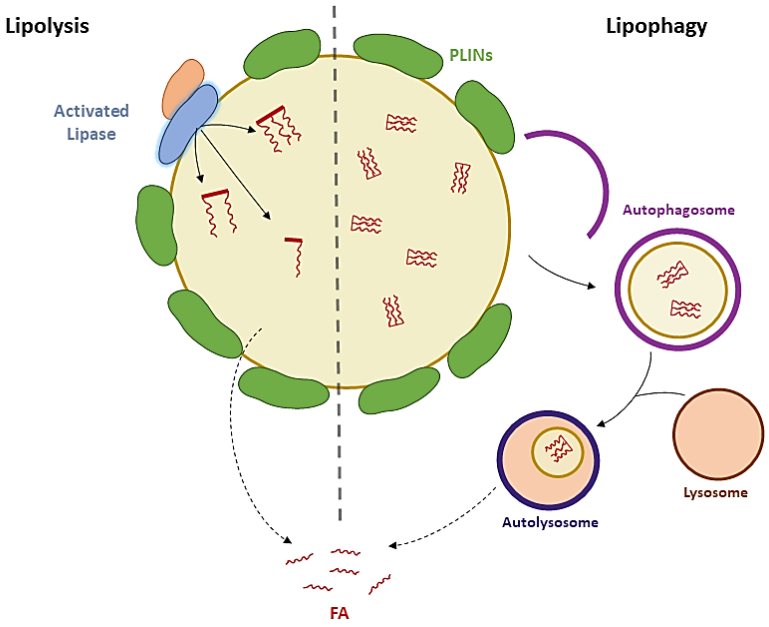

Figure 5. **Lipolysis vs Lipophagy.** While lipolysis (left) involves changes in the LD-associated lipases' activity, which, upon activation, hydrolyse the stored neutral lipids into fatty acids, lipophagy (right) leads to the release of FA to the cytosol through intervention of lytic compartments like lysosomes and autophagic machinery.

1.2.4 Lipid droplet functions

Although, for a long time, LDs were seen only as cellular storage vesicles, their crucial role for cellular homeostasis is growing. Several new functions keep being discovered, and while some need to be further clarified at the molecular level, others are already well established. LD functions go from storage of nutrients and toxic molecules to regulation of lipid, and even protein metabolism and homeostasis (Welte and Gould, 2017; Cohen, 2018).

1.2.4.1 Lipid metabolism

As organelles that store neutral lipids, LDs are a major cellular regulator of membranes and energy homeostasis (Welte and Gould, 2017). During nutrient shortage or cell starvation, cells can rely on LDs as a source of phospholipid precursors and cholesterol to maintain the balance of lipid flux that goes to membranes (for growth) or to storage (for stress survival) (Barbosa *et al.*, 2015; Shpilka *et al.*, 2015; Velázquez and Graef, 2016; Velázquez *et al.*, 2016; Yang *et al.*, 2016). Furthermore, through processes of lipolysis and lipophagy, neutral lipids stored in these organelles can be broken down to release FAs critical for cellular energy production via mitochondria or peroxisome β-oxidation (Kerner and Hoppel, 2000; Eaton, 2002).

1.2.4.2 Storage of vitamins and signalling precursors

Curiously, besides being key organelles for cellular energy and membranes homeostasis, LDs also provide a physiologically relevant storage site for fat-soluble vitamins and their metabolites, as vitamin E, in plants, cyanobacteria, and human adipocytes (Traber and Kayden, 1987; Peramuna and Summers, 2014; Spicher and Kessler, 2015), and vitamin A, mainly in the human liver but also

in the intestine, lung, kidney, and adipocytes (Nagy *et al.*, 1997; Senoo, Kojima and Sato, 2007; Schreiber *et al.*, 2012; Senoo *et al.*, 2013; Blaner *et al.*, 2016).

Moreover, the lipid core can accommodate precursors of molecules involved in intercellular communication, such as steroid hormones and FA signals (Papackova and Cahova, 2015; Shen, Azhar and Kraemer, 2016). For example, in specialized endocrine cells, LDs accumulate cholesteryl esters which are an important source for the biosynthesis of various steroid hormones via the mitochondria (Kraemer *et al.*, 2013). Proteomic analyses revealed that LDs can be purified alongside with certain steroidogenic enzymes in several types of steroid-producing cells, leading to the suggestion that LDs may also act as a storage site for such enzymes and/or be involved in the transfer of steroid intermediates (Yamaguchi *et al.*, 2015; Shen, Azhar and Kraemer, 2016). Furthermore, precursors of eicosanoids, a family of signalling lipids, which include leukotrienes, prostaglandins, and thromboxanes, can also be found in this organelle. All these lipids are known to be ultimately derived from arachidonic acid (AA) which, besides being released from membrane phospholipids, can be further derived from AA-rich triglycerides located in LDs, through the activity of the adipose triglyceride lipase (ATGL) (Bozza *et al.*, 2011; Dichlberger *et al.*, 2011, 2014; Schlager *et al.*, 2015; Schreiber and Zechner, 2015). Since both eicosanoid precursors and eicosanoid-producing enzymes have been identified in LDs, it is thought that they can be more than just a passive source site of AA, being even part of the regulation of eicosanoid production (Bozza *et al.*, 2011).

1.2.4.3 Cellular detoxification

Since many toxic molecules, either exogenous or endogenous, have lipophilic properties (Welte and Gould, 2017) and several man-made environmental toxicants split into triglycerides in preference to phospholipids (Sandermann, 2003), LDs are fundamental in selectively collecting numerous toxicants in the cell. Several examples of this function can be highlighted. For example, LDs and triglyceride biosynthesis genes are necessary for providing perylenequinones (PQ), toxins produced by a variety of fungal species, resistance in the producing fungus. Moreover, LDs are believed to decrease the generation of ROS induced by these toxins (Chang *et al.*, 2015). By a similar rationale, LDs can represent a therapeutically relevant pathway for drug resistance since many prodrugs and drugs accumulate in this organelle, hence LD biogenesis inhibitors might be considered adjuncts to improve drug efficacy (Sandoz *et al.*, 2014; Verbrugge *et al.*, 2016). The anticancer prodrug CHR2863, for example, moves to LDs before the conversion into its active form, and, upon selection for resistance to this medicine, myelomonocytic cell sublines were found to exhibit a higher abundance of LDs (Verbrugge *et al.*, 2016).

1.2.4.4 Managing cell stress

More than responding to nutritional and genetic changes, LDs also respond to cell's stress being involved in stress mitigation by maintaining lipid homeostasis or sequestering harmful lipid molecules. Cell's stress can have different sources as nutrient deficiency, excessive free FAs, and/or redox perturbations (Welte and Gould, 2017).

FA excess or ER stress are triggers of the unfolded protein response (UPR) that aims to restore protein homeostasis (Pineau and Ferreira, 2010; Oakes and Papa, 2015; Volmer and Ron, 2015;

Han and Kaufman, 2016). LDs have been reported to be more abundant upon UPR activation (Vevea *et al.*, 2015). Even though it is not yet clear whether this happens through involvement in autophagy and/or increase of the FA storage, LDs are clearly an agent of ER quality control that plays a role in removing misfolded proteins and re-establishing the lipid homeostasis there (Olzmann, Kopito and Christianson, 2013; Christianson and Ye, 2014; Welte and Gould, 2017).

ER stress as well as several other triggers such as mitochondrial dysfunction, hypoxia, and chemical pro-oxidants, can lead to oxidative stress, which is present in some pathologies, including cancer and non-alcoholic fatty liver disease (Welte and Gould, 2017), that are further associated with LDs accumulation (Ashraf and Sheikh, 2015; Liu *et al.*, 2015; Koizume and Miyagi, 2016). Such stress happens when ROS cellular concentration escalates for harmful levels, where the cellular defence mechanisms, that comprise the activity of glutathione peroxidase, superoxide dismutase, and catalase, are not sufficient to protect the cell (Welte and Gould, 2017). Although it has been reported a correlation between LDs and oxidative stress in various cell types, just a few studies have suggested a role for LDs in this context (Bensaad *et al.*, 2014; Liu *et al.*, 2015). However, more studies are required to further clarify LDs' role in oxidative stress regulation.

1.2.5 Lipid droplets-related diseases

LDs act as cellular protector agents and their dysfunction is associated with a variety of human pathologies, like obesity, neutral lipid storage disease, atherosclerosis and associated cardiovascular diseases, diabetes mellitus, and fatty liver diseases (Krahmer, Farese and Walther, 2013; Onal *et al.*, 2017; Welte and Gould, 2017).

Mutations in one of the genes that encode for LDs proteins ATGL or CGI-58 are linked to the development of neutral lipid storage disease (NLSD), a heterogeneous rare autosomal recessive disorder (Lefèvre *et al.*, 2001; Fischer *et al.*, 2007). Mutations in genes associated with LDs synthesis, regulation, and storage have also been associated with the development of lipodystrophies, rare genetic disorders characterised by selective but variable loss of adipose tissue (Garg and Agarwal, 2009). Deficiency of LDs may occur as result of defects in neutral lipid synthesis, ultimately leading to formation of anomalous or degenerative white adipose tissue. Moreover, this defective LD biosynthesis in adipose tissue frequently drives to massive hepatic steatosis which successively may lead to metabolic defects, as insulin resistance, diabetes mellitus, and hypertension (Hegele, 2004).

Lipophagy dysfunction has also been associated with the development of fatty liver diseases or steatotic liver diseases, as non-alcoholic and alcoholic steatohepatitis, which are associated with increased levels of lipid storage in LDs (Madrigal-Matute and Cuervo, 2016). These disorders may also progress to chronic liver injury, fibrosis, or even hepatocellular carcinoma (Dolganiuc *et al.*, 2012; Czaja, 2016).

LDs have also been associated with more complex disorders as obesity or atherosclerosis, diseases that may have different causes and may be multifactorial origins (Onal *et al.*, 2017). However, their role on these pathologies is still unclear and further studies are needed.

1.2.6 Lipid droplets in viral infections

Viruses have evolved to disrupt LDs' functions in the host cells. Dengue virus (DENV), for example, upregulates the breakdown of LDs via autophagy inducing the release of FA and their β-oxidation for viral replication centres formation and energy production, thus sustaining viral replication (Heaton and Randall, 2010).

However, most of the reported interactions between viruses and LDs suggest that viruses exploit this organelle for its own advantage, improving viral replication and dissemination. As mentioned in section 1.1.4, a well-known modulator of LDs is HCV, that through its core and NS5A proteins, localizes at LDs via a DGAT1-dependent delivery process, which is thought to improve viral RNA encapsulation (Hourioux *et al.*, 2007; Herker *et al.*, 2010; Harris *et al.*, 2011; Camus *et al.*, 2013; Filipe and McLauchlan, 2015; Meyers *et al.*, 2016; Zhang, Lan and Sanyal, 2017). Similarly, capsid protein of DENV after being translated in ER is transiently translocated to LDs (Carvalho *et al.*, 2012; Iglesias *et al.*, 2015), which seems to be important for formation of new infectious particles (Samsa *et al.*, 2009).

As HCV, the relocation of LDs to the cytosolic inclusion bodies where viral replication occurs, also appears to be crucial for production of new rotavirus particles (Cheung *et al.*, 2010). It was also reported that rotavirus infection modulates several lipid classes related to distinct cellular processes (Gaunt *et al.*, 2013), hence suggesting a broader metabolic function of LDs for this viruses' life cycle.

LDs may also have a role in cellular antiviral defence since the virus inhibitory protein ER-associated interferon inducible (viperin) protein, an antiviral protein that localizes at ER and LDs in uninfected cells, relocalizes to a variety of cellular compartments upon infection (Hinson and Cresswell, 2009; Welte and Gould, 2017). Although the function of viperin at LDs is still unclear, it has been suggested that it may use LDs to target viruses that exploit this organelle for assembly or may accumulate on LDs simply for storage. It has been shown that localization of viperin at LDs and ER is essential for its activity against HCV, since it interacts with viral proteins at the LD surface (Helbig *et al.*, 2011). However, the same was not observed during DENV infection, since it has been shown the protein's antiviral activity in this context was independent from the terminal responsible for targeting to organellar membranes (Helbig *et al.*, 2013).

1.3 Peroxisomes

Peroxisomes are ubiquitous cytoplasmic organelles delimited by a single bilayer membrane that encloses a granular matrix and a crystalline core of oxidative enzymes. This dynamic organelle is highly variable in shape and size, responding promptly to cellular or environmental alterations through changes in size, number, morphology, and function (Lodhi and Semenkovich, 2014). Most are spherical or ovoid, with a diameter of approximately 100 to 200 nm, although in some conditions their size can increase 5 to 10 times, and can even present a tubular form (Lodhi and Semenkovich, 2014; Lazarow, 2016).

Although the term "peroxisome" has only been proposed in 1965 by Christian de Duve, the first report about peroxisomes dates back to 1954 by Rhodin, when they were still named

"microbodies". De Duve found that these microbodies contained enzymes related to hydrogen peroxide metabolism, hence, designating these subcellular organelles as peroxisomes (De Duve and Baudhuin, 1966; Tolbert and Essner, 1981).

1.3.1 Biogenesis

The origin of peroxisomes remains a controversial topic. It is, however, generally accepted that two different pathways govern the organelle's biogenesis. Peroxisomes can be formed by (i) growth and division of pre-existing organelles or (ii) arise *de novo* (**Figure 6**).

The growth and division model from pre-existing peroxisomes consists in peroxisomal membrane protrusion, elongation or tubulation, constriction, and final fission (Hua and Kim, 2016; Kim, 2017) (**Figure 6A**). PEX11β coordinates and regulates the division process by initiating membrane remodelling and elongation (Opaliński *et al.*, 2011; Yoshida *et al.*, 2015; Su *et al.*, 2018). It contains amphipathic helices that are inserted into the peroxisomal membrane causing its bending which leads to membrane elongation (Su *et al.*, 2018). Then, the anchor proteins, mitochondria fusion factor (MFF) and mitochondrial fission 1 (FIS1), promote the activation of dynamin-like protein-1 (DLP1), which upon formation of ring-like structures around peroxisome membrane, induces membrane fission through GTP hydrolysis (Kobayashi, Tanaka and Fujiki, 2007; Itoyama *et al.*, 2013; Williams *et al.*, 2015; Hua and Kim, 2016). In the end of this process new peroxisomes are formed, appearing smaller or with similar size and composition to the original peroxisome.

Nevertheless, in cells that lack pre-existing peroxisomes, it was observed that new, mature organelles could be formed *de novo* from the ER. In mutant cells lacking peroxisomes due to the loss of the membrane biogenesis factors PEX3, PEX16 and PEX19, upon their re-introduction, these were targeted to the ER, being retained in pre-peroxisomal vesicles (ppV), which are then released to form import-competent peroxisomes (Kim, 2017). However, new similar studies in human cells revealed that PEX3 and PEX14 can also target mitochondria, inducing the release of ppV from this organelle. In this study, PEX16 was targeted to ER being then released in ppV that fuses with mitochondria-derived ppV, generating new import-competent peroxisomes (Kim, 2017; Sugiura *et al.*, 2017) (**Figure 6B**).

Formation of fully mature peroxisomes depends on the insertion of peroxisomal membrane proteins (PMPs), import of matrix proteins and incorporation of lipids. Upon PMPs translation, PEX19 binds to their membrane peroxisomal targeting signal (mPTS), transporting them to peroxisomes, where PEX16 and PEX3 mediate their insertion into the organelle's membrane (Sacksteder and Gould, 2000; Jones, Morrell and Gould, 2004; Rottensteiner *et al.*, 2004). This process is essential for the formation of the complex import system that transports peroxisomal matrix proteins into the organelle. After protein synthesis, the peroxisomal targeting signal (PTS) is recognized in the cytosol either by PEX5 (for PTS1) or PEX7 (for PTS2). PTS1 is a carboxyl terminus-located tripeptide, while PTS2 is a bigger peptide found at the amino terminus of the peroxisomal matrix protein. The receptor-bound matrix proteins are then transported to docking sites at the peroxisome membrane. The peroxisome's protein import machinery comprises not only these docking sites that, together with PEX5, form a pore but also a re-exportation complex that recycles PEX5 and PEX7 back to the cytosol through a process driven by ubiquitination and

adenosine triphosphate (ATP) hydrolysis (Nair, Purdue and Lazarow, 2004; Hettema *et al.*, 2014; Francisco *et al.*, 2017; Barros-Barbosa *et al.*, 2019).

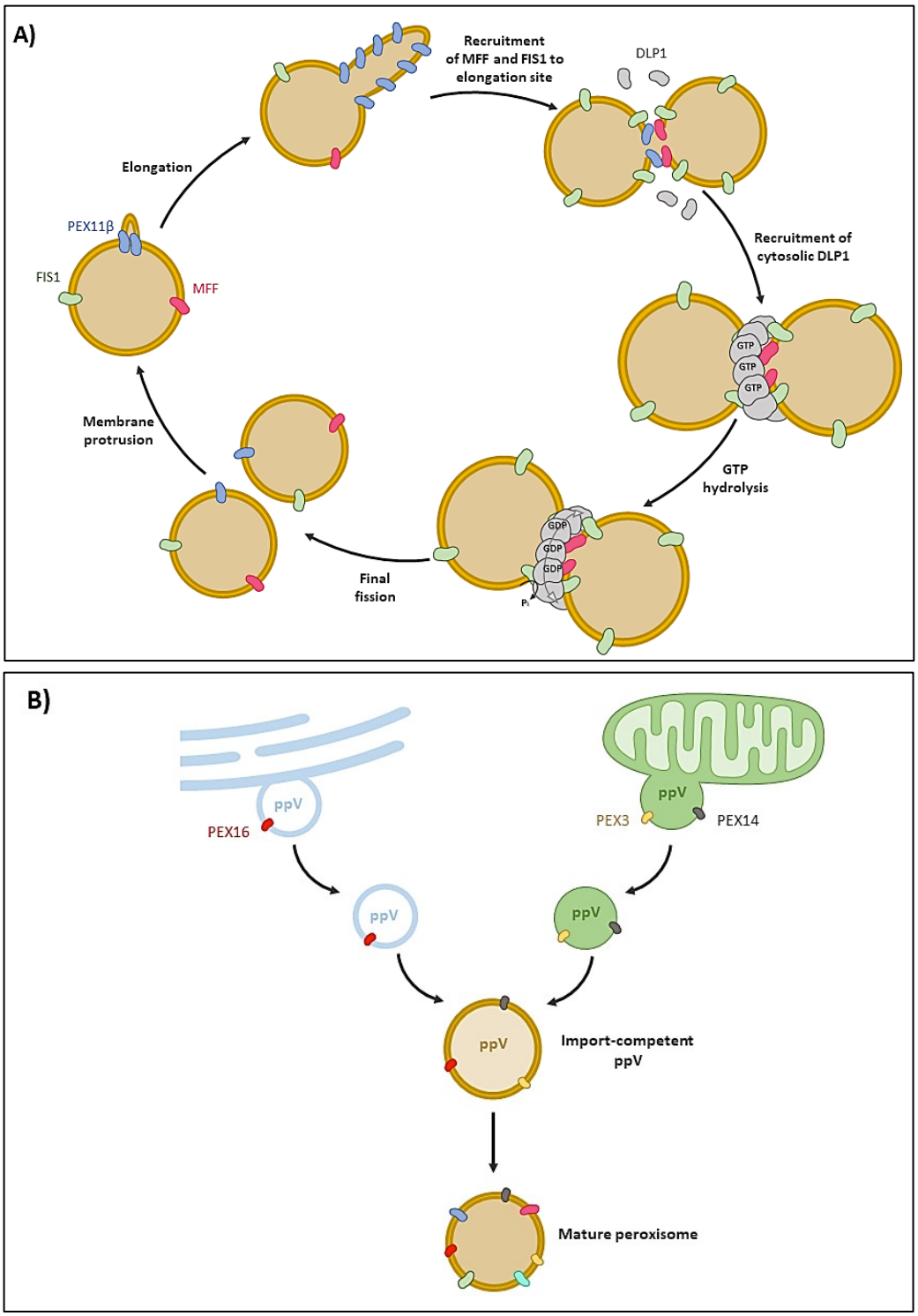

Figure 6. **Representation of peroxisome biogenesis.** A) Growth and division model. B) De novo formation.

1.3.2 Peroxisome degradation

Peroxisomes' homeostasis is a dynamic process that not only depends on peroxisome biogenesis but also on peroxisome degradation, or pexophagy, being the estimated half-life of mammalian peroxisomes approximately 1.5 to 2 days (Price *et al.*, 1962; Poole, Leighton and De Duve, 1969; Huybrechts *et al.*, 2009). Three main pathways for peroxisome degradation are accepted: (i) the Lon protease system, (ii) autolysis and (iii) pexophagy.

The Lon protease system is responsible for the degradation of excess of peroxisomal matrix proteins (Katarzyna and Suresh, 2016). Autolysis, on the other hand, depends on the activity of 15-lipoxygenase (15-LOX), enzyme that, upon integration into organelles' membranes converts poly-unsaturated fatty acids into conjugated hydroperoxide, disrupts peroxisomal membrane inducing the diffusion of peroxisomal components to the cytoplasm, which will be degraded by the proteosome (Maccarrone, Melino and Finazzi-Agrò, 2001).

Peroxisomes are mainly degraded by pexophagy, which follows the autophagy-lysosome pathway that consists in the engulfment of peroxisomes in autophagosomes that then fuse with lysosomes. In mammalian cells, pexophagy may occur through three different pathways: (i) ubiquitinated PMPs are recognized by p62, which leads to the recruitment of an autophagosome after interaction with LC3-II (Kim *et al.*, 2008); (ii) depending on the nutrient conditions, by competing with PEX5, LC3-II interacts directly with PEX14 , inducing the formation of the autophagosome (Hara-Kuge and Fujiki, 2008); (iii) NBR1 and p62 both bind to an ubiquitinated PMP or directly to the peroxisomal membrane, activating the autophagosome formation (Deosaran *et al.*, 2013). While progresses have been made to clarify the mechanisms behind peroxisomes degradation, as well as pexophagy, more research is needed.

As an organelle implicated in a range of cellular metabolic and signalling mechanisms (as described below), the strict regulation of peroxisomes' abundance and function is critical for cells and organisms. Several studies have demonstrated that impairment of pexophagy can result IN age-related phenotypes, being associated with cellular senescence and aging (Koepke *et al.*, 2008; Salmon, Richardson and Pérez, 2010; Baker *et al.*, 2011).

1.3.3 Peroxisome metabolic functions

Peroxisomes show functional diversity depending on the organism where they reside: in fungi they are known for the biosynthesis of penicillin and methanol degradation, in trypanosomes they are responsible for glycolysis, while in plants, photorespiration and glyoxylate cycle (Islinger and Schrader, 2011).

In mammalian cells, peroxisomes are mainly involved in the production and scavenging of reactive oxygen/nitrogen species (ROS/RNS) as well as in the metabolism of lipids, including β-oxidation of very long-chain fatty acids (VLCFA), α-oxidation of branched-chain fatty acids (BCFA), synthesis of bile acids and ether-linked phospholipids (Wanders and Waterham, 2006) (**Figure 7**).

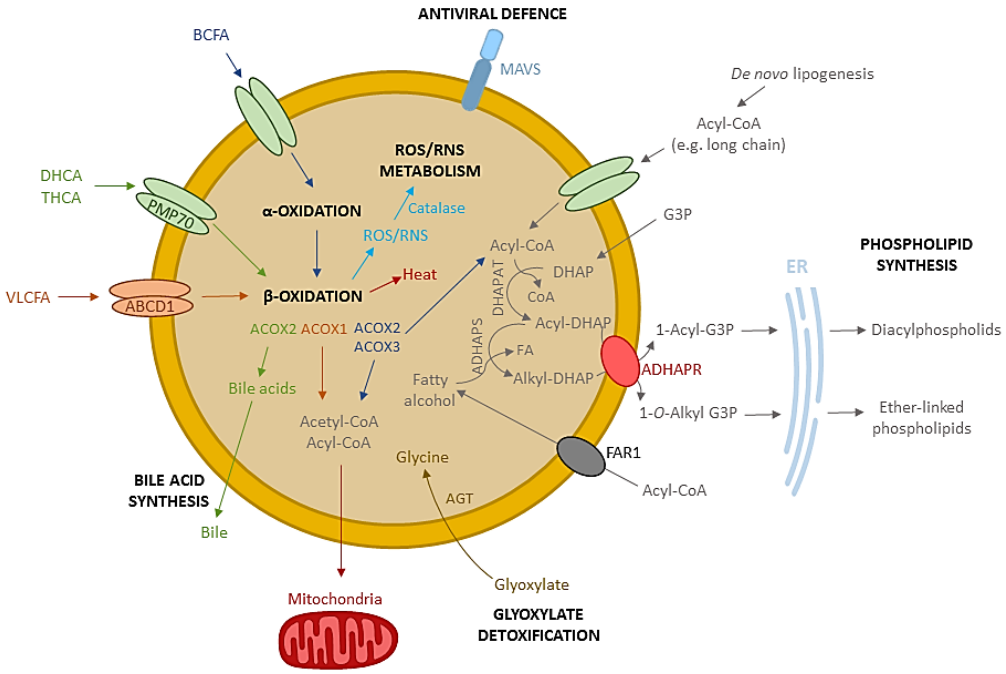

***Figure 7*. Peroxisome main metabolic functions.** *ABCD1*: ATP-binding cassette transporter D subfamily 1; *ACOX*: acyl-CoA oxidase; *ADHAPR*: Acyl/Alkyl dihydroxyacetone phosphate reductase; *ADHAPS*: alkyl dihydroxyacetone phosphate synthase; *AGT*: Alanine-glyoxylate transaminase; *CoA*: Coenzyme A; *DHAP*: Dihydroxyacetone phosphate; *DHAPAT*: dihydroxyacetone-phosphate acyltransferase; *DHCA*: 3α-, 7α-dihydroxy-5β-cholestanoic acid; *FAR1*: Fatty acyl-CoA reductase 1; *G3P*: glycerol 3-phosphate; *MAVS*: Mitochondrial antiviral signalling; *THCA*: 3α-, 7α-, 12α-trihydroxy-5β-cholestanoic acid.

1.3.3.1 ROS and RNS metabolism at peroxisomes

Catabolic and anabolic reactions mediated by peroxisomal oxidases generate potentially damaging by-products that mainly consist in ROS and RNS, such as hydrogen peroxide (H_2O_2), superoxide ($O2^-$), nitric oxide (NO), and hydroxyl radicals ($^{\bullet}OH$). To compensate, and as a protective mechanism, peroxisomes transport in their lumen a diverse range of metabolizing enzymes responsible for ROS and RNS degradation, such as catalase or peroxiredoxin 5, but also non-enzymatic antioxidant compounds such as glutathione, and others that act as scavengers and help to counteract oxidative stress (Fransen *et al.*, 2012) (**Figure 7**).

Peroxisome oxidases use oxygen (O_2) molecules to oxidize several substrates like uric acid, D-amino acids, acyl-Coenzime A (acyl-CoA), polyamines, pipecolic acid, and L-α-hydroxy acids, resulting in the production of one molecule of hydrogen peroxide (H_2O_2) per cycle of fatty acid β-oxidation. The decomposition of H_2O_2 occurs through two alternative mechanisms: the peroxidic oxidation of H_2O_2 and substrates, such as ethanol to acetaldehyde and water (H_2O), or the 'catalytic' dismutation of $2H_2O_2$ to $2H_2O$ and O_2 (**Figure 8**). The first prevails when H_2O_2 is present at low rates, whereas the later takes over when H_2O_2 is being produced quickly. Moreover, catalase's reaction rate is proportional to the substrate concentration, hence it functions faster and faster as the production of H_2O_2 increases, never reaching a plateau, preventing substantial leakage of the ROS. Nevertheless, H_2O_2 is an important cellular signalling mediator in various

signalling transduction pathways that, e.g., regulate cell fate or cellular defence against pathogens (De Duve and Baudhuin, 1966; Tolbert and Essner, 1981; Fransen *et al.*, 2012).

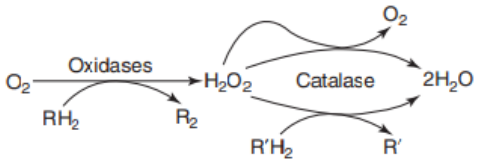

Figure 8. **Degradation reaction of H2O2 mediated by catalase.**

1.3.3.2 Peroxisome fatty acid oxidation

Peroxisomes are one of the main sites for fatty acid oxidation, being the only organelle that performs α-oxidation of BCFA and the preferential site of β-oxidation of VLCFA in animal cells (Lodhi and Semenkovich, 2014) (**Figure 7**).

Fatty acid oxidation depends first on the fatty acyl-CoA uptake into peroxisomes. Three ATP-binding cassette transporter D subfamily (ABCDs) proteins, which localize at peroxisomal membrane, are required (Wanders *et al.*, 2007). ABCD1 (also known as adrenoleukodystrophy protein or ALDP) homodimer is engaged in transporting VLCFA from the cytosol to the peroxisomal lumen for β-oxidation (Roermund *et al.*, 2008). ABCD2, particularly abundant in adipose tissue, is thought to act in the import of dietary erucic acid (C22:1) (J. Liu *et al.*, 2012). ABCD3 (also designated as PMP70) imports long-chain fatty acids (LCFA) and BCFA (Imanaka *et al.*, 1999).

VLCFA, which consist in fatty acids with 22 or more carbon atoms, are β-oxidized preferentially at peroxisomes (Singh *et al.*, 1984). VLCFA oxidation comprises the removal of two carbons at the carboxyl terminus of the molecule. Moreover, it is thought that there is also a link between peroxisomal and microsomal fatty acid metabolism since LCFA and VLCFA can also be metabolized by ω-oxidation. This oxidation process occurs in microsomes, vesicles derived from the smooth ER, and consists in the removal of the carbon most distant from the carboxyl terminus, originating dicarboxylic acids that can then be further metabolized by β-oxidation in peroxisomes (Reddy and Hashimoto, 2001).

Peroxisomes β-oxidation is a four-step reaction that involves (i) the removal of two-hydrogen (or dehydrogenation) and introduction of a *trans* double bond between the α and β carbons of the fatty acyl-CoA molecule; (ii) hydration across the double bond resulting in 3-L-hydroxyacyl-CoA; (iii) dehydrogenation forming 3-ketoacyl CoA; and finally (iv) thiolytic cleavage of the terminal acetyl-CoA group, resulting in a new acyl-CoA molecule with less two carbons. Importantly, this mechanism in peroxisomes is energetically less favourable than the mitochondrial one. Peroxisomal β-oxidation is first catalysed by acyl-CoA oxidases (ACOX), then the L- and D-bifunctional (LBP and DBP) proteins catalyse the second and third reactions, being the fourth reaction catalysed by the peroxisomal thiolases, 3-oxoacyl-CoA thiolase (ACAA1) and sterol carrier protein X (SCPx) (Herzog *et al.*, 2018).

BCFA, such as phytanic acid, have a methyl group on the third carbon atom (ϒ position), which prevents them to undergo β-oxidation. Peroxisomal α-oxidation is, therefore, essential for the

metabolism of these fatty acids since they can only be oxidized in peroxisomes or in mitochondria after undergoing oxidative decarboxylation (α-oxidation) to remove the terminal carboxyl group as carbon dioxide (CO2) (Verhoeven *et al.*, 1998; Wanders *et al.*, 2001) .

1.3.3.3 Peroxisome lipid synthesis

Peroxisomes are essential for the synthesis of ether-linked phospholipids and bile acids (**Figure 7**). Ether-linked phospholipids, such as alkyl ether phospholipids and plasmalogens, represent approximately 20% of the total phospholipid content in humans. However, tissue levels of these lipids vary significantly: they are particularly abundant in the brain, heart, and white blood cells but minimal in the liver (Nagan and Zoeller, 2001; Braverman and Moser, 2012). Interestingly, despite their scant concentration, many enzymes that are involved in their synthesis have been purified from the liver, suggesting that this organ may secrete them in the form of lipoproteins instead of storing them (Vance, 1990; Bräutigam *et al.*, 1996).

Ether phospholipid synthesis is a peroxisome-unique function that is mandatory to produce precursors of all ether lipids in mammals, including platelet activating factors and plasmalogens (Hajra and Das, 1996). Moreover, this pathway is interconnected with the peroxisomal β-oxidation in a physiologically relevant way, since acetyl-CoAs produced during peroxisomal fatty acid oxidation are preferentially channelled towards the ether lipid synthesis pathway (Hayashi and Oohashi, 1995). Their synthesis starts with the formation of dihydroxyacetone phosphate (DHAP) through dehydrogenation of glycerol 3-phosphate, which is then used as a building block for the synthesis of phospholipids that continues at ER. In parallel, fatty acids are activated to fatty acyl-CoA by a peroxisome-membrane-associated acyl-CoA synthetase. Acyl-CoAs are then used by dihydroxyacetone-phosphate acyltransferase (DHAPAT) to acylate DHAP, resulting in acyl-DHAP. Acyl-CoAs may also be reduced to a fatty alcohol by fatty acyl CoA reductase 1 (FAR1) in an NADPH-dependent manner, that can be used by ADHAPS to convert acyl-DHAP into alkyl-DHAP. Finally, acyl-DHAP and alkyl-DHAP are reduced to 1-Acyl G3P (also known as lysophosphatidic acid (LPA)), and 1-*O*-Alkyl G3P (AGP) respectively, by Acyl/Alkyl DHAP reductase (ADHAPR) (Hajra and Das, 1996; Lodhi and Semenkovich, 2014). The subsequent steps for diacylphospholipid and ether-linked phospholipid synthesis using, respectively, LPA and AGP occur in the ER (Hajra and Das, 1996).

Bile acids synthesis is the primary pathway for cholesterol catabolism and occurs exclusively in the liver. The synthesis of bile acids starts with the conversion of hydrophobic cholesterol into more water-soluble compounds in organelles as ER and mitochondria. However, the intermediates 3α-, 7α-dihydroxy-5β-cholestanoic acid (DHCA) and 3α-, 7α-, 12α-trihydroxy-5β-cholestanoic acid (THCA) can only be metabolized by peroxisomes (Staels and Fonseca, 2009; Berendse *et al.*, 2016). At this organelle, DHCA and THCA undergo shortening through β-oxidation, reaction described above, after which they are processed by the enzyme bile acid-CoA: amino acid N-acyltransferase (BAAT), producing tauro/glycocholate and tauro/glycochenodeoxycholate, end products of peroxisomal bile acid metabolism that are then exported by unknown mechanisms (Berendse *et al.*, 2016).

1.3.4 Peroxisomal Disorders

As important organelles for cellular homeostasis, peroxisomes are also essential for humans' health. Peroxisome dysfunctions have been associated with several genetic disorders, which can be divided into two subgroups: peroxisome biogenesis disorders (PBDs) and peroxisome function disorders or single peroxisomal enzyme deficiencies. These diseases are clinically heterogeneous (Aubourg and Wanders, 2013; Lodhi and Semenkovich, 2014; Wanders, 2014).

The Zellweger spectrum disorders and the rhizomelic chondrodysplasia punctata type 1 (RCDP1) and type 5 (RCDP5) are included in the PBDs subgroup. These diseases are caused by mutations in one of the *Pex* genes involved in peroxisomal biogenesis, thus being associated with the most severe phenotypes of peroxisomal disorders. Mutations on these genes may result in a virtual absence of peroxisomes in any cells or in a phenotype known as 'ghost peroxisomes' which consist of empty membrane compartments due to defects in the import machinery for peroxisomal matrix enzymes. These defective peroxisomes are usually bigger, less abundant, and deficient in most peroxisomal enzymes, including catalase (Islinger and Schrader, 2011; Aubourg and Wanders, 2013; Barøy *et al.*, 2015).

Disorders caused by an impaired peroxisomal function comprehend those due to defects in a single peroxisomal protein but with an intact peroxisomal structure, such as adult Refsum disease (ARD), X-linked adrenoleukodystrophy (X-ALD), RCDP2, RCDP3, and RCDP4 (Lodhi and Semenkovich, 2014; Wanders, 2014; Argyriou, D'Agostino and Braverman, 2016). The first one's primary defect is a mutation in the peroxisomal enzyme phytanoyl-CoA hydroxylase that catalyses the first step in α-oxidation. This is the only fatty acid α-oxidation deficiency-related disorder identified so far. Consequently, this disorder is biochemically characterised by accumulation of phytanic acid, a branched chain fatty acid found in dairy products that must be first α-oxidized in peroxisomes prior to β-oxidation in mitochondria (Wierzbicki *et al.*, 2002; Lodhi and Semenkovich, 2014; Wanders, 2014). On the other hand, X-ALD is caused by mutations in *ABCD1* and so, it is a peroxisomal β-oxidation disorder (Guimarães *et al.*, 2004; Lodhi and Semenkovich, 2014; Wanders, 2014). Finally, RCDP2, RCDP3, and RCDP4 are caused by mutations in DHAPAT, ADHAPS, and FAR1, respectively, thereby being associated with defects in ether lipid synthesis (Aubourg and Wanders, 2013; Wanders, 2014; Argyriou, D'Agostino and Braverman, 2016).

Moreover, a different group of diseases, fission disorders, also compromise peroxisomes' normal function by affecting division of peroxisomes, although not exclusively, since peroxisomal division depends on Pex11β, DLP1, MFF, and FIS1 proteins, all of which, except the former, are shared with mitochondria (Fujiki *et al.*, 2020). Indeed, human disorders with impaired DLP1, and MFF function have been reported and associated with defective division of both mitochondria and peroxisomes (Waterham *et al.*, 2007; Passmore *et al.*, 2020).

1.3.5 Peroxisomes in viral infections

One of the most recent functions attributed to peroxisomes is their role as signalling platforms in cellular antiviral defence, and, therefore, their importance for the virus-host interplay gained relevance. It is now accepted that peroxisomes can have both anti- and pro-viral roles in different viral infections (Ferreira, Marques and Ribeiro, 2019; Ferreira *et al.*, 2021).

It was discovered that the mitochondrial antiviral signalling (MAVS) protein localizes not only at mitochondria or mitochondria-associated membranes of the ER (Seth *et al.*, 2005; Horner *et al.*, 2011), but also at peroxisomes (Dixit *et al.*, 2010). MAVS is the adaptor protein of the retinoic-inducible gene-I (RIG-I)-like receptors (RLRs), which are soluble RNA helicases that recognise viral RNA in the cytosol. Upon recognition of viral RNA, RIG-I or melanoma differentiation-associated protein 5 (MDA5) suffer a conformational change that allows the activation of MAVS, which after forming an high order signalosome activates a downstream signalling cascade that culminates with the expression of interferons (IFNs), IFN-stimulated genes (ISGs) and pro-inflammatory cytokines (Ferreira, Marques and Ribeiro, 2019) (**Figure 9**). However, differences in kinetics and antiviral gene expression set by peroxisomal MAVS and mitochondrial MAVS were observed. While peroxisomal MAVS signalling leads to a fast but short-termed type I IFN-independent expression of ISGs, mitochondrial MAVS triggers a later but sustained type I IFN-dependent expression (Dixit *et al.*, 2010).

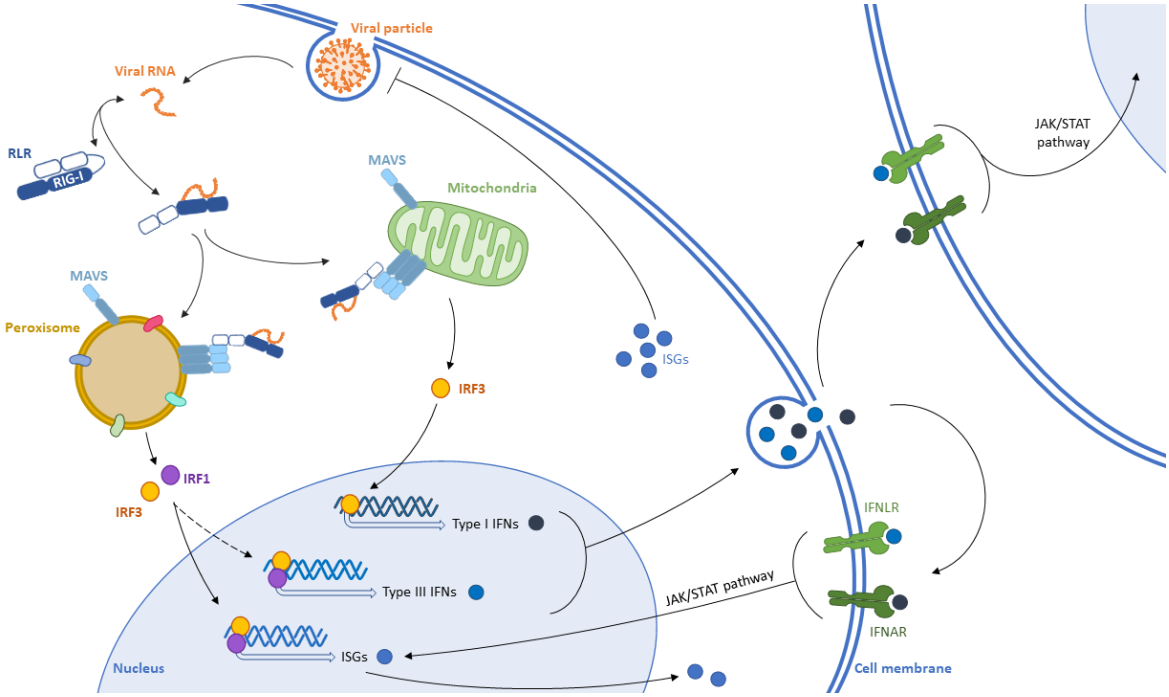

Figure 9. **MAVS-dependent antiviral signalling. RIG-I-like receptor antiviral signalling pathway.** When a virus infects a cell, the viral RNA is released into the cytosol which can be detected by RIG-I in RLRs. Then, the receptors travel to mitochondria and peroxisomes inducing the activation of their adaptor protein MAVS. Upon MAVS activation, a downstream signalling is activated, culminating with the production of type I IFNs and ISGs. Peroxisomal MAVS-dependent antiviral response relates to a rapid production of ISGs through IRF1 and IRF3, whereas mitochondria signalling drives a delayed but sustained response via IRF3. Once secreted, IFNs bind to specific receptors on the cell surface, thus activating the JAK/STAT pathway that results in an amplifying loop of ISGs. The conjugation of these responses restricts viral replication and spreading to neighbouring cells. *IFNAR*: Interferon-alpha/beta receptor; *IFNLR*: Interferon Lambda Receptor; *IRF*: Interferon regulatory factor; *JAK/STAT*: Janus kinase/signal transducer and activator of transcription.

Strongly supporting the critical role of peroxisomes in cellular antiviral defence, a diverse range of viruses have developed specific mechanisms to evade the peroxisome-dependent antiviral signalling (Ferreira *et al.*, 2021). One example of this is the HCV, which cleaves MAVS at

peroxisomes via its NS3/4A serine protease complex, inhibiting the peroxisomal-dependent antiviral signalling (Ferreira *et al.*, 2016), besides interfering with MAVS downstream signalling from mitochondria and MAMs as had been previously shown (Meylan *et al.*, 2005; Horner *et al.*, 2011). Furthermore, NS3/4A was shown to localize at peroxisomes even in the absence of MAVS and to disrupt downstream signalling with similar kinetics as in mitochondria (Ferreira *et al.*, 2016). Additionally, DENV, Zika virus (ZIKV) and West Nile virus (WNV), flaviviruses such as HCV, were also suggested to evade the peroxisomal-dependent antiviral signalling by sequestering PEX19 via their capsid protein, impairing peroxisome biogenesis and inducing peroxisome number reduction (You *et al.*, 2015). Several other viruses, such as human cytomegalovirus (HCMV) or herpes simplex virus 1 (HSV-1), are other examples of viruses that evade the peroxisomes-dependent antiviral signalling (Magalhães *et al.*, 2016; Zheng and Su, 2017; Wong *et al.*, 2019).

Interestingly, viruses can also exploit peroxisomes for efficient viral replication and dissemination. The human immunodeficiency virus (HIV), Kaposi's sarcoma associated herpesvirus (KSHV) or HCMV were reported to target and modulate the peroxisomal lipid metabolism and biogenesis (Ferreira *et al.*, 2021). The flaviviruses WNV and ZIKV have been shown to interfere with cellular lipid metabolism. WNV manipulates infected cells lipid metabolism to increase glycerophospholipids and sphingolipids (Martin-Acebes *et al.*, 2014), while in the serum of ZIKV infected patients, increased levels of plasmalogens were observed (Queiroz *et al.*, 2019). These results suggest that flaviviruses may modulate cellular lipid metabolism, including peroxisomal metabolism for remodelling and curvature of cellular membranes. Curiously, while highly dependent on the cellular lipid metabolism, not much is known about peroxisomes role in HCV infection. It has been shown that HCV leads to the accumulation of VLCFA (Lupberger *et al.*, 2019). Additional studies are, hence, necessary to understand if peroxisomal β-oxidation of VLCFA influence HCV infection and propagation.

1.4 Interplay between peroxisomes and lipid droplets

LDs and peroxisomes not only establish a strong network with other cellular organelles, but they also rely in one another to accomplish their functions (Schrader *et al.*, 2013; Gao and Goodman, 2015; Schuldiner and Bohnert, 2017; Schrader, Kamoshita and Islinger, 2019; Wang *et al.*, 2021). Since both organelles derive from ER, an intimate interplay was expected.

Actual contact sites between LDs and peroxisomes have been reported in yeast by Binns et al., who have shown peroxisomal adherence to LDs' core by extended cellular processes, named pexopodia, along with an enrichment of LDs in peroxisomal enzymes related to β-oxidation (Binns *et al.*, 2006). In fact, as previously referred, in mammals, the VLCFA β-oxidation occurs preferentially in peroxisomes, and in some yeasts and plants they are the only site of intracellular β-oxidation (Lodhi and Semenkovich, 2014). Apposition of both organelles' membranes led to key points of communication, aiding in the transfer and exchange of metabolites. Whether this inter-organellar close association occurs in mammalian cells as well is not completely clear yet, but some lines of evidence, mainly in hepatic and adipose cells, have been emerging (Lodhi and Semenkovich, 2014). First, several studies using immunogold and 3,3'-diaminobenzidine (DAB) staining have shown the formation of small dumbbell-shaped peroxisomes at LDs periphery

(Novikoff *et al.*, 1980; Novikoff and Novikoff, 1982; Blanchette-Mackie *et al.*, 1995). Later, tubulo-reticular clusters of peroxisomes were detected in close association with LDs by live cell imaging (Schrader, 2001). More recently, a bimolecular fluorescence multiple complementation assay has shown several protein-protein interactions between peroxisomal markers and LD-associated proteins (Pu *et al.*, 2011). A close peroxisome-LD interaction would require a well-coordinated control of both lipid trafficking and metabolism. Accordingly, upon energy demand, this interorganellar crosstalk, which connects LDs to peroxisomes, promotes the mobilization of VLCFA from TG stored at LDs via lipolysis that are then degraded by peroxisomal β-oxidation (Shai, Schuldiner and Zalckvar, 2016). This has been further associated with CIDE-ATGL-PPARα pathway in murine adipocytes (Wang *et al.*, 2021). Consistently, impaired peroxisomal β-oxidation or deficit of peroxisomes was shown to be related to enlarged LDs as well as variations in their number (Schrader, Kamoshita and Islinger, 2019). Nevertheless, there is evidence that lipid trafficking is bidirectional, since it was also demonstrated that ether-linked lipids produced at peroxisome can be stored at LDs (Bartz *et al.*, 2007).

Even though contact sites between organelles have captured a lot of interest from the scientific community, there are still several questions that remain to be answered. Despite the existence of several studies reporting the interplay between LDs and peroxisomes there is a lack of knowledge regarding the regulation of their interplay and how contacts are established. In baker's yeast, where pexopodia was reported, a protein-protein interaction analysis revealed that two resident LD proteins, ERG6 and PET10, interact with different peroxisomal proteins, but it was not conclusive whether such proteins constitute an actual tether (Pu *et al.*, 2011). More recently, hereditary spastic paraplegia protein M1 (Spastin), a membrane-bound AAA ATPase present in LDs, was identified as a tether of these two organelles. Spastin was found to interact with ABCD1, a peroxisomal fatty acid transporter. Furthermore, this tethering complex was demonstrated to cooperate with two ESCRT-III proteins, which facilitate FA trafficking from LDs to peroxisomes, probably by inducing morphology alterations on LD membrane (Chang *et al.*, 2019).

More studies are required to better comprehend the interplay between peroxisomes and LDs and to understand the role that their crosstalk may play during viral infections.

II. OBJECTIVES

2.1 Objectives

HCV represents a major cause of death worldwide, presenting a burden not only for public health but also for economy. Although antiviral treatment can cure more than 95% of infected patients, access to diagnosis and treatment are still low, and no effective vaccine exists.

To establish infection and efficiently disseminate, HCV manipulates several host cell's functions, being highly dependent on cellular lipid metabolism. HCV induces profound changes on intracellular membrane architecture to form specialized replication complexes and virions use lipids release pathways for cell exiting. To manipulate lipid metabolism, it is well known that HCV modulates LD functions as well as their subcellular localization for its advantage.

Peroxisomes have been established as important platforms for the cellular immune response, and it has been described that HCV targets this organelle to abolish antiviral signalling. While peroxisomes are critical organelles for the cellular lipid metabolism, and are known interactors of LDs, their role on HCV infection as a metabolic organelle is still undetermined.

The main goal of this project is to create specialized tools that allow the study of the role of peroxisomes and their interplay with LDs for HCV propagation, through life cell imaging. These tools involve the creation of fluorescent fusion proteins constructs to generate stable cell lines with fluorescently stained LDs and peroxisomes. To achieve this, the following specific aims were proposed:

1. Develop plasmids coding peroxisome and LD-targeted fluorescent fusion transgenes for mammalian expression and for lentiviral transduction;
2. Study the expression phenotype of the developed fluorescent fusion proteins;
3. Analyse peroxisome morphology and subcellular distribution in cells expressing HCV core protein.

III. MATERIAL AND METHODS

3.1 Material

3.1.1 Bacterial strains

- DH5α competent *E. coli* bacteria

3.1.2 Vectors

- Provided by Dr. Eva Herker (Institute of Virology, Marburg):
  - Packaging vector: pCMV-ΔR9 (Naldini *et al.*, 1996)
  - Envelope vector: pCMV VSV.G (Naldini *et al.*, 1996)

3.1.3 Plasmids

- MXS-chaining vector (Addgene #62394)
- MXS_tdTomato (Addgene #62407)
- MXS_iRFP670 (Addgene #62411)
- MXS_bGHpA (Addgene #62425)
- Provided by Dr. Eva Herker (Institute of Virology, Marburg):
  - pSicoR-MS1-EF1α-mCherry (Wissing *et al.*, 2011)
  - JF559 A3Nt-GFP (Poppelreuther *et al.*, 2012)
  - HCV-2a-Core-3XFLAG (Ramage *et al.*, 2015)

3.1.4 Chemicals, reagents, and markers

	Company	Catalog Number
Agar	ForMedium	AGA03
Agarose	Roth	2267.4
Ampicillin sodium salt	Sigma-Aldrich	A9518-5G
Bovine serum albumin (BSA)	NZYTech	SPMB125
Collagen	Corning	354236
GelGreen Nucleic Acid Gel Stain 10000X	Biotium	41004
Glycerol	Roth	3783.1
LB Broth (powder)	NZYtech	MB14502
Mowiol 4-88	AppliChem	A90110100
N-propyl-gallate	Fluka	02370
O'GeneRuler DNA Ladder Mix	ThermoFisher Scientific	SM0333
Paraformaldehyde (PFA)	Sigma-Aldrich	158127
Penicillin/Streptomycin	BioWest	L0022-100
Sodium Azide	Fluka	71289
Triton X-100	Sigma-Aldrich	T8787

3.1.5 Solutions and buffers

- 0.2%Triton X-100: 0.2% Triton X-100 in 1x PBS
- 1x PBS: 1.39M NaCl, 80mM Na_2HPO_4, 0.0268M KCl, 0.0147M KH2PO4, pH 7.36 (prepared from 10x PBS diluted in ddH2O)

- 1x TAE: 0.04M Tris, 0.02M Acetic Acid, 1mM EDTA, pH 8 (prepared from TAE 50x diluted in ddH2O)
- Annealing Buffer: 200mM potassium acetate, 60mM HEPES-KOH pH 7.4, and 4mM Magnesium acetate
- 1% Agarose gel: 1g agarose and 5µL of GelGreen Nucleic Acid Gel Stain 10000X (Biotium) in 100mL 1x TAE; heat the mixture until obtain a homogenous solution
- 1% BSA: 2% BSA diluted in 1x PBS
- Homemade 10x DNA Loading Dye: 250mg Bromophenol Blue, 33mL Tris-HCl pH 7.6 (150mM), 60mL glycerol in ddH_2O up to 100mL
- LB medium: 20g LB in 1000 mL ddH2O
- LB/Agar: 2g agar and 20g LB in 1000 mL ddH2O
- Mounting Medium:
    - Mowiol: 12g Mowiol 4-88, 20mL Glycerol, 40mL PBS
    - N-propyl-Gallate: 2.5% (w/v) n-propyl-gallate; 50% glycerol, in PBS
    - Mounting medium: mixture of 3:1 ratio of Mowiol over N-propyl-Gallate
- 4% PFA: 20g PFA in 450 mL ddH2O, 4 drops 1 M NaOH, 50 mL 10x PBS

3.1.6 Primers

Table 2. **List of the primers and oligos used**

Primer's Designation		Sequence (5' → 3')
Primer 1	MXS EF1a HTLV fw	AATACGCGTAACTCGAGGGATCTGCGATCGCTCCGG
Primer 2	MXS EF1a HTLV rev	CTAGTCGACGCTAGCGTAGGCGCCGGTC
Primer 3	MXS Col fw	TTACCGCCTTTGAGTGAG
Primer 4	MXS Col rev	TTGTCTCATGAGCGGATAC
Primer 5	MXS iRFP fw	AATACGCGTAACTCGAGATGGCGCGTAAGGTCGATCTC
Primer 6	iRFP-PTS1 rev	CTAGTCGACTCAGAGTTTGCTGCGTTGGTGGTGGGCGGC
Primer 7	MXS EGFP fw	AATACGCGTAACTCGAGATGGTGAGCAAGGGCGAGG
Primer 8	EGFP-PTS1 rev	CTAGTCGACTCAGAGTTTGCTCTTGTACAGCTCGTCCATG
Primer 9	MXS ACSL fw	AATACGCGTAACTCGAGATGAATAACCACGTGTCTT
Primer 10	SalI BamHI ACSL rev	CTAGTCGACGGTGGATCCGCAAGCCAAT
Primer 11	ACSL link tdTomato fw	GCGGATCCACCGGTCGCCACCATGGTGAGCAAGGGCGAGG
Primer 12	MXS tdTomato rev	CTAGTCGACTCACTTGTACAGCTCGTCCATGCCG
Oligo MCS sense	pSicoR XbaI MCS sense	CTAGAGGAGGCGCGCCGGACTCGAGGGAGTCGACGCCGGATCCGCCG
Oligo MCS antisense	pSicoR EcoRI MCS as	AATTCGGCGGATCCGGCGTCGACTCCCTCGAGTCCGGCGCGCTCCT
Primer S1		TGCAGGGGAAAGAATAGTAGAC

3.1.7 Kits

- NucleoBond Xtra Midi/Maxi (Macherey-Nagel)
- E.Z.N.A. Gel Extraction Kit (Omega Bio-tek)

- NucleoSpin Plasmid, Mini kit for plasmid DNA (Macherey-Nagel)
- MXS-chaining kit (Addgene)

3.1.8 Databases and Software

- Zen 3.3 (blue edition)
- Basic Local Alignment Search (BLAST) Tool, National Center for Biotechnology Information (NCBI)
- Excel, Microsoft
- Serial Cloner

3.1.9 Enzymes

***Table 3*. Summarised information about the enzymes used**

Enzyme	Buffer	Manufacture
MluI	NEBuffer 3.1	New England Biolabs
SalI		
BamHI		
PvuI		
XhoI	NEBuffer 3.1 / CutSmart Buffer	
BsrGI	NEBuffer 2.1 / NEBuffer 3.1	
AgeI	NEBuffer 1.1	
XbaI	NEBuffer 2.1 / CutSmart Buffer	
EcoRI-HF	CutSmart Buffer	
AscI		
BamHI-HF		
KpnI	NEBuffer 2.1	
NheI		
T4 DNA Ligase	T4 DNA Ligase Reaction Buffer	
Quick CIP	-	
Taq DNA polymerase	Taq Buffer (10X), with KCl	ThermoFisher Scientific
Polynucleotide Kinase (New England Biolabs)	T4 DNA Ligase Buffer (ThermoFisher Scientific)	

3.1.10 Cell lines

- HEK293T: human embryonic kidney 293 cells that express a mutant version of the SV40 large T antigen
- Huh7: human hepatoma permanent cell line established from hepatoma tissue

3.1.11 Cell culture solutions

- Dulbecco's Modified Eagle Medium (DMEM), (4,5 g/L), w/ L-Glutamine, w/o Sodium Pyruvate (BioWest and Gibco)

- 1x Dulbecco's Phosphate Buffered Saline w/o Calcium w/o Magnesium (BioWest and Gibco)
- 1x Trypsin-EDTA in PBS w/o Calcium w/o Magnesium w/o Phenol Red (BioWest and Gibco)
- Fetal Bovine Serum (FBS), qualified, E.U.-approved, South America origin (Gibco)
- 1x Opti-MEM Reduced-Serum Medium liquid (Gibco)

3.1.12 Transfection Reagents

- Polyethyleneimine linear (PEI) (PolySciences)
- FuGENE HD Transfection Reagent (Promega)
- Polybrene (Merck Millipore)

3.1.13 Antibodies

Table 4. **Detailed information about the antibodies and dyes used in immunofluorescence analyses**

Antibody	Species	Clonality	Dilution	Company	Reference
Primary Antibodies					
PMP70	Mouse	Monoclonal	1:200	Sigma-Aldrich	SAB4200181
Flag	Rabbit	Polyclonal	1:500	Sigma-Aldrich	F7425
Secondary Antibodies					
TRITC	Donkey	Polyclonal	1:100	Jackson immunoresearch	711-025-152 705-025-147
Alexa 488	Donkey	Polyclonal	1:400	Invitrogen	A-21202 A-21206
BODIPY 665	-	-	1:20000	Invitrogen	B3932
BODIPY 493/503	-	-	1:750	Invitrogen	D3922
Hoechst Dye	-	-	1:2000	PolySciences	33258/09460

3.1.14 Equipment

- Analytical balance VWR (Sartorius)
- Basic pH meter PB-11 (Sartorius)
- Centrifuge Heraeus Pico and Fresco 17 (Thermo Scientific)
- CO_2 incubator MCO-17AIC (Sanyo)
- Confocal Laser Scanning Microscope TCS PS5 II (Leica Microsystems)
- DS-11 Series Spectrophotometer (DeNovix)
- Eclipse Ts2 microscope (Nikon)
- Electromagnetic agitator VMS-C7 (VWR)
- Electrophoresis Power Suply EPS 3501 XL Power Supply, GE Healthcare
- Incubation shaker CERTOMAT BS-1 (Sartorius)
- NanoDrop Lite Spectrophotometer (Thermo Scientific)
- Pipettes Eppendorf Research (Eppendorf)
- Shaker, Mini-Rocker PMR-30 (Grant Bio)
- Thermal cycler ProFlex™ 3 x 32-well PCR System (Thermo Scientific)

- Thermomixer Comfort 1.5 (Eppendorf)
- Ultracentrifuge Optima LE-80K (Beckman)
- UV-3100 PC Spectrophotometer (VWR)
- Vaccum gas pump (VWR)
- Vertical Laminar Flow Hood (HERAEUS HeraSafe)
- Water Bath VW36 (VWR)
- Zeiss Axio Imager Z1 microscope (Zeiss)
- Zeiss LSM 880 with Airyscan confocal microscope (Zeiss)
- EVOS M5000 Imaging System (Thermo Scientific)

3.2 Methods

3.2.1 Cloning

To analyse simultaneously LDs and peroxisomes by live cell imaging, 11 different plasmids were developed (**Table 5**).

All polymerase chain reactions (PCRs) indicated below were performed in a thermal cycler ProFlex™ 3 x 32-well PCR System (Thermo Scientific) and all the necessary DNA concentration measurements were obtained in a NanoDrop Lite Spectrophotometer (Thermo Scientific).

Table 5. **Developed MXS plasmids**

MXS39	MXS plasmid only containing the EF1α HTLV promoter
MXS40	MXS iRFP-PTS1 bGHpA
MXS41	MXS EGFP-PTS1 bGHpA
MXS42	MXS EF1α HTLV::iRFP-PTS1 bGHpA
MXS43	MXS EF1α HTLV::EGFP-PTS1 bGHpA
MXS44	MXS ACSL
MXS45	MXS ACSL-tdTomato
MXS46	MXS EF1α HTLV::ACSL-tdTomato
MXS47	MXS EF1α HTLV::ACSL-tdTomato bGHpA
MXS48	MXS EF1α HTLV::ACSL-tdTomato bGHpA_EF1α HTLV::EGFP-PTS1 bGHpA
MXS49	MXS EF1α HTLV::ACSL-tdTomato bGHpA_EF1α HTLV::iRFP-PTS1 bGHpA

3.2.1.1 MXS EF1α HTLV plasmid cloning strategy

To drive high level expression of the MXS constructs, EF1α HTLV promoter from the pSico-R-MS1-EF1α-mCherry plasmid was first cloned into the MXS-chaining vector (Addgene #62394) (MXS38), to create the construct MXS EF1α HTLV (MXS39) (**Figure 10**).

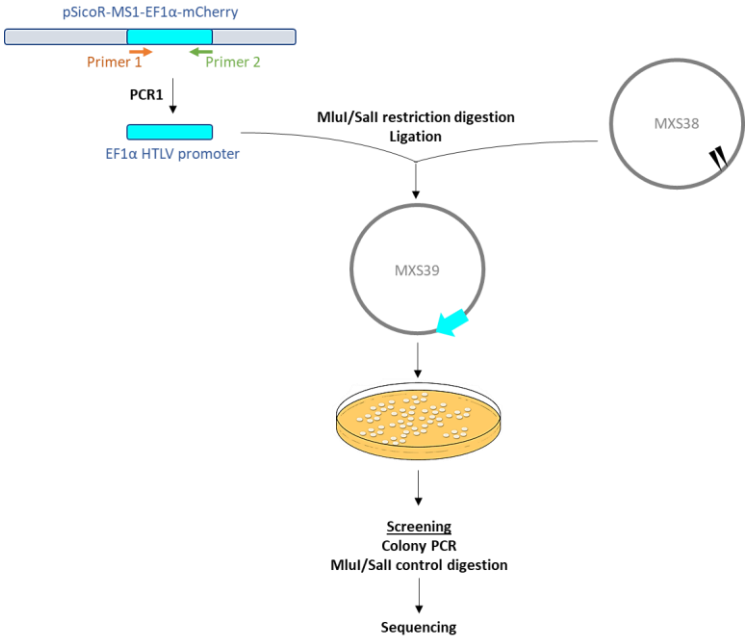

Figure 10. **Schematic representation of MXS EF1α HTLV (MXS39) cloning.**

3.2.1.1.a. Polymerase Chain Reaction (PCR)

The EF1α HTLV promoter sequence was amplified by PCR (PCR 1) using the lentiviral plasmid pSicoR-MS1-EF1α-mCherry (given by Dr. Eva Herker, Institute of Virology, Marburg – see section 3.1.3) as template and the Primers 1 and 2 (**Table 2**). The PCR reaction mix composition and conditions are described in **Table 6** and **Table 7**, respectively.

Table 6. **PCR reaction master mix**

Component	Volume
5x Phusion HF Buffer (Thermo Scientific)	10 µL
10 mM dNTPs	1 µL
DMSO	2 µL
Forward Primer (10µM)	2.5 µL
Reverse Primer (10µM)	2.5 µL
DNA Template	100 ng
Phusion DNA Polymerase (Thermo Scientific)	0.5 µL
Nuclease free water	Up to 50 µL

Table 7. **PCR 1 conditions**

Cycle step	Nº of Cycles	Temperature	Time (min:sec)
Initial Denaturation	1x	98°C	2:00
Denaturation	25x	98°C	0:10
Annealing		65°C	0:30
Extension		72°C	0:30
Final Extension	1x	72°C	10:00
Final Hold	1x	4°C	∞

3.2.1.1.b. DNA isolation and purification after PCR

After DNA amplification, the 576 bp amplified product was isolated by electrophoresis and purified by gel extraction. For this, the whole PCR reaction product was mixed with homemade loading dye, to allow running front identification of samples, before loading in a 1% agarose gel. A DNA Ladder Mix was also loaded to help identify the DNA of interest by its size. Gel ran at 150V for 40 minutes in 1x TAE, and after identifying and excising the interest DNA band, DNA was purified by following the Spin protocol from the E.Z.N.A.® Gel Extraction Kit (Omega Bio-tek).

3.2.1.1.c. Restriction Enzyme Digestion and Ligation

To insert the EF1α HTLV promoter sequence in the MXS38 vector, a restriction enzyme digestion of both DNAs was performed using MluI and SalI enzymes (New England Biolabs). For this, 1 µg of each DNA were digested with 0.5 µL of each enzyme, in 2 µL of NEBuffer 3.1 (New England Biolabs) and supplemented with nuclease free water for a final volume of 20 µL, for at least 1 hour at 37°C.

Before ligation and to avoid vector self-ligation, vector DNA was dephosphorylated by treatment with 1 µL of Quick CIP (New England Biolabs) for 1 hour at 37°C.

Both insert and vector were separated by electrophoresis in a 1% agarose gel and the expected fragments (1927 bp for vector, and 564 bp for insert) were isolated and purified by following gel extraction protocol (as described in section 3.2.1.1.b). Undigested vector was also loaded as a negative digestion control. The concentration of the purified digested products was then measured using a NanoDrop spectrophotometer.

Insert and vector ligation was performed using T4 DNA Ligase (New England Biolabs) and by following manufactures' protocol in a final volume of 10 µL, which was incubated for 15 minutes at room temperature. Insert was added in a 3:1 molar ratio over 20 ng of digested and dephosphorylated vector (according to formula presented in **Figure 11**). To have a control for analysing vector self-ligation, a control reaction was performed without adding insert.

$$Mass\ of\ insert\ (ng) = \frac{Mass\ of\ vector\ (ng) \times\ Size\ of\ insert\ (kb)}{Size\ of\ vector\ (kb)} \times Molar\ ratio(\frac{Insert}{Vector})$$

Figure 11. **Mathematical formula to calculate mass of insert to be used in a ligation protocol**

3.2.1.1.d. Transformation

For each ligation condition, 5 µL of the ligation reaction were mixed with 50 µL of competent DH5α *E. coli* and incubated on ice for 30 minutes before performing a heat shock at 42°C for 20 seconds followed by a 2-minute incubation on ice. For recovery, 300 µL of LB medium without antibiotics were added to bacteria/ligation mix, which was then incubated for 20 minutes at 37°C with a 350-rpm shaking. Afterwards, pelleted bacteria, obtained after a full speed centrifugation for 1 minute, were resuspended in 200 µL of supernatant and plated on selective LB agar/ampicillin plates using a triangular steel spreader, and incubated overnight at 37°C.

3.2.1.1.e. Colony Screening

To identify positive colonies, a Colony PCR was performed where picked colonies were first spread in a LB/ampicillin plate (master plate) before being emerged in the colony PCR master mix (**Table 8**) containing the Primers 3 and 4 (**Table 2**). Targeted DNA was amplified using the PCR conditions described in **Table 9**.

Table 8. **Colony PCR reaction master mix**

Component	Volume
10x Taq Buffer, with KCl (ThermoFisher Scientific)	2 µL
10 mM dNTPs	0.4 µL
$MgCl_2$	1.6 µL
Forward Primer (10µM)	1 µL
Reverse Primer (10µM)	1 µL
Taq DNA Polymerase (ThermoFisher Scientific)	0.1 µL
Nuclease free water	Up to 20 µL

Table 9. **PCR conditions for identification of positive colonies (Colony PCR)**

Cycle step	Nº of Cycles	Temperature	Time (min:sec)
Initial Denaturation	1x	94°C	10:00
Denaturation	20x	94°C	0:30
Annealing		55°C	0:30
Extension		72°C	1:00
Final Extension	1x	72°C	7:00
Final Hold	1x	4°C	∞

As described previously, amplified PCR products were analysed by electrophoresis to identify positive colonies.

Prepared master plates were incubated overnight at 37°C, after which, bacteria inoculums of the positive clones were prepared in duplicate using 3 mL of LB medium with ampicillin which were then incubated overnight at 37°C with a 200-rpm shacking. In the following day, plasmid DNA was isolated and purified using the NucleoSpin Plasmid Mini kit (Macherey-Nagel).

Plasmids DNA sequence were then confirmed by restriction enzyme digestion using MluI and SalI, as described previously, and by Sanger sequencing following the SupremeRun Tube instructions (Eurofins). After sequence confirmation, positive bacteria were inoculated again to prepare glycerol stocks and high quantities of transfection grade DNA using the NucleoBond® Xtra Midi or Maxi kit (Macherey-Nagel), to obtain the MXS39 plasmid DNA.

3.2.1.2 MXS EF1α HTLV::iRFP-PTS1 bGHpA and MXS EF1α HTLV::EGFP-PTS1 bGHpA plasmids cloning strategy

To analyse peroxisomes during live cell imaging, two constructs that express different fluorescent fusion proteins targeting peroxisomes (iRFP-PTS1 and EGFP-PTS1) were developed (**Figure 12**).

Figure 12. **Schematic representation of MXS EF1α HTLV::iRFP-PTS1 bGHpA (MXS42) and MXS EF1α HTLV::EGFP-PTS1 bGHpA (MXS43) plasmids cloning.**

For iRFP-PTS1 amplification, the MXS-iRFP670 plasmid (Addgene #62411) from MXS-chaining kit was used as template together with the Primers 5 and 6 (**Table 2**) (PCR 2). For EGFP-PTS1 amplification, the JF559-A3Nt-GFP plasmid (kindly provided by Dr. Eva Herker, Institute of Virology, Marburg – see section 3.1.3) was used as template along with the Primers 7 and 8 (**Table 2**) (PCR 3).

PCR reaction master mixes composition and conditions used are described in **Table 6** and **Table 10**.

Table 10. **PCR 2 and PCR 3 conditions**

	Cycle step	Nº of Cycles	Temperature	Time (min:sec)
PCR 2	**Initial Denaturation**	1x	98°C	2:00
	Denaturation	25x	98°C	0:10
	Annealing		65°C	0:30
	Extension		72°C	0:30
	Final Extension	1x	72°C	10:00
	Final Hold	1x	4°C	∞
PCR 3	**Initial Denaturation**	1x	98°C	2:00
	Denaturation	25x	98°C	0:10
	Annealing		60°C	0:30
	Extension		72°C	0:30
	Final Extension	1x	72°C	10:00
	Final Hold	1x	4°C	∞

After each amplification, DNA was isolated and purified. The expected size of the iRFP-PTS1 sequence was 971bp, whereas for the EGFP-PTS1 sequence was 755bp long.

First, to produce MXS iRFP-PTS1 bGHpA (MXS40) and MXS EGFP-PTS1 bGHpA (MXS41) constructs, 1 µg of iRFP-PTS1 and EGFP-PTS1 fragments were digested with 0.5 µL of MluI and SalI restriction enzymes (New England Biolabs). MXS_bGHpA plasmid (Addgene #62425) (vector) was digested with 0.5 µL of both MluI and XhoI restriction enzymes (New England Biolabs). After vector dephosphorylation, both inserts and vector were isolated and purified before proceeding with ligation. The expected sizes for the digested fragments were 2168 bp for the vector, 959bp for the iRFP-PTS1, and 743bp for the EGFP-PTS1.

Ligation products were then transformed and grown colonies were screened for positive clones by colony PCR, control restriction digestion, and by Sanger sequencing. The chosen positive clone was then amplified originating the MXS40 and MXS41 plasmids. Subsequently, to maximize expression of the two constructs, EF1α HTLV promoter sequence was inserted. To this end, 1 µg of both MXS40 and MXS41 plasmids (vectors) were digested with 0.5 µL of MluI and XhoI restriction enzymes (New England Biolabs), while 0.5 µg of MXS39 plasmid were digested with 0.5 µL of both MluI and SalI restriction enzymes (New England Biolabs) to isolate EF1α HTLV sequence (insert). After vectors dephosphorylation, DNAs were isolated and purified before proceeding with ligation, as described before.

Ligation products were then transformed and grown colonies were also screened for positive clones by colony PCR and restriction enzyme digestion. The confirmed sequences originated the MXS EF1α HTLV::iRFP-PTS1 bGHpA (MXS42) and MXS EF1α HTLV::EGFP-PTS1 bGHpA (MXS43) plasmid DNAs (**Figure 15**) which were then amplified as midi or maxipreps to obtain high quantities of DNA for subsequent experiments.

The method behind restriction enzyme digestion, dephosphorylation and ligation indicated in this section were followed as described in section 3.2.1.1.c with the specific alterations indicated here. Transformation and colony screening were also performed as described in sections 3.2.1.1.d and 3.2.1.1.e and minor changes were specified in this section as well.

3.2.1.3 MXS EF1α HTLV::ACSL-tdTomato bGHpA plasmid cloning strategy

To analyse LDs by live cell imaging, MXS EF1α HTLV::ACSL-tdTomato bGHpA (MXS47) plasmid was developed. To this end, ACSL sequence, which corresponds to the sequence coding for the first 135 amino acids of the long-chain acyl-coenzyme A synthetase (ACSL) 3, was first inserted in the MXS38 plasmid, generating the MSX ACSL (MXS44) plasmid and posteriorly tdTomato sequence was added, generating the MXS ACSL-tdTomato (MXS45) plasmid. The EF1α HTLV sequence was then inserted in this construct (MXS46) as well as the bGHpA, thus creating the MXS47 construct (**Figure 13**) that, upon expression, produces a tdTomato fusion protein that is targeted to LDs.

To obtain the ACSL-tdTomato sequence, two amplification reactions were performed. ACSL sequence was obtained by using JF559-A3Nt-GFP plasmid (given by Dr. Eva Herker's, Institute of Virology, Marburg – see section 3.1.3) as template with the Primers 9 and 10 (**Table 2**) (PCR 4). At the same time, tdTomato sequence was amplified by using the MXS_tdTomato plasmid (Addgene

#62407) as template and the Primers 11 and 12 (**Table 2**) (PCR 5). The reaction mixes composition and amplification conditions are described in **Table 6** and **Table 11**, respectively**.**

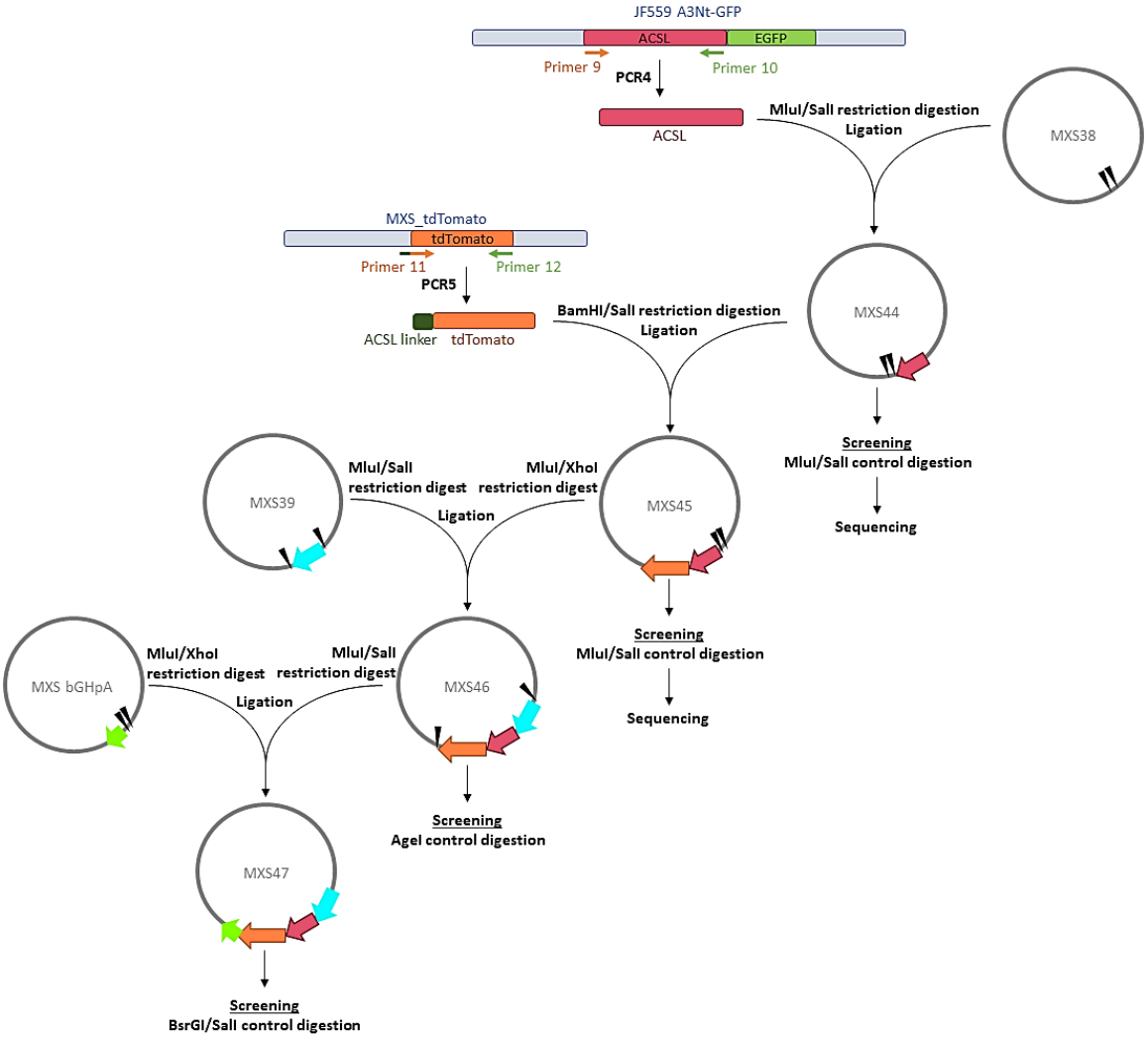

Figure 13. **Schematic representation of MXS EF1α HTLV::ACSL-tdTomato bGHpA (MXS47) cloning.**

In the end of amplification, PCR products were isolated by electrophoresis and purified by gel extraction as described on section 3.2.1.1b. The expected DNA size of the amplified ACSL sequence was 442 bp, and amplified tdTomato sequence was 1461 bp.

To create the MXS44 plasmid, the amplified ACSL sequence and the vector MXS38 were both digested with MluI and SalI (New England Biolabs). Digestion was followed by vector dephosphorylation, DNA electrophoresis and ligation. Ligation mix was then transformed and grown colonies were screened by restriction enzyme digestion. Positive clones were sequenced, and the selected one was then used for DNA amplification and purification.

The MXS44 construct was then used together with the amplified tdTomato sequence (obtained with PCR 5) to generate the MXS45 plasmid. To this end, a restriction enzyme digestion of MXS44 plasmid (vector) and tdTomato sequence (insert) was performed with BamHI and SalI restriction enzymes (New England Biolabs). After vector dephosphorylation and ligation of these two

sequences, the ligation product was used to transform bacteria. Then, for colony screening, restriction enzyme digestion was performed, and positive clones were sequenced. The selected colony was then used for DNA amplification and purification.

Table 11. **PCR 4 and PCR 5 conditions**

	Cycle step	Nº of Cycles	Temperature	Time (min:sec)
PCR 4	**Initial Denaturation**	1x	98°C	2:00
	Denaturation	30x	98°C	0:10
	Annealing		55°C	0:30
	Extension		72°C	0:20
	Final Extension	1x	72°C	10:00
	Final Hold	1x	4°C	∞
PCR 5	**Initial Denaturation**	1x	98°C	2:00
	Denaturation	7x	98°C	0:10
	Annealing		61°C	0:30
	Extension		72°C	1:30
	Denaturation	23x	98°C	0:10
	Annealing		66°C	0:30
	Extension		72°C	1:30
	Final Extension	1x	72°C	10:00
	Final Hold	1x	4°C	∞

To drive high expression levels of the construct, the EF1α HTLV promoter sequence was inserted. For this, MXS45 plasmid (vector) was digested with the MluI and XhoI restriction enzymes (New England Biolabs), and MXS39 was digested with MluI and SalI (New England Biolabs). Digested vector was then dephosphorylated before proceeding with ligation. Ligation products were then transformed into bacterial cells and obtained colonies were screened by restriction enzyme digestion. The selected positive colony was then used for DNA amplification and purification, producing the MXS46 DNA plasmid.

Finally, to transform the MXS46 construct into a transcriptable sequence, the bGHpA terminator sequence was added. To this end, MXS_bGHpA plasmid (vector) was digested with the MluI and XhoI restriction enzymes (New England Biolabs), and MXS46 was digested with MluI and SalI (New England Biolabs). Digested vector was then dephosphorylated before proceeding to ligation, which was followed by bacteria transformation with ligated product. Upon colony screening by restriction enzyme digestion, the selected colony was then used for DNA amplification and purification producing the transcriptable MXS47 plasmid (**Figure 15**).

The method behind restriction enzyme digestion, dephosphorylation and ligation indicated in this section was followed as described in section 3.2.1.1.c with specific alterations that are indicated here. Moreover, vector and insert ligation described in this section used 15 to 35 ng of the digested and dephosphorylated vector, and because of the different insert/vector size ratios, depending on the condition, 3:1 or 1:1 ratio was used. Transformation and colony screening were also performed as described in section 3.2.1.1.d and 3.2.1.1.e and minor changes were specified in this section as well.

3.2.1.4 MXS EF1α HTLV::ACSL-tdTomato bGHpA_EF1α HTLV::EGFP-PTS1 bGHpA and MXS EF1α HTLV::ACSL-tdTomato bGHpA_EF1α HTLV::iRFP-PTS1 bGHpA plasmids cloning strategy

To develop MXS plasmids that express two fusion proteins that would target both peroxisomes and LDs, EF1α HTLV::ACSL-tdTomato bGHpA sequence was inserted into the MXS42 and MXS43 plasmids (**Figure 14**). To this end, 1 µg of MXS47 was digested with 1 µL of both MluI and SalI restriction enzymes (New England Biolabs) to isolate ACSL-tdTomato sequence (insert) and 1 µg of MXS42 and MXS43 plasmids (vectors) were digested with 1 µL of both MluI and XhoI restriction enzymes (New England Biolabs). Upon vectors dephosphorylation, vectors and insert were isolated by DNA electrophoresis, which was followed by ligation.

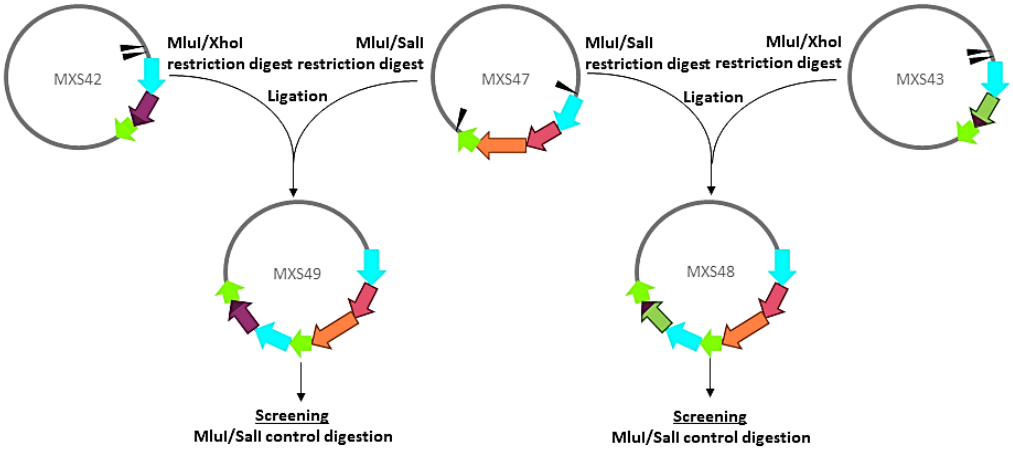

Figure 14. **Schematic representation of EF1α HTLV::ACSL-tdTomato bGHpA_EF1α HTLV::EGFP-PTS1 bGHpA (MXS48) and MXS EF1α HTLV::ACSL-tdTomato bGHpA_EF1α HTLV::iRFP-PTS1 bGHpA (MXS49) cloning approach.**

Bacteria were then transformed with the ligation products and grown colonies were screened for positive clones by restriction enzyme digestion with 0.5 µL of both MluI and SalI (New England Biolabs). For the plasmid containing the iRFP and tdTomato fusion proteins sequences, positive clones presented a 4416bp band. On the other hand, for the plasmid containing the sequences of EGFP and tdTomato, positive clones presented a 4200bp band. Identified positive clone DNA was then amplified to obtain MXS EF1α HTLV::ACSL-tdTomato bGHpA_EF1α HTLV::EGFP-PTS1 bGHpA (MXS48) and MXS EF1α HTLV::ACSL-tdTomato bGHpA_EF1α HTLV::iRFP-PTS1 bGHpA (MXS49) (**Figure 15**).

The restriction enzyme digestion, dephosphorylation and ligation indicated in this section were conducted as described in section 3.2.1.1.c with the specific alterations indicated here. Transformation and colony screening were also performed as described in sections 3.2.1.1.d and 3.2.1.1.e and minor changes were specified in this section as well.

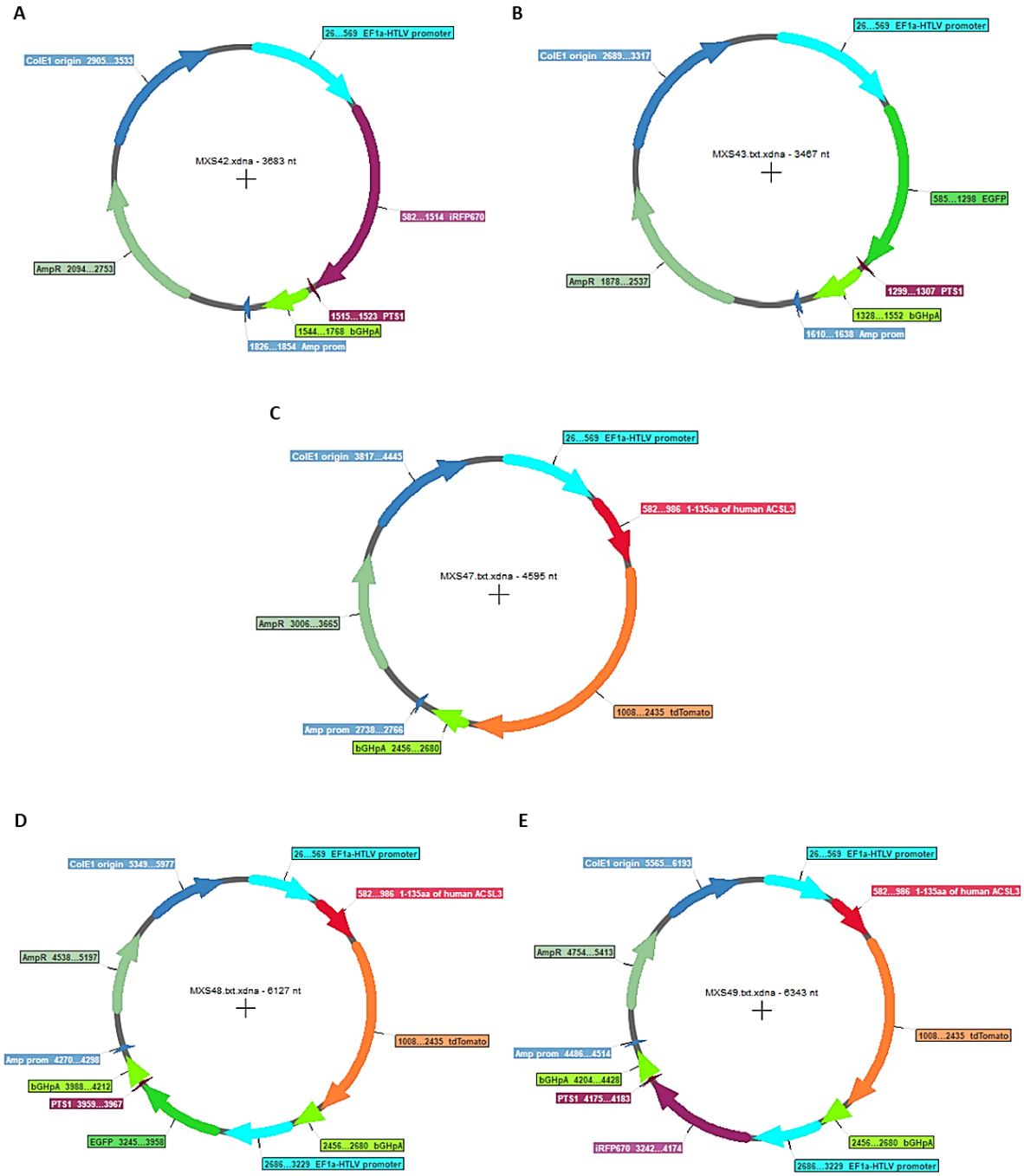

Figure 15. **Graphic maps of the five transcriptable high-expression MXS plasmids constructed. (A)** MXS EF1α HTLV::iRFP-PTS1 bGHpA (MXS42), **(B)** MXS EF1α HTLV::EGFP-PTS1 bGHpA (MXS43), **(C)** MXS EF1α HTLV::ACSL-tdTomato bGHpA (MXS47), **(D)** MXS EF1α HTLV::ACSL-tdTomato bGHpA_EF1α HTLV::EGFP-PTS1 bGHpA (MXS48), and **(E)** MXS EF1α HTLV::ACSL-tdTomato bGHpA_EF1α HTLV::iRFP-PTS1 bGHpA (MXS49).

3.2.1.5 Cloning strategy to insert the developed reporter cassettes into a lentiviral plasmid

To construct the lentiviral plasmids containing either the combined or the single reporter cassettes, the MXS42, MXS43, MXS47, MXS48, MXS49 organelle-targeting constructs were cloned into a pSicoR-MS1 lentiviral vector (**Figure 16**).

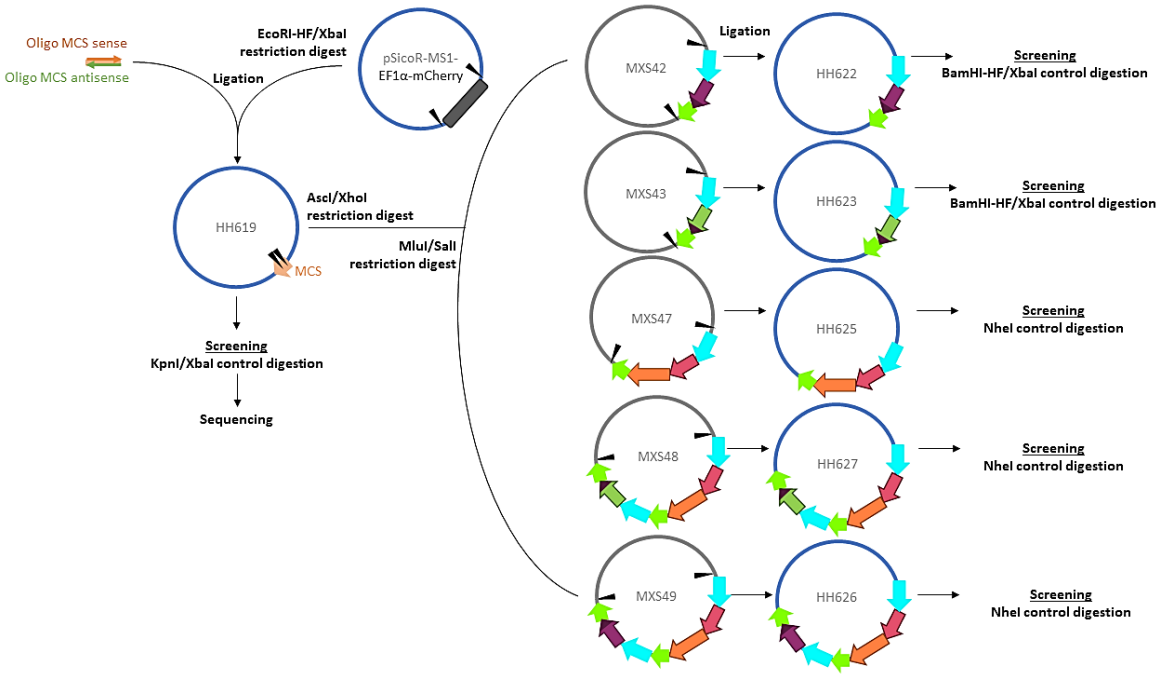

Figure 16. **Schematic representation of lentiviral plasmids cloning.**

To insert the developed LD and/or peroxisome-targeting construct from the MXS backbone into the lentiviral vector it was necessary to introduce the required restriction sites in a multiple cloning site (MCS). For this, 3 µg of the pSicoR-MS1-EF1α-mCherry plasmid (given by Dr. Eva Herker, Institute of Virology, Marburg – see section 3.1.3) were digested with 0.5 µL of EcoRI-HF and XbaI restriction enzymes (New England Biolabs) to remove the EF1α-mCherry sequence. This was followed by vector dephosphorylation, and isolation by DNA electrophoresis and gel purification.

In parallel, the sense and antisense oligos were phosphorylated and annealed to be then used as the insert in this subcloning. For the phosphorylation of the Oligos MCS sense and antisense (**Table 2**), 2 µL of each were mixed with 1 µL of T4 DNA Ligase Buffer (ThermoFisher Scientific) and 0.4 µL of Polynucleotide Kinase (New England Biolabs) with a final volume of 10 µL each and were incubated at 37°C for 45 minutes followed by an incubation at 65°C for 20 minutes. Thereafter, for the annealing, 5 µL of each phosphorylation reaction were mixed with 25 µL of Annealing Buffer in a final volume of 50 µL. This mix was incubated at 95°C for 5 minutes and then the temperature of incubation was progressively decreased 1°C every minute for 88 minutes.

Then, ligation of vectors with the annealed oligos was performed by mixing 1 µL of the annealing reaction with 2 µL of the digested and dephosphorylated vectors. Ligation products were then transformed into bacteria and grown colonies were screened for positive clones by restriction enzyme digestion with 0.5 µL of both KpnI and XbaI (New England Biolabs). Afterwards, the DNA from a chosen positive clone was sent for sequencing together with Primer S1 (**Table 2**). After sequence confirmation, pSicoR-MS1-MCS plasmid was amplified and stored in glycerol stocks (HH619).

To insert the MXS sequence into the lentiviral vector, 1 µg of the HH619 plasmid (vector) was digested with 1 µL of AscI and XhoI restriction enzymes (New England Biolabs) while 1 µg of each of the 5 MXS plasmids were digested with 1 µL of both MluI and SalI restriction enzymes (New England Biolabs). Vector was then dephosphorylated, and all DNAs were separated through electrophoresis and purified.

Each MXS insert was cloned into the vector, and ligation products were then transformed. Grown colonies were screened for positive clones by restriction enzyme digestion with 1 µL of both BamHI-HF and XbaI for MXS42 and MXS43-containing lentiviral plasmids, and 1 µL of NheI (New England Biolabs) for MXS47, MXS48 and MXS49-containing lentiviral plasmids. After sequence confirmation, lentiviral plasmids were amplified and stored in glycerol stocks (**Figure 17**).

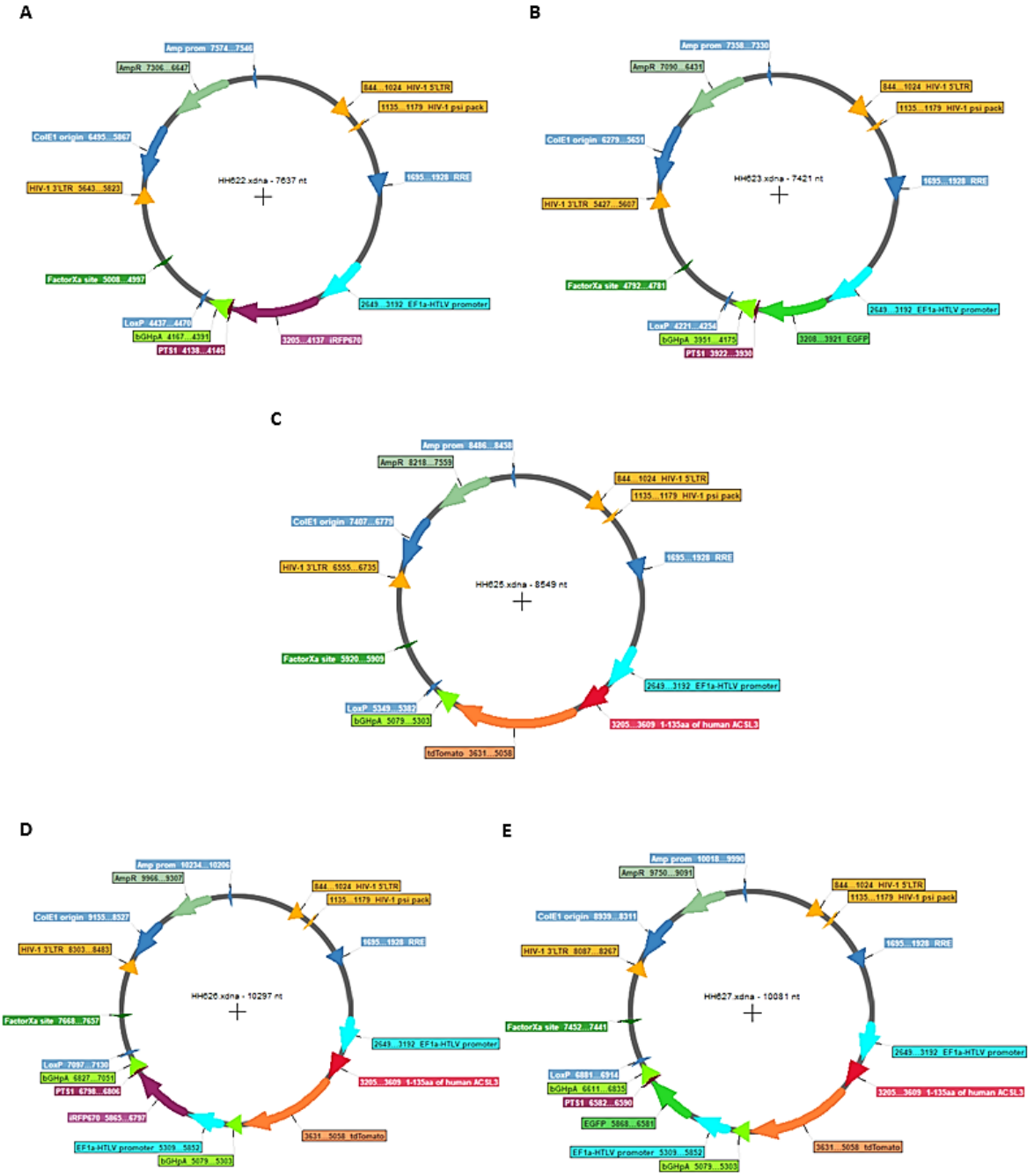

Figure 17. **Graphic maps of the five lentiviral plasmids constructed. (A)** pSicoR-MS1 EF1α HTLV::iRFP-PTS1 bGHpA (HH622), **(B)** pSicoR-MS1 EF1α HTLV::EGFP-PTS1 bGHpA (HH623) **(C)** pSicoR-MS1 EF1α HTLV::ACSL-tdTomato bGHpA (HH625) **(D)** pSicoR-MS1 EF1α HTLV::ACSL-tdTomato bGHpA_EF1α HTLV::iRFP-PTS1 bGHpA (HH626), and **(E)** pSicoR-MS1 EF1α HTLV::ACSL-tdTomato bGHpA_EF1α HTLV::EGFP-PTS1 bGHpA (HH627).

The method behind restriction enzyme digestion, dephosphorylation and ligation indicated in this section was followed as described in section 3.2.1.1.c along with the specific alterations indicated here. Transformation and colony screening were also performed as described in section 3.2.1.1.d and 3.2.1.1.e and minor changes were specified in this section as well.

3.2.2 Cell Maintenance

For this project, high-passage Huh7 cells (kindly given by Dr. Eva Herker, Institute of Virology, Marburg) and the HEK293T cells (kindly given by Dr. Friedemman, Weber Institute of Virology, Justus-Liebig University) were used. These cells were routinely cultured in DMEM, high glucose supplemented with 10% FBS, 1% penicillin and streptomycin (DMEM +/+) and incubated at 37°C in a humidified atmosphere containing 5% CO_2. When cells reach a certain confluence, their passage was conducted, normally from 1 to 2 times a week.

For passage, cells were washed with DPBS and, after a 5-minute incubation with 1.5 mL trypsin-EDTA at 37°C and 5% CO_2, they were resuspended by adding 3.5 mL of DMEM +/+ and pipetting up and down to break cell agglomerates. Next, a centrifugation at 1000 rpm for 3 minutes at room temperature was performed to remove cell debris. The supernatant was discarded, the cell pellet was resuspended in 5 ml of DMEM +/+, and cells were seeded in a 10 cm dish, in a defined dilution depending on the following experiments that would be conducted. For experiments that required a specific number of cells, cells were counted after cell pellet resuspension using a Neubauer counting chamber.

3.2.3 Transfection Methods

3.2.3.1 Polyethylenimine (PEI)

In a 24-well plate with glass coverslips in the bottom, $2x10^4$ Huh7 cells were seeded in 0.5 mL of DMEM +/+ per well. In the following day, for each well, 0.5 µg of the DNA was diluted in 30 µL of serum-free media (DMEM high glucose without supplementation with FBS nor antibiotics). Subsequently, 4 µL of PEI reagent were added to the DNA mix, in a 1:8 ratio of DNA over PEI, vortexed and then incubated for 20 minutes at room temperature. The cell media was renewed, and the transfection mix was added dropwise in the well. The plate was then incubated at 37°C and 5% CO_2.

3.2.3.2 FUGENE HD

In a 6-well plate with two or three coverslips in each well, $2x10^5$ Huh7 cells were seeded in 2 mL of DMEM +/+ per well. In the following day, for each well, 1 µg of the DNA was diluted in a volume up to 100 µL of Opti-MEM. This mixture was incubated for 5 minutes at room temperature. Subsequently, 3 µL of FuGENE HD reagent were added to the DNA solution and vortexed immediately. After a 15-minute incubation at room temperature, the DNA/FuGENE HD mixture

was added to the well with changed media in a dropwise manner. The plate was then incubated at 37°C and 5% CO_2 for about 48 hours.

3.2.4 Lentivirus production and concentration

HEK293T cells were seeded in collagen-coated 10 cm dishes and for each lentivirus 5 dishes were prepared ($2x10^6$ cells per dish). After 24-hour incubation, cells were transfected with PEI reagent, in which 8 µg of transfer vector, 6 µg of pCMV-ΔR9 (packaging plasmid kindly provided by Dr. Eva Herker, Institute of Virology, Marburg – see section 3.1.2), and 2.4 µg of pCMV VSV.G (envelope plasmid kindly provided by Dr. Eva Herker, Institute of Virology, Marburg – see section 3.1.2) were diluted in 500 µL of DMEM not supplemented with antibiotics nor FBS (DMEM-/-). Then, 99 µL of PEI reagent was added, in a 1:6 ratio of DNA over PEI, which, after steadily vortexed, was incubated for 20 minutes at room temperature. Meanwhile, cell media was replaced with 5 mL of DMEM supplemented only with 10% FBS (DMEM +/-), and, at the end of the incubation, the transfection mix was added in a dropwise manner. Dishes were incubated at 37°C in a humidified atmosphere containing 5% CO_2 for 6 to 8 hours, after which cell media was changed to 5 mL of DMEM +/+. Afterwards, the dishes were incubated once again at the same conditions of temperature and CO_2.

Finally, 3 days after transfection, cells were checked for fluorescence with a EVOS M5000 Imaging System (ThermoFisher Scientific) before collecting cell supernatant. Cell supernatant of 5 dishes was transferred to a 50 mL falcon, which was then spined down for 5 minutes at 1200 rpm at room temperature to discard cell debris. Debris-free supernatant was collected and evenly distributed into ultracentrifuge tubes, which were submitted to an ultracentrifugation at 65000 rpm for 30 minutes at 4°C in an Optima LE-80K ultracentrifuge (Beckman) using the Beckman type 80 Ti rotor. Following ultracentrifugation, almost all supernatant was aspirated to resuspend lentivirus present in pellet in only 1 mL of supernatant. At last, aliquots of 100 µL or 200 µL were prepared and kept at -80°C.

3.2.5 Lentivirus titration

Lentivirus titration was conducted both to confirm the efficiency of lentivirus production and determine the amount of the lentivirus to use in further studies, as well as to check the subcellular localization of the fusion protein or proteins encoded by these viruses. Huh7 cells were seeded in DMEM +/+ in a 12-well plate with coverslips ($1.5x10^4$ cells per well). The day after, cell media was changed to 1 mL of DMEM +/+ supplemented with Polybrene (1:1000 dilution) and different volume of lentivirus aliquots were added to each well, always keeping one well untransduced. The day after transduction, cell media was changed to 1 mL of DMEM +/+ and 72 hours post-transduction, cell media was aspirated, and cells were fixed with 4% paraformaldehyde at room temperature for 20 minutes, after which they were washed three times with PBS and stored at 4°C until further processing.

3.2.6 Immunofluorescence

Immunofluorescence staining protocol is entirely performed at room temperature. Cells grown in glass coverslips were always washed three times with 1x PBS before being fixated with 4%

paraformaldehyde for 20 minutes, permeabilized with 0.2% Triton X-100 for 10 minutes and blocked with 1% BSA for 10 minutes. Cells were then stained with 20 µL of primary antibody for 1 hour, then with 20 µL of the secondary antibody for the same time, both in a humid environment, and finally with 20 µL of Hoechst dye for 3 minutes, always protected from the light. After each of these staining steps, cells were washed three times with 1x PBS. Lastly, coverslips were washed in ddH_2O, mounted in glass slides with Mowiol mounting medium and dried overnight. Glass slides were then stored at 4°C.

Fixed cells were observed with a Zeiss AxioImager Z1 upright widefield or a Nikon Eclipse Ts2 inverted fluorescence microscope, equipped with the appropriate filter sets. Confocal images were acquired with a Zeiss LSM 880 with Airyscan or a Leica CSLM TCS sp5 II microscope, using the Plan-Apochromat 63x/1.40 oil objective, and the lasers Diode 405 nm, 488 nm Argon-ion laser, DPSS 561 nm laser and HeNe 633 nm were used for imaging of samples stained with Hoechst dye, Alexa Fluor 488 dye or expressing EGFP, TRITC dye or expressing tdTomato, and expressing iRFP670, respectively.

IV. RESULTS

4.1 Results

4.1.1 Development of a plasmid-based strategy to visualize peroxisomes and lipid droplets by fluorescence microscopy

One of the current projects in our laboratory involves the study of the interplay between peroxisomes and LDs during HCV infection. To be able to simultaneously analyse the organelles' intracellular localization, morphology, and motility in the context of viral infections, we aimed to develop a system that would allow the direct visualisation of both LDs and peroxisomes by life cell imaging. This can be achieved by expressing fluorescent proteins that target these organelles by being tagged with specific organelle-specific localization signals.

We aimed to create a single plasmid system that leads to the expression of two different fluorescent proteins targeting both peroxisomes and LDs. To accomplish this, we made use of the MXS-chaining method, which was designed to allow the assembly of constructs for imaging analysis in mammalian cell culture systems (Sladitschek and Neveu, 2015). This method offers a library of cassettes that can be tailored to develop a specific construct. The MXS-chaining vector backbone is based on pUC19 with resistance to ampicillin and on pMB1 replicon to achieve high copy replication of the plasmid with a multiple cloning site that includes MluI-XhoI-SalI restriction sites. Each individual building block is flanked by MluI and XhoI at the 5' end and by SalI at the 3' end, which allows that, upon a double digestion with MluI and SalI of one individual block, it can be inserted into a vector digested with both MluI and XhoI. The SalI and the XhoI overhangs are compatible, producing a translatable scar sequence that cannot be further recognized by either of the employed enzymes and that is translated into valine-glutamic acid (Sladitschek and Neveu, 2015).

Before creating the double plasmid expressing both the peroxisome- and LD-localized proteins, we constructed individual plasmids expressing the fusion proteins targeted to each of these organelles. As described before, peroxisomal matrix proteins are imported into peroxisomes due to the recognition of specific amino acid sequences, PTS1 or PTS2, by PEX5 or PEX7, respectively. For the purpose of this project, and in order to be able to obtain different fluorescent protein combinations which would simplify and strengthen our future analyses, we aimed to create two plasmids expressing the fluorescent proteins iRFP670 and EGFP tagged with the PTS1 (or SKL, serine-lysine-leucine) sequence (Miura *et al.*, 1992) (the MXS42 and MXS43 plasmids, respectively) (**Table 12**) (see section 3.2.1.2).

The mechanisms behind protein targeting to LDs are still unclear, and no targeting sequences have been described so far. Nevertheless, several studies have reported that ACSL3 specifically localizes at LDs in mammalian cells. This protein belongs to the ACSL family, which comprises five different mammalian isoforms and catalyses FA synthesis from substrates such as LCFA, ATP, and CoA (Fujimoto *et al.*, 2007). To construct a plasmid that targets the fluorescent protein tdTomato to LDs (MXS47), we used the sequence encoding for the first 135 amino acids of ACSL3 as a targeting sequence (Poppelreuther *et al.*, 2012) (**Table 12**) (see section 3.2.1.3). In order to create the combined plasmids to allow simultaneous visualisation of peroxisomes and LDS (MXS48 and

MXS49) (**Table 12**), we devised a cloning strategy in which the fusion fluorescent protein, with specific targeting signals to localize at each of the organelles, where inserted in MXS-chaining vectors. For the individual and the double plasmids, specific promoters and terminators were used (see section 3.2.1.4).

Table 12. **Summary list of the transcriptable MXS plasmids constructed**

MXS42	MXS EF1α HTLV::iRFP-PTS1 bGHpA
MXS43	MXS EF1α HTLV::EGFP-PTS1 bGHpA
MXS47	MXS EF1α HTLV::ACSL-tdTomato bGHpA
MXS48	MXS EF1α HTLV::ACSL-tdTomato bGHpA_EF1α HTLV::EGFP-PTS1 bGHpA
MXS49	MXS EF1α HTLV::ACSL-tdTomato bGHpA_EF1α HTLV::iRFP-PTS1 bGHpA

To enhance the expression of the inserted sequence, we added the composite promoter EF1α HTLV at its 5' end, which comprises the human Elongation Factor-1α (EF1α) core promoter, the R segment and part of the U5 sequence (R-U5') of the Human T-Cell Leukemia Virus (HTLV) Type 1 Long Terminal Repeat. This enhanced promoter presents stronger activity, yields longer expression of a transgene *in vivo* and promotes RNA stability (Poulain *et al.*, 2017). Moreover, at the 3' end, a bGHpA terminator, supplied in the MXS-chaining kit, was also added. bGHpA is a bovine growth hormone transcription terminator/polyadenylation sequence that, as a terminator, defines the end of the transgene transcription, inducing the process of releasing of newly synthesized RNAs from the transcription machinery (Goodwin and Rottman, 1992). While several other terminators with higher activity could be used, bGHpA terminator is better suited when lentivirus production is intended (Zufferey *et al.*, 1999; Wodrich, Schambach and Kräusslich, 2000; Hager *et al.*, 2008). With this, five different MXS constructs were developed (**Table 12**).

To verify the subcellular localization of the designed MXS plasmids, Huh7 cells were transfected with each of the 5 constructed MXS plasmids by using PEI or FuGENE HD transfection reagents (see section 3.2.3). After 24 or 48 hours, respectively, of incubation with the transfection mix, cells were subjected to immunofluorescence analysis with an antibody against the peroxisomal marker protein PMP70 or with BODIPY, a nonpolar lipid tracer that stains LDs. Confocal microscopy analysis showed a perfect colocalization between the overexpressed iRFP-PTS1 (MXS42) or EGFP-PTS1 (MXS43) and the peroxisomal protein PMP70 (**Figure 18A**). ACSL-tdTomato (MXS47) also clearly colocalized with LDs stained with BODIPY (**Figure 18B**). MXS48 and MXS49 overexpression, as expected, led to a peroxisome and LD staining pattern similar to the ones observed with MXS42, MXS43 and MXS47 overexpression (**Figure 18C,D**). Interestingly, when LDs were big enough, ACSL-tdTomato could be spotted at the LD membranes, surrounding the lumen where BODIPY was located (**Figure 18B,D**).

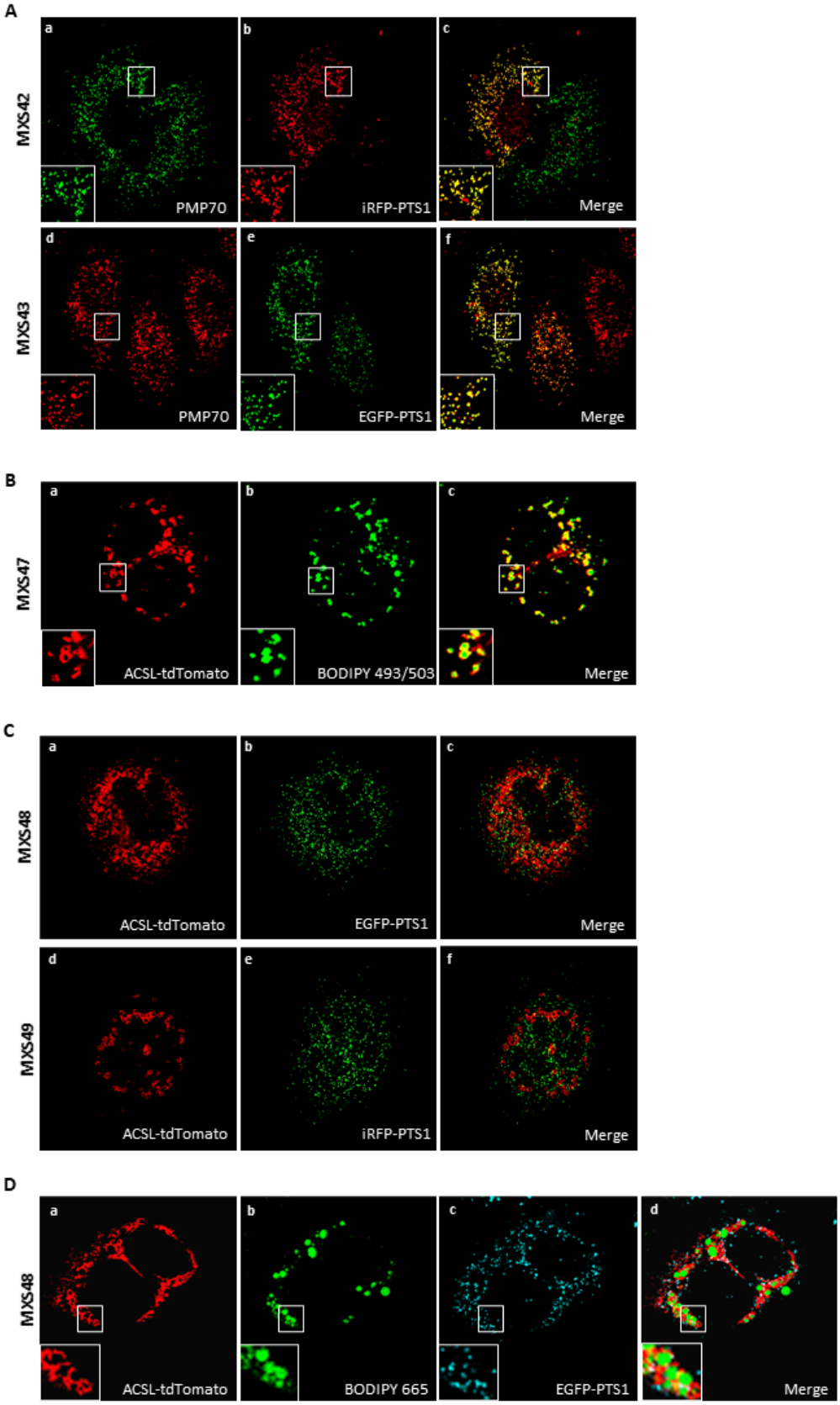

Figure 18. **Subcellular localization of the expressed fluorescent proteins from the developed MXS constructs. (A) iRFP-PTS1 and EGFP-PTS1, expressed from MXS42 and MXS43, respectively, colocalize with**

peroxisomes. Antibody against the peroxisomal protein PMP70 was used. (a-c) Huh7 cells transfected with MXS42. (a) PMP70, (b) iRFP670, (c) merge of a) and b); (d-f) Huh7 cells transfected with MXS43. (d) anti-PMP70, (e) EGFP, (f) merge of d) and e). **(B) ACSL-tdTomato expressed by MXS47 colocalize with LDs**. (a-d) Huh7 cells transfected with MXS47. BODIPY was used to stain LDs. (a) tdTomato, (b) BODIPY 493/503, (c) merge of a) and b). **(C) ACSL-tdTomato and EGFP-PTS1 or iRFP-PTS1 expressed by MXS48 or MXS49, respectively, show a peroxisomal and LD-specific staining pattern.** (a-c) Huh7 cells transfected with MXS48. (a) tdTomato, (b) EGFP, (c) merge of a) and b). (d-f) Huh7 cells transfected with MXS49. (d) tdTomato, (e) iRFP670, (f) merge of d) and e). **(D) MXS48 overexpression in Huh7 cells stained with BODIPY.** (a) tdTomato, (b) BODIPY665, (c) EGFP, (d) merge image of a), b) and c).

During confocal microscopy analysis of transfected cells, we observed that cells overexpressing MXS42 or MXS43 presented different staining patterns. Besides the normal peroxisomal staining in a dot-like pattern, some transfected cells also presented a strong cytosolic signal **(Figure 19).** While different transfection reagents were tested, in all conditions both patterns were observed. These differences were also observed in cells transfected with the MXS plasmids containing the combined reporter cassettes (data not shown).

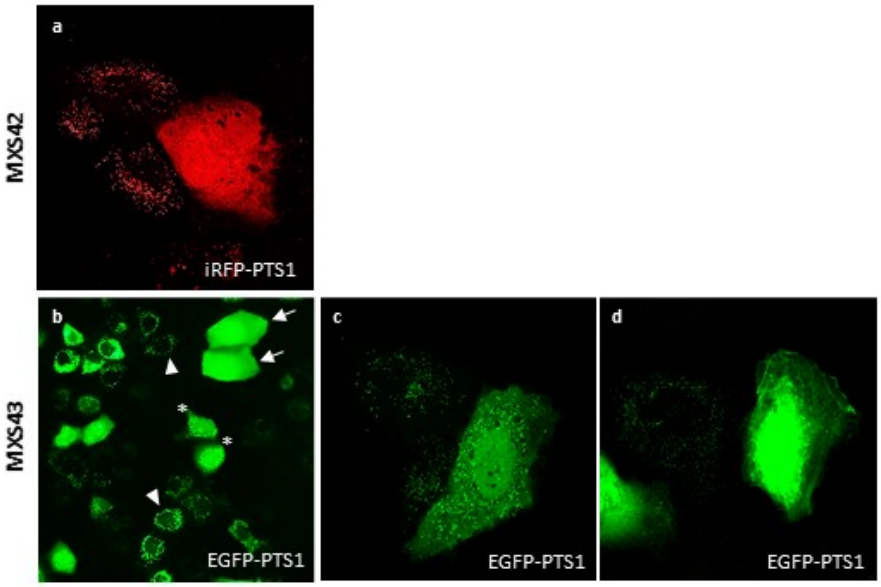

***Figure 19*. Different phenotypes of fluorescent fusion proteins that localize at peroxisomes.** (a) MXS42 transfected Huh7 cells using PEI, expressing iRFP-PTS1. (b-d) Huh7 cells transfected with MXS43 using FuGENE HD (b) and PEI (c-d) expressing EGFP-PTS1. (b) three distinct phenotypes of EGFP-PTS1 expression: specific dot-like pattern (arrow tops), cytosolic staining (complete arrows), and mix of both (asterisks).

A detailed analysis of ACSL-tdTomato overexpression also revealed different LD staining phenotypes. While in some cells LDs were dispersed through the cytosol (**Figure 20a**), in some others bigger LDs agglomerated in the perinuclear region (**Figure 20b**), and a reticular staining was also often observed (**Figure 20c**). These differences were also observed in cells transfected with the MXS plasmids containing the combined reporter cassettes (data not shown).

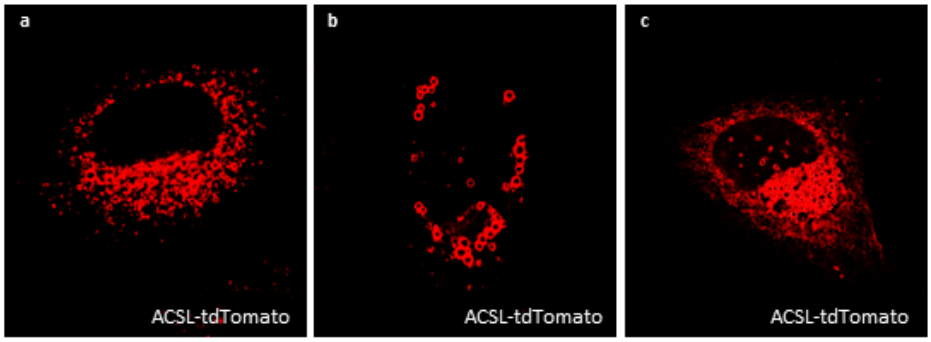

Figure 20. **Different phenotypes observed for ACSL-tdTomato fusion protein.** (a-c) Huh7 cells transfected with MXS47 overexpressing the fluorescent fusion protein ACSL-tdTomato. (a) LDs dispersed through the cytosol. (b) Bigger LDs agglomerated in the perinuclear region. (c) LD and reticular staining.

4.1.2 Development of a lentiviral system to visualize peroxisomes and lipid droplets by fluorescence microscopy

One of the goals of this project was to generate Huh7 stable cell lines that express the fluorescent fusion proteins targeted to peroxisomes and LDs to allow organelle interplay and morphology analyses through the course of HCV infection. To that end, the reporter cassettes from the five MXS plasmids were inserted in a lentiviral vector backbone (see section 3.2.1.5) **(Table 13)**.

Table 13. **Summary list of the constructed pSicoR-MS1 lentiviral plasmids**

HH622	pSicoR-MS1 EF1α HTLV::iRFP-PTS1 bGHpA
HH623	pSicoR-MS1 EF1α HTLV::EGFP-PTS1 bGHpA
HH625	pSicoR-MS1 EF1α HTLV::ACSL Lipotracker-tdTomato bGHpA
HH626	pSicoR-MS1 EF1α HTLV::ACSL Lipotracker-tdTomato bGHpA_EF1α HTLV::iRFP-PTS1 bGHpA
HH627	pSicoR-MS1 EF1α HTLV::ACSL Lipotracker-tdTomato bGHpA_EF1α HTLV::EGFP-PTS1 bGHpA

Lentiviruses can be used either for gene silencing by delivery of shRNA or CRISPR/Cas9 or for stable overexpression of a gene of interest (Tandon *et al.*, 2018). These are widely used for efficient transfer of large transgene fragments and its stable integration into host genome, which ensures long-term expression essential for the generation of stable cell lines (Naldini *et al.*, 1996; Walther and Stein, 2000; Tandon *et al.*, 2018). Furthermore, they infect both dividing and non-dividing cells without generating immune response (Suzuki and Suzuki, 2011).

We have used three HIV-1-based lentiviral vectors - transfer, packaging, and envelope vectors- to produce the required lentiviral particles. The pCMV-ΔR9 packaging vector preserves several original genes from the virus, encoding the human cytomegalovirus (hCMV) immediate early promoter as well, which drives the expression of the viral proteins. However, this vector is replication-defective since some sequences have been deleted (Naldini *et al.*, 1996). On the other hand, the pCMV VSV.G envelope vector encodes the vesicular stomatitis virus (VSV) G envelope protein, which, due to its wide infectivity, improves lentivirus tropism (Burns *et al.*, 1993; Naldini

et al., 1996; Walther and Stein, 2000; Suzuki and Suzuki, 2011). The pSicoR transfer vectors (**Table 13**), besides the long terminal repeat (LTR) sequences flanking the gene of interest that are required for gene integration into the host genome, also contain a *psi* packaging signal, a part of the *env* gene containing the rev response element (RRE) and an internal promoter (EF1α-HTLV) (Walther and Stein, 2000; Suzuki and Suzuki, 2011). For safety reasons, transfer vectors are replication-incompetent.

To verify the subcellular localization of the fluorescent fusion proteins expressed by the produced lentiviruses (see section 3.2.4), Huh7 cells were transduced with the lentiviruses and, 72 hours after, cells were processed for confocal microscopy analysis. As expected, both HH622 and HH623 transduced cells, which express iRFP-PTS1 and EGFP-PTS1, respectively, showed a clear peroxisomal staining (**Figure 21A (a,b)**). In HH625 transduced cells, however, ASCL-tdTomato was found concentrated in aggregated structures and no LD staining was observed (**Figure 21A (c)**). Similarly, HH626 and HH627 transduced cells, which express both fusion fluorescent proteins targeting peroxisomes and LDs, also presented these aggregates with only some light peroxisomal staining (**Figure 21B,C**).

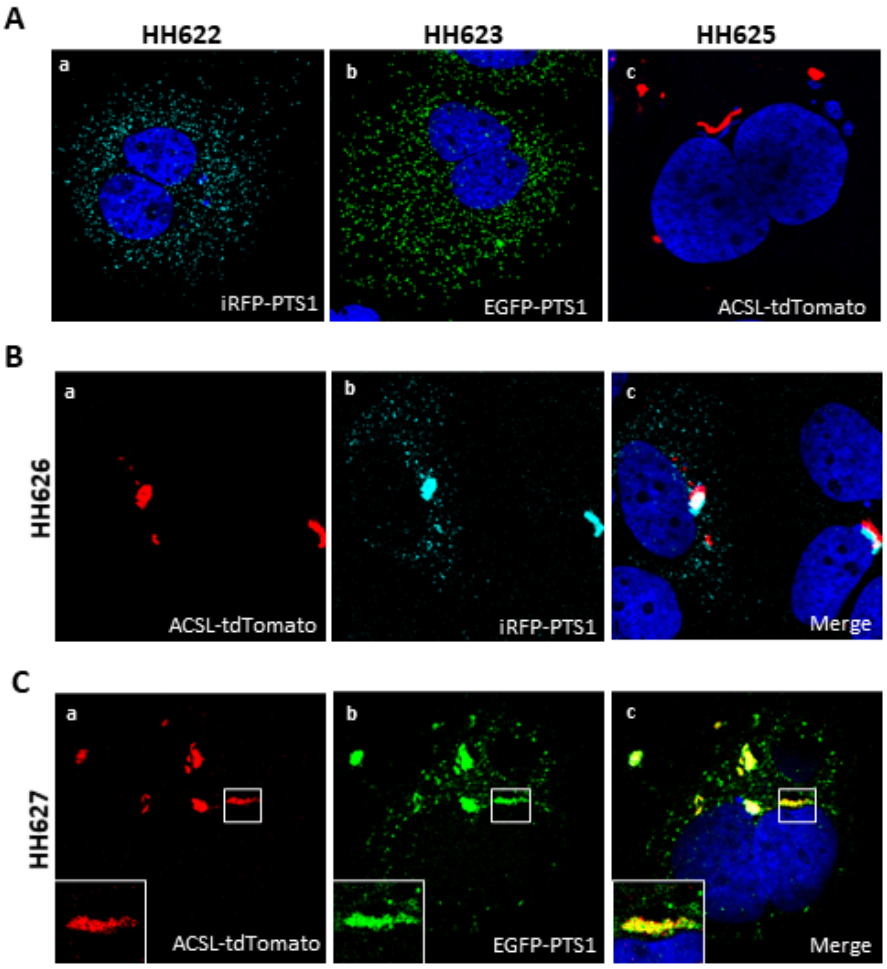

Figure 21. **Subcellular localization of fluorescent proteins expressed from the developed lentiviral constructs. (A) Huh7 cells transduced with the single fluorescent fusion protein lentiviruses.** (a) iRFP-PTS1 expressed by HH622 transduced Huh7 cells. (b) EGFP-PTS1 expressed by HH623 transduced Huh7 cells. (c)

ACSL-tdTomato expressed by HH625 transduced Huh7 cells. **(B) iRFP-PTS1 and ACSL-tdTomato expressed by HH626 transduced Huh7 cells**. (a) ACSL-tdTomato. (b) iRFP670-PTS1. (c) merge of a) and b). **(C) EGFP-PTS1 and ACSL-tdTomato expressed by HH626 transduced Huh7 cells**. (a) ACSL-tdTomato. (b) EGFP-PTS1. (c) merge of a) and b). **(A-C)** Nuclei were stained with Hoechst.

4.1.3 Peroxisomes' subcellular localization and morphology upon overexpression of HCV core protein

As previously described, during HCV infection, the viral core protein targets both the ER and LDs in hepatic and non-hepatic cells, independently of the HCV genotype (Barba *et al.*, 1997; Okamoto *et al.*, 2004; Piodi *et al.*, 2008; Boson *et al.*, 2011; Qiang and Jhaveri, 2012; Galli, Ramirez and Bukh, 2021). Moreover, it is well established that the progressive coating of LD surface by core is associated with LD agglomeration around the nucleus, a critical step for viral assembly and release (Boulant *et al.*, 2008). However, current understanding of the role of peroxisomes in HCV infection is still scarce.

Contrarily to the extensively studied role of HCV core protein in the subcellular redistribution of LDs, its effect on peroxisome morphology and intracellular organization has not yet been explored. As peroxisomes play an important role on the cellular lipid metabolism and have been reported to interact with LDs, we aimed to investigate peroxisomal localization and morphology features upon HCV core overexpression, using the tools developed and described in the previous sections. To that end, Huh7 cells were transfected with a plasmid expressing the HCV core protein, HCV-2a-Core-3XFLAG (provided by Dr. Eva Herker, Institute of Virology, Marburg – see section 3.1.3). Twenty-four hours after, cells were processed for immunofluorescence analysis. As expected, HCV core protein presented both an LD and reticular staining patterns (**Figure 22**). Our preliminary data indicated that, while some colocalization between peroxisomes and LDs could be observed, no significant peroxisome morphological alterations or cellular redistribution could be clearly identified.

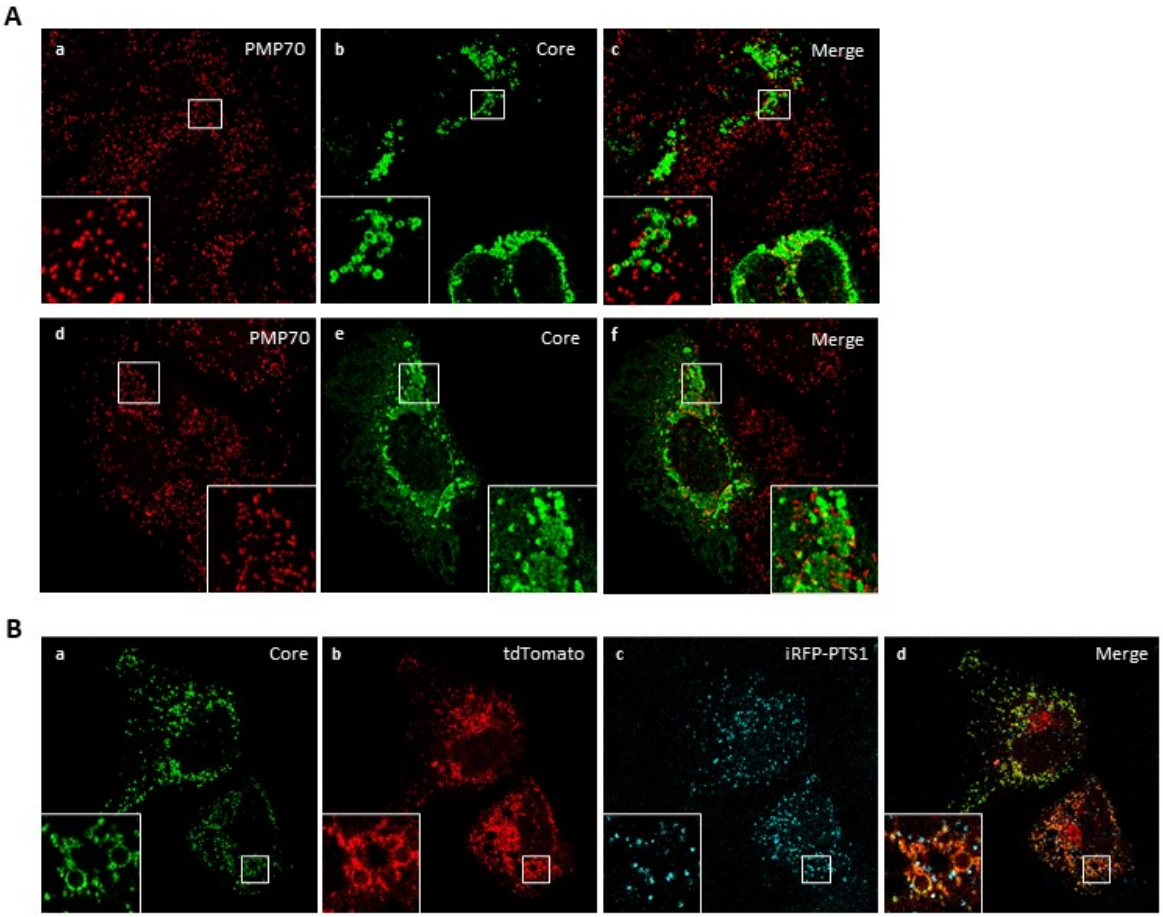

Figure 22. **Peroxisomes' subcellular localization and morphology upon overexpression of HCV core protein. (A)** (a-f) Huh7 cells transfected with the HCV-2a-Core-3XFLAG plasmid. (a, d) PMP70 staining using antibodies anti-PMP70, (b, e) Core stained with the antibody anti-Flag, (c, f) merge images of a) and b), and d) and e), respectively. **(B)** (a-d) Huh7 cells co-transfected with HCV 2a Core-3XFLAG and MXS49. (a) Core stained with the antibody anti-Flag, (b) ACSL-tdTomato, (c) iRFP670-PTS1, and (d) merge of a-c.

V. DISCUSSION

5.1 Discussion

HCV replication and dissemination is extremely dependent on the host cell's lipid metabolism. This virus takes advantage of cellular organelles such as LDs and ER, to build specialized compartments for replication and assembly and for the release of its new virions. Nevertheless, information on the role of peroxisomes in HCV infection is still scarce.

One of the projects currently being developed in our laboratory involves the study of peroxisome morphology, subcellular distribution, and interaction with LDs throughout HCV infection. To accomplish this, specific tools had to be developed to allow the monitoring of both organelles by live cell imaging.

The MXS-chaining method was used to produce not only single fluorescent fusion proteins-encoding plasmids tagged with organelle localization signals, but also plasmids that combine both peroxisomes- and LD-targeted fluorescent fusion proteins. The PTS1 sequence was used to localize iRFP or EGFP at peroxisomes, and the N-terminal of ACSL3 sequence was used to target tdTomato to LDs. However, besides localizing at peroxisomes, iRFP and EGFP staining was also detected at the cytosol. This occurs when cellular expression is extremely high resulting in a blockage of the peroxisomal import system, which had been already described (Rosenthal *et al.*, 2020). Expression of ACSL-tdTomato always presented a specific LD pattern but different LD phenotypes including different size and subcellular distribution. In basal conditions, LDs are mostly found dispersed throughout the cytoplasm. However, we observed a preferential redistribution of LDs at the perinuclear region in some cells, which could be related to the fluorescent fusion protein overexpression. Since ACSL3 enzyme, besides targeting to LDs, can also be found at ER, and selective permeabilization and *in silico* studies have shown that the N-terminal hydrophobic amino acids form an amphipathic helix restricted to the cytosolic leaflet of the ER membrane (Poppelreuther *et al.*, 2012), it may be suggested that, upon high levels of expression and accumulation at LD surface, the expressed ACSL-tdTomato could also be recruited to or retained in the ER associated with emerging LDs, leading to the observed LD staining that clues for LD relocation. One other possible explanation for the perinuclear phenotype is that the targeting of the overexpressed fusion protein to the LD surface may have an effect similar to the one observed with the targeting of HCV core protein to LDs which also affects the organelle's size and subcellular distribution to a preferential agglomeration around the nucleus.

To better study these organelles throughout HCV infection, we also aimed to produce cell lines stably expressing these fluorescent fusion proteins. To this end, lentiviral plasmids derived from the MXS constructs were created. Interestingly, iRFP-PTS1 and EGFP-PTS1 proteins' localization on transduced cells has significantly improved. Since lentiviruses stably integrate transgenes in the cells' genome, this not only ensures long-term expression, essential for the generation of stable cell lines, but also allows better regulation of transgenes expression (Page, Fusil and Cosset, 2020). Hence, the localization of peroxisome-targeted fluorescent proteins showed to be more specific using the lentiviral system. On the contrary, LD-targeted fluorescent proteins expressed with lentiviral system HH625 did not localize at LDs but produced big agglomerates on transduced cells. This was also observed in iRFP-PTS1 and EGFP-PTS1 expressed by lentivirus containing the plasmids with combined reporter cassettes, HH626 and HH627. This organelle aggregation may be

due to the higher time of incubation that could aggravate the effect of the expressed fluorescence protein in LDs distribution which could also explained the presence of the same aggregates in the peroxisomal fluorescence channels upon transduction with lentiviruses expressing both fusion proteins, possibly due to interactions between the two different fluorescent proteins.

We furthermore co-expressed the peroxisome and LD-targeted fluorescent proteins with HCV core protein. Upon analysis of co-transfected cells, it was possible to observe colocalization between peroxisomes, HCV core protein, and LDs, although no significant peroxisome morphological alterations or cellular redistribution were observed. Nevertheless, further studies to analyse peroxisomal subcellular localization as well as morphology are required. Image and quantitative analyses should be performed in the future to better evaluate the effect of HCV core protein on peroxisomes.

VI. FINAL REMARKS

6.1 Conclusions

Peroxisomes are critical platforms for the cellular lipid metabolism and several of their functions depend on their interplay with other organelles, such as LDs. While it is already known that HCV is highly dependent of host cell's lipid metabolism, and modulates LDs for efficient viral replication and dissemination, the role of peroxisomes in HCV infection is still unknown.

With this project we were able to successfully develop plasmid- and lentivirus-based systems to analyse peroxisome dynamics by fluorescence microscopy and life cell imaging, respectively. These tools are crucial for one of the main projects being currently developed in our laboratory: the study of the importance of peroxisomes for HCV life cycle.

Our preliminary results on the overexpression of the peroxisome-localizing fluorescent fusion protein with HCV core, revealed that this viral protein may not affect peroxisome morphology or subcellular distribution. However, further studies are required to perform quantitative image analysis of peroxisomes size, shape, and cellular localization, not only upon HCV core protein overexpression, but also during HCV infection. Additionally, besides analysing this organelle by microscopy, it would be required to analyse peroxisomal enzymes and lipid species throughout infection. Moreover, while we are now able to study peroxisomes and their interplay with LDs using the developed constructs, and even to produce stable cell lines with fluorescent peroxisomes, it will be necessary to reanalyse the lentivirus construct expressing LD-targeting fluorescent fusion protein to eliminate the issue of organelle aggregation that we have observed.

VII. REFERENCES

7.1 References

Anjum, S. *et al.* (2013) 'Sequence and structural analysis of 3' untranslated region of hepatitis C virus, genotype 3a, from Pakistani isolates', *Hepatitis Monthly*, 13(5), pp. 1–7. doi: 10.5812/hepatmon.8390.

Argyriou, C., D'Agostino, M. D. and Braverman, N. (2016) 'Peroxisome biogenesis disorders', *Translational Science of Rare Diseases*, 1(2), pp. 111–144. doi: 10.3233/trd-160003.

Ashraf, N. U. and Sheikh, T. A. (2015) 'Endoplasmic reticulum stress and Oxidative stress in the pathogenesis of Non-alcoholic fatty liver disease', *Free Radical Research*, 49(12), pp. 1405–1418. doi: 10.3109/10715762.2015.1078461.

Aubourg, P. and Wanders, R. (2013) *Peroxisomal disorders*. 1st edn, *Handbook of Clinical Neurology*. 1st edn. Elsevier B.V. doi: 10.1016/B978-0-444-59565-2.00028-9.

Aziz, A. A. (2018) 'Hepatitis C Virus: Virology and Genotypes', in *Hepatitis C in Developing Countries: Current and Future Challenges*. Elsevier Inc., pp. 3–11. doi: 10.1016/B978-0-12-803233-6.00001-1.

Baker, D. J. *et al.* (2011) 'Clearance of p16 Ink4a-positive senescent cells delays ageing-associated disorders', *Nature*, 479(7372), pp. 232–236. doi: 10.1038/nature10600.

Barba, G. *et al.* (1997) 'Hepatitis C virus core protein shows a cytoplasmic localization and associates to cellular lipid storage droplets', *Proceedings of the National Academy of Sciences of the United States of America*, 94(4), pp. 1200–1205. doi: 10.1073/pnas.94.4.1200.

Barbosa, A. D. *et al.* (2015) 'Lipid partitioning at the nuclear envelope controls membrane biogenesis', *Molecular Biology of the Cell*, 26(20), pp. 3641–3657. doi: 10.1091/mbc.E15-03-0173.

Barøy, T. *et al.* (2015) 'A novel type of rhizomelic chondrodysplasia punctata, RCDP5, is caused by loss of the PEX5 long isoform', *Human Molecular Genetics*, 24(20), pp. 5845–5854. doi: 10.1093/hmg/ddv305.

Barros-Barbosa, A. *et al.* (2019) 'The intrinsically disordered nature of the peroxisomal protein translocation machinery', *FEBS Journal*, 286(1), pp. 24–38. doi: 10.1111/febs.14704.

Bartenschlager, R. *et al.* (2011) 'Assembly of infectious hepatitis C virus particles', *Trends in Microbiology*, 19(2), pp. 95–103. doi: 10.1016/j.tim.2010.11.005.

Bartenschlager, R. and Lohmann, V. (2000) 'Replication of Hepatitis C Virus', *Journal of General Virology*, 81, pp. 1631–1648. doi: 10.1016/B978-1-4377-0881-3.00007-3.

Bartz, R. *et al.* (2007) 'Lipidomics reveals that adiposomes store ether lipids and mediate phospholipid traffic', *Journal of Lipid Research*, 48(4), pp. 837–847. doi: 10.1194/jlr.M600413-JLR200.

Benga, W. J. A. *et al.* (2010) 'Apolipoprotein E interacts with hepatitis C virus nonstructural protein 5A and

determines assembly of infectious particles', *Hepatology*, 51(1), pp. 43–53. doi: 10.1002/hep.23278.

Bensaad, K. *et al.* (2014) 'Fatty acid uptake and lipid storage induced by HIF-1α contribute to cell growth and survival after hypoxia-reoxygenation', *Cell Reports*, 9(1), pp. 349–365. doi: 10.1016/j.celrep.2014.08.056.

Berendse, K. *et al.* (2016) 'Cholic acid therapy in Zellweger spectrum disorders', *Journal of Inherited Metabolic Disease*, 39(6), pp. 859–868. doi: 10.1007/s10545-016-9962-9.

Bickel, P. E., Tansey, J. T. and Welte, M. A. (2009) 'PAT proteins, an ancient family of lipid droplet proteins that regulate cellular lipid stores', *Biochim Biophys Acta*, 1791(6), pp. 419–440. doi: 10.1016/j.bbalip.2009.04.002.PAT.

Binns, D. *et al.* (2006) 'An intimate collaboration between peroxisomes and lipid bodies', *Journal of Cell Biology*, 173(5), pp. 719–731. doi: 10.1083/jcb.200511125.

Blanchette-Mackie, E. J. *et al.* (1995) 'Perilipin is located on the surface layer of intracellular lipid droplets in adipocytes', *Journal of Lipid Research*, 36(6), pp. 1211–1226. doi: 10.1016/s0022-2275(20)41129-0.

Blaner, W. S. *et al.* (2016) *Vitamin A absorption, storage and mobilization*, *Sub-Cellular Biochemistry*. doi: 10.1007/978-94-024-0945-1_4.

Boson, B. *et al.* (2011) 'A concerted action of hepatitis C virus P7 and nonstructural protein 2 regulates core localization at the endoplasmic reticulum and virus assembly', *PLoS Pathogens*, 7(7). doi: 10.1371/journal.ppat.1002144.

Boulant, S. *et al.* (2005) 'Hepatitis C Virus Core Protein Is a Dimeric Alpha-Helical Protein Exhibiting Membrane Protein Features', *Journal of Virology*, 79(17), pp. 11353–11365. doi: 10.1128/jvi.79.17.11353-11365.2005.

Boulant, S. *et al.* (2006) 'Structural determinants that target the hepatitis C virus core protein to lipid droplets', *Journal of Biological Chemistry*, 281(31), pp. 22236–22247. doi: 10.1074/jbc.M601031200.

Boulant, S. *et al.* (2008) 'Hepatitis C virus core protein induces lipid droplet redistribution in a microtubule- and dynein-dependent manner', *Traffic*, 9(8), pp. 1268–1282. doi: 10.1111/j.1600-0854.2008.00767.x.

Bozza, P. T. *et al.* (2011) 'Lipid body function in eicosanoid synthesis: An update', *Prostaglandins Leukotrienes and Essential Fatty Acids*, 85(5), pp. 205–213. doi: 10.1016/j.plefa.2011.04.020.

Bräutigam, C. *et al.* (1996) 'Plasmalogen phospholipids in plasma lipoproteins of normolipidemic donors and patients with hypercholesterolemia treated by LDL apheresis', *Atherosclerosis*, 119(1), pp. 77–88. doi: 10.1016/0021-9150(95)05632-7.

Braverman, N. E. and Moser, A. B. (2012) 'Functions of plasmalogen lipids in health and disease', *Biochimica*

et Biophysica Acta - Molecular Basis of Disease, 1822(9), pp. 1442–1452. doi: 10.1016/j.bbadis.2012.05.008.

Brown, D. A. (2001) 'Lipid droplets: Proteins floating on a pool of fat', *Current Biology*, 11(11), pp. 446–449. doi: 10.1016/S0960-9822(01)00257-3.

Burns, J. C. *et al.* (1993) 'Vesicular stomatitis virus G glycoprotein pseudotyped retroviral vectors: concentration to very high titer and efficient gene transfer into mammalian and nonmammalian cells', *Proc. Natl. Acad. Sci. USA*, 90, pp. 8033–8037.

Camus, G. *et al.* (2013) 'Diacylglycerol acyltransferase-1 localizes hepatitis C virus NS5A protein to lipid droplets and enhances NS5A interaction with the viral capsid core', *Journal of Biological Chemistry*, 288(14), pp. 9915–9923. doi: 10.1074/jbc.M112.434910.

Carvalho, F. A. *et al.* (2012) 'Dengue Virus Capsid Protein Binding to Hepatic Lipid Droplets (LD) Is Potassium Ion Dependent and Is Mediated by LD Surface Proteins', *Journal of Virology*, 86(4), pp. 2096–2108. doi: 10.1128/jvi.06796-11.

Catanese, M. T. *et al.* (2013) 'Ultrastructural analysis of hepatitis C virus particles', *Proceedings of the National Academy of Sciences of the United States of America*, 110(23), pp. 9505–9510. doi: 10.1073/pnas.1307527110.

Chang, C. L. *et al.* (2019) 'Spastin tethers lipid droplets to peroxisomes and directs fatty acid trafficking through ESCRT-III', *Journal of Cell Biology*, 218(8), pp. 2583–2599. doi: 10.1083/jcb.201902061.

Chang, W. *et al.* (2015) 'Trapping toxins within lipid droplets is a resistance mechanism in fungi', *Scientific Reports*, 5(44), pp. 1–11. doi: 10.1038/srep15133.

Cheung, W. *et al.* (2010) 'Rotaviruses Associate with Cellular Lipid Droplet Components To Replicate in Viroplasms, and Compounds Disrupting or Blocking Lipid Droplets Inhibit Viroplasm Formation and Viral Replication', *Journal of Virology*, 84(13), pp. 6782–6798. doi: 10.1128/jvi.01757-09.

Chevaliez, S. and Pawlotsky, J. (2006) 'Chapter 1: HCV Genome and Life Cycle', in *Hepatitis C viruses: genomes and molecular biology*, pp. 5–47.

Chitraju, C. *et al.* (2017) 'Triglyceride Synthesis by DGAT1 Protects Adipocytes from Lipid-Induced ER Stress during Lipolysis', *Cell Metabolism*, 26(2), pp. 407-418.e3. doi: 10.1016/j.cmet.2017.07.012.

Choo, Q.-L. *et al.* (1989) 'Isolation of a cDNA clone derived from a blood-borne non-A, non-B viral hepatitis genome', *Science*, 244(4902), pp. 359–362. Available at: www.sciencemag.org.

Christianson, J. C. and Ye, Y. (2014) 'Cleaning up in the endoplasmic reticulum: Ubiquitin in charge', *Nature Structural and Molecular Biology*, 21(4), pp. 325–335. doi: 10.1038/nsmb.2793.

Cocquerel, L., Voisset, C. and Dubuisson, J. (2006) 'Hepatitis C virus entry: Potential receptors and their

biological functions', *Journal of General Virology*, 87(5), pp. 1075–1084. doi: 10.1099/vir.0.81646-0.

Cohen, S. (2018) *Lipid Droplets as Organelles*. 1st edn, *International Review of Cell and Molecular Biology*. 1st edn. Elsevier Inc. doi: 10.1016/bs.ircmb.2017.12.007.

Coller, K. E. *et al.* (2009) 'RNA interference and single particle tracking analysis of hepatitis C virus endocytosis', *PLoS Pathogens*, 5(12). doi: 10.1371/journal.ppat.1000702.

Coller, K. E. *et al.* (2012) 'Molecular determinants and dynamics of hepatitis C virus secretion', *PLoS Pathogens*, 8(1). doi: 10.1371/journal.ppat.1002466.

Counihan, N. A., Rawlinson, S. M. and Lindenbach, B. D. (2011) 'Trafficking of hepatitis C virus core protein during virus particle assembly', *PLoS Pathogens*, 7(10). doi: 10.1371/journal.ppat.1002302.

Cun, W., Jiang, J. and Luo, G. (2010) 'The C-Terminal α-Helix Domain of Apolipoprotein E Is Required for Interaction with Nonstructural Protein 5A and Assembly of Hepatitis C Virus', *Journal of Virology*, 84(21), pp. 11532–11541. doi: 10.1128/jvi.01021-10.

Czaja, M. J. (2016) 'Function of Autophagy in Nonalcoholic Fatty Liver Disease', *Dig Dis Sci.*, 61(5), pp. 1304–1313. doi: 10.1007/s10620-015-4025-x.Function.

Deosaran, E. *et al.* (2013) 'NBR1 acts as an autophagy receptor for peroxisomes', *Journal of Cell Science*, 126(4), pp. 939–952. doi: 10.1242/jcs.114819.

Dichlberger, A. *et al.* (2011) 'Lipid body formation during maturation of human mast cells', *Journal of Lipid Research*, 52(12), pp. 2198–2208. doi: 10.1194/jlr.M019737.

Dichlberger, A. *et al.* (2014) 'Adipose triglyceride lipase regulates eicosanoid production in activated human mast cells', *Journal of Lipid Research*, 55(12), pp. 2471–2478. doi: 10.1194/jlr.M048553.

Dixit, E. *et al.* (2010) 'Peroxisomes Are Signaling Platforms for Antiviral Innate Immunity', *Cell*, 141(4), pp. 668–681. doi: 10.1016/j.cell.2010.04.018.

Dolganiuc, A. *et al.* (2012) 'Autophagy in Alcohol-Induced Liver Diseases', *Alcoholism: Clinical and Experimental Research*, 36(8), pp. 1301–1308. doi: 10.1111/j.1530-0277.2012.01742.x.

Dustin, L. B. *et al.* (2016) 'Hepatitis C virus: life cycle in cells, infection and host response, and analysis of molecular markers influencing the outcome of infection and response to therapy', *Clinical Microbiology and Infection*, 22(10), pp. 826–832. doi: 10.1016/j.cmi.2016.08.025.

De Duve, C. and Baudhuin, P. (1966) 'Peroxisomes (microbodies and related particles).', *Physiological reviews*, 46(2), pp. 323–357. doi: 10.1152/physrev.1966.46.2.323.

Eaton, S. (2002) 'Control of mitochondrial β-oxidation flux', *Progress in Lipid Research*, 41(3), pp. 197–239.

doi: 10.1016/S0163-7827(01)00024-8.

Egger, D. *et al.* (2002) 'Expression of Hepatitis C Virus Proteins Induces Distinct Membrane Alterations Including a Candidate Viral Replication Complex', *Journal of Virology*, 76(12), pp. 5974–5984. doi: 10.1128/jvi.76.12.5974-5984.2002.

Enomoto, N. and Sato, C. (1995) 'Hepatitis C virus quasispecies populations during chronic hepatitis C infection', *Trends in Microbiology*, 3(11), pp. 445–447. doi: 10.1016/S0966-842X(00)89000-9.

Farese, R. V. and Walther, T. C. (2009) 'Lipid Droplets Finally Get a Little R-E-S-P-E-C-T', *Cell*, 139(5), pp. 855–860. doi: 10.1016/j.cell.2009.11.005.

Ferreira, A. R. *et al.* (2016) 'Hepatitis C virus NS3-4A inhibits the peroxisomal MAVS-dependent antiviral signalling response', *Journal of Cellular and Molecular Medicine*, 20(4), pp. 750–757. doi: 10.1111/jcmm.12801.

Ferreira, A. R. *et al.* (2021) 'Emerging roles of peroxisomes in viral infections', *Trends in Cell Biology*, xx(xx), pp. 1–16. doi: 10.1016/j.tcb.2021.09.010.

Ferreira, A. R., Marques, M. and Ribeiro, D. (2019) 'Peroxisomes and innate immunity: Antiviral response and beyond', *International Journal of Molecular Sciences*, 20(15). doi: 10.3390/ijms20153795.

Filipe, A. and McLauchlan, J. (2015) 'Hepatitis C virus and lipid droplets: Finding a niche', *Trends in Molecular Medicine*, 21(1), pp. 34–42. doi: 10.1016/j.molmed.2014.11.003.

Fischer, J. *et al.* (2007) 'The gene encoding adipose triglyceride lipase (PNPLA2) is mutated in neutral lipid storage disease with myopathy', *Nature Genetics*, 39(1), pp. 28–30. doi: 10.1038/ng1951.

Francisco, T. *et al.* (2017) 'Protein transport into peroxisomes: Knowns and unknowns', *BioEssays*, 39(10), pp. 1–8. doi: 10.1002/bies.201700047.

Fransen, M. *et al.* (2012) 'Role of peroxisomes in ROS/RNS-metabolism: Implications for human disease', *Biochimica et Biophysica Acta - Molecular Basis of Disease*, 1822(9), pp. 1363–1373. doi: 10.1016/j.bbadis.2011.12.001.

Fujiki, Y. *et al.* (2020) 'Recent insights into peroxisome biogenesis and associated diseases', *Journal of Cell Science*, 133(9), pp. 1–9. doi: 10.1242/jcs.236943.

Fujimoto, T. *et al.* (2001) 'Caveolin-2 is targeted to lipid droplets, a new "membrane domain" in the cell', *Journal of Cell Biology*, 152(5), pp. 1079–1085. doi: 10.1083/jcb.152.5.1079.

Fujimoto, Y. *et al.* (2007) 'Involvement of ACSL in local synthesis of neutral lipids in cytoplasmic lipid droplets in human hepatocyte HuH7', *Journal of Lipid Research*, 48(6), pp. 1280–1292. doi: 10.1194/jlr.M700050-JLR200.

Galli, A., Ramirez, S. and Bukh, J. (2021) 'Lipid Droplets Accumulation during Hepatitis C Virus Infection in Cell-Culture Varies among Genotype 1–3 Strains and Does Not Correlate with Virus Replication', *Viruses*, 13(3), p. 289.

Gao, Q. and Goodman, J. M. (2015) 'The lipid droplet-a well-connected organelle', *Frontiers in Cell and Developmental Biology*, 3(AUG), pp. 1–12. doi: 10.3389/fcell.2015.00049.

Garg, A. and Agarwal, A. K. (2009) 'Lipodystrophies: Disorders of adipose tissue biology', *Biochim Biophys Acta*, 1791(6), pp. 507–513. doi: 10.1016/j.bbalip.2008.12.014.Lipodystrophies.

Gastaminza, P. *et al.* (2008) 'Cellular Determinants of Hepatitis C Virus Assembly, Maturation, Degradation, and Secretion', *Journal of Virology*, 82(5), pp. 2120–2129. doi: 10.1128/jvi.02053-07.

Gaunt, E. R. *et al.* (2013) 'Lipidome analysis of rotavirus-infected cells confirms the close interaction of lipid droplets with viroplasms', *Journal of General Virology*, 94(PART7), pp. 1576–1586. doi: 10.1099/vir.0.049635-0.

Gong, J. *et al.* (2011) 'Fsp27 promotes lipid droplet growth by lipid exchange and transfer at lipid droplet contact sites', *Journal of Cell Biology*, 195(6), pp. 953–963. doi: 10.1083/jcb.201104142.

Goodwin, E. C. and Rottman, F. M. (1992) 'The 3'-flanking sequence of the bovine growth hormone gene contains novel elements required for efficient and accurate polyadenylation', *Journal of Biological Chemistry*, 267(23), pp. 16330–16334. doi: 10.1016/s0021-9258(18)42005-4.

Gosert, R. *et al.* (2003) 'Identification of the Hepatitis C Virus RNA Replication Complex in Huh-7 Cells Harboring Subgenomic Replicons', *Journal of Virology*, 77(9), pp. 5487–5492. doi: 10.1128/jvi.77.9.5487-5492.2003.

Guimarães, C. P. *et al.* (2004) 'Mouse liver PMP70 and ALDP: Homomeric interactions prevail in vivo', *Biochimica et Biophysica Acta - Molecular Basis of Disease*, 1689(3), pp. 235–243. doi: 10.1016/j.bbadis.2004.04.001.

Guo, Y. *et al.* (2008) 'Functional genomic screen reveals genes involved in lipid-droplet formation and utilization', *Nature*, 453(7195), pp. 657–661. doi: 10.1038/nature06928.

Hager, S. *et al.* (2008) 'An internal polyadenylation signal substantially increases expression levels of lentivirus-delivered transgenes but has the potential to reduce viral titer in a promoter-dependent manner', *Human Gene Therapy*, 19(8), pp. 840–850. doi: 10.1089/hum.2007.165.

Hajra, A. K. . and Das, A. K. (1996) 'Lipid Biosynthesis in Peroxisomes', *ANNALS NEW YORK ACADEMY OF SCIENCES*, 804(1), pp. 129–141. Available at: http://dx.doi.org/10.1016/j.meatsci.2017.01.005%0Ahttps://linkinghub.elsevier.com/retrieve/pii/S0309174016301395.

Han, J. and Kaufman, R. J. (2016) 'The role of ER stress in lipid metabolism and lipotoxicity', *Journal of Lipid Research*, 57(8), pp. 1329–1338. doi: 10.1194/jlr.R067595.

Hara-Kuge, S. and Fujiki, Y. (2008) 'The peroxin Pex14p is involved in LC3-dependent degradation of mammalian peroxisomes', *Experimental Cell Research*, 314(19), pp. 3531–3541. doi: 10.1016/j.yexcr.2008.09.015.

Harris, C. *et al.* (2011) 'Hepatitis C virus core protein decreases lipid droplet turnover: A mechanism for core-induced steatosis', *Journal of Biological Chemistry*, 286(49), pp. 42615–42625. doi: 10.1074/jbc.M111.285148.

Hashimoto, T. *et al.* (2012) 'Active involvement of micro-lipid droplets and lipiddroplet-associated proteins in hormone-stimulated lipolysis in adipocytes', *Journal of Cell Science*, 125(24), pp. 6127–6136. doi: 10.1242/jcs.113084.

Hayashi, H. and Oohashi, M. (1995) 'Incorporation of acetyl-CoA generated from peroxisomal β-oxidation into ethanolamine plasmalogen of rat liver', *Biochimica et Biophysica Acta*, 1254(3), pp. 319–325.

Heaton, N. S. and Randall, G. (2010) 'Dengue virus-induced autophagy regulates lipid metabolism', *Cell Host and Microbe*, 8(5), pp. 422–432. doi: 10.1016/j.chom.2010.10.006.

Hegele, R. A. (2004) 'Phenomics, Lipodystrophy, and the Metabolic Syndrome', *Trends Cardiovasc Med*, 14(4), pp. 133–137. doi: 10.1007/s11883-002-0048-9.

Helbig, K. J. *et al.* (2011) 'The antiviral protein viperin inhibits hepatitis C virus replication via interaction with nonstructural protein 5A', *Hepatology*, 54(5), pp. 1506–1517. doi: 10.1002/hep.24542.

Helbig, K. J. *et al.* (2013) 'Viperin Is Induced following Dengue Virus Type-2 (DENV-2) Infection and Has Anti-viral Actions Requiring the C-terminal End of Viperin', *PLoS Neglected Tropical Diseases*, 7(4). doi: 10.1371/journal.pntd.0002178.

Herker, E. *et al.* (2010) 'Efficient Hepatitis C Virus Particle Formation Requires Diacylglycerol Acyltransferase 1 (DGAT1)', *Nat Med*, 16(11), pp. 1295–1298. doi: 10.1038/nm.2238.Efficient.

Herzog, K. *et al.* (2018) 'Functional characterisation of peroxisomal β-oxidation disorders in fibroblasts using lipidomics', *Journal of Inherited Metabolic Disease*, 41(3), pp. 479–487. doi: 10.1007/s10545-017-0076-9.

Hettema, E. H. *et al.* (2014) 'Evolving models for peroxisome biogenesis', *Current Opinion in Cell Biology*, 29(1), pp. 25–30. doi: 10.1016/j.ceb.2014.02.002.

Hinson, E. R. and Cresswell, P. (2009) 'The antiviral protein, viperin, localizes to lipid droplets via its N-terminal amphipathic α-helix', *Proceedings of the National Academy of Sciences of the United States of America*, 106(48), pp. 20452–20457. doi: 10.1073/pnas.0911679106.

Hodges, B. D. M. and Wu, C. C. (2010) 'Proteomic insights into an expanded cellular role for cytoplasmic lipid droplets', *Journal of Lipid Research*, 51(2), pp. 262–273. doi: 10.1194/jlr.R003582.

Hoffman, B. and Liu, Q. (2011) 'Hepatitis C viral protein translation: Mechanisms and implications in developing antivirals', *Liver International*, 31(10), pp. 1449–1467. doi: 10.1111/j.1478-3231.2011.02543.x.

Hope, R. G. and McLauchlan, J. (2000) 'Sequence motifs required for lipid droplet association and protein stability are unique to the hepatitis C virus core protein', *Journal of General Virology*, 81(8), pp. 1913–1925. doi: 10.1099/0022-1317-81-8-1913.

Horner, S. M. *et al.* (2011) 'Mitochondrial-associated endoplasmic reticulum membranes (MAM) form innate immune synapses and are targeted by hepatitis C virus', *Proceedings of the National Academy of Sciences of the United States of America*, 108(35), pp. 14590–14595. doi: 10.1073/pnas.1110133108.

Hourioux, C. *et al.* (2007) 'The genotype 3-specific hepatitis C virus core protein residue phenylalanine 164 increases steatosis in an in vitro cellular model', *Gut*, 56(9), pp. 1302–1308. doi: 10.1136/gut.2006.108647.

Hua, R. and Kim, P. K. (2016) 'Multiple paths to peroxisomes: Mechanism of peroxisome maintenance in mammals', *Biochimica et Biophysica Acta - Molecular Cell Research*, 1863(5), pp. 881–891. doi: 10.1016/j.bbamcr.2015.09.026.

Huybrechts, S. J. *et al.* (2009) 'Peroxisome dynamics in cultured mammalian cells', *Traffic*, 10(11), pp. 1722–1733. doi: 10.1111/j.1600-0854.2009.00970.x.

Iglesias, N. G. *et al.* (2015) 'Dengue Virus Uses a Non-Canonical Function of the Host GBF1-Arf-COPI System for Capsid Protein Accumulation on Lipid Droplets', *Traffic*, 16(9), pp. 962–977. doi: 10.1111/tra.12305.

Imanaka, T. *et al.* (1999) 'Characterization of the 70-kDa peroxisomal membrane protein, an ATP binding cassette transporter', *Journal of Biological Chemistry*, 274(17), pp. 11968–11976. doi: 10.1074/jbc.274.17.11968.

Islinger, M. and Schrader, M. (2011) 'Peroxisomes', *Current Biology*, 21(19), pp. 800–801. doi: 10.1016/j.cub.2011.07.024.

Itabe, H. *et al.* (2017) 'Perilipins: a diversity of intracellular lipid droplet proteins', *Lipids in Health and Disease*, 16(1), pp. 1–11. doi: 10.1186/s12944-017-0473-y.

Itoyama, A. *et al.* (2013) 'Mff functions with Pex11pβ and DLP1 in peroxisomal fission', *Biology Open*, 2(10), pp. 998–1006. doi: 10.1242/bio.20135298.

Jambunathan, S. *et al.* (2011) 'FSP27 promotes lipid droplet clustering and then fusion to regulate triglyceride accumulation', *PLoS ONE*, 6(12), pp. 1–12. doi: 10.1371/journal.pone.0028614.

Jirasko, V. *et al.* (2010) 'Structural and functional studies of nonstructural protein 2 of the hepatitis C virus

reveal its key role as organizer of virion assembly', *PLoS Pathogens*, 6(12). doi: 10.1371/journal.ppat.1001233.

Jones, D. M. and McLauchlan, J. (2010) 'Hepatitis C virus: Assembly and release of virus particles', *Journal of Biological Chemistry*, 285(30), pp. 22733–22739. doi: 10.1074/jbc.R110.133017.

Jones, J. M., Morrell, J. C. and Gould, S. J. (2004) 'PEX19 is a predominantly cytosolic chaperone and import receptor for class 1 peroxisomal membrane proteins', *Journal of Cell Biology*, 164(1), pp. 57–67. doi: 10.1083/jcb.200304111.

Kapadia, S. B. and Chisari, F. V. (2005) 'Hepatitis C virus RNA replication is regulated by host geranylgeranylation and fatty acids', *Proceedings of the National Academy of Sciences of the United States of America*, 102(7), pp. 2561–2566. doi: 10.1073/pnas.0409834102.

Katarzyna, Z. R. and Suresh, S. (2016) 'Autophagic degradation of peroxisomes in mammals', *Biochemical Society Transactions*, 44(2), pp. 431–440. doi: 10.1042/BST20150268.

Kerner, J. and Hoppel, C. (2000) 'Fatty acid import into mitochondria', *Biochimica et Biophysica Acta - Molecular and Cell Biology of Lipids*, 1486(1), pp. 1–17. doi: 10.1016/S1388-1981(00)00044-5.

Kim, P. (2017) 'Peroxisome Biogenesis: A Union between Two Organelles', *Current Biology*, 27(7), pp. R271–R274. doi: 10.1016/j.cub.2017.02.052.

Kim, P. K. *et al.* (2008) 'Ubiquitin signals autophagic degradation of cytosolic proteins and peroxisomes', *Proceedings of the National Academy of Sciences of the United States of America*, 105(52), pp. 20567–20574. doi: 10.1073/pnas.0810611105.

Kobayashi, S., Tanaka, A. and Fujiki, Y. (2007) 'Fis1, DLP1, and Pex11p coordinately regulate peroxisome morphogenesis', *Experimental Cell Research*, 313(8), pp. 1675–1686. doi: 10.1016/j.yexcr.2007.02.028.

Koepke, J. I. *et al.* (2008) 'Progeric effects of catalase inactivation in human cells', *Toxicology and Applied Pharmacology*, 232(1), pp. 99–108. doi: 10.1016/j.taap.2008.06.004.

Koizume, S. and Miyagi, Y. (2016) 'Lipid droplets: A key cellular organelle associated with cancer cell survival under normoxia and hypoxia', *International Journal of Molecular Sciences*, 17(9), pp. 1–23. doi: 10.3390/ijms17091430.

Kory, N., Farese, R. V. and Walther, T. C. (2016) 'Targeting Fat: Mechanisms of Protein Localization to Lipid Droplets', *Trends in Cell Biology*, 26(7), pp. 535–546. doi: 10.1016/j.tcb.2016.02.007.

Kraemer, F. B. *et al.* (2013) 'Cholesterol ester droplets and steroidogenesis', *Molecular and Cellular Endocrinology*, 371(1–2), pp. 15–19. doi: 10.1016/j.mce.2012.10.012.

Krahmer, N. *et al.* (2011) 'Phosphatidylcholine synthesis for lipid droplet expansion is mediated by localized

activation of CTP:Phosphocholine cytidylyltransferase', *Cell Metabolism*, 14(4), pp. 504–515. doi: 10.1016/j.cmet.2011.07.013.

Krahmer, N., Farese, R. V. and Walther, T. C. (2013) 'Balancing the fat: Lipid droplets and human disease', *EMBO Molecular Medicine*, 5(7), pp. 973–983. doi: 10.1002/emmm.201100671.

Lazarow, P. B. (2016) 'Peroxisomes', *Encyclopedia of Cell Biology*, 2, pp. 248–272. doi: 10.1016/B978-0-12-394447-4.20022-9.

Lefèvre, C. *et al.* (2001) 'Mutations in CGI-58, the gene encoding a new protein of the esterase/lipase/thioesterase subfamily, in Chanarin-Dorfman syndrome', *American Journal of Human Genetics*, 69(5), pp. 1002–1012. doi: 10.1086/324121.

Lindenbach, B. D. and Rice, C. M. (2005) 'Unravelling hepatitis C virus replication from genome to function', *Nature*, 436(7053), pp. 933–938. doi: 10.1038/nature04077.

Lindenbach, B. D. and Rice, C. M. (2013) 'The ins and outs of hepatitis C virus entry and assembly', *Nat Rev Microbiol.*, 11(10), pp. 688–700. doi: 10.1038/nrmicro3098.The.

Liu, H. M. *et al.* (2012) 'Hepatitis C virus translation preferentially depends on active RNA replication', *PLoS ONE*, 7(8). doi: 10.1371/journal.pone.0043600.

Liu, J. *et al.* (2012) 'The absence of ABCD2 sensitizes mice to disruptions in lipid metabolism by dietary erucic acid', *Journal of Lipid Research*, 53(6), pp. 1071–1079. doi: 10.1194/jlr.M022160.

Liu, L. *et al.* (2015) 'Glial lipid droplets and ROS induced by mitochondrial defects promote neurodegeneration', *Cell*, 160(1–2), pp. 177–190. doi: 10.1016/j.cell.2014.12.019.

Lodhi, I. J. and Semenkovich, C. F. (2014) 'Peroxisomes: A nexus for lipid metabolism and cellular signaling', *Cell Metabolism*, 19(3), pp. 380–392. doi: 10.1016/j.cmet.2014.01.002.

Londos, C. *et al.* (1999) 'Perilipins, ADRP, and other proteins that associate with intracellular neutral lipid droplets in animal cells', *Seminars in Cell and Developmental Biology*, 10(1), pp. 51–58. doi: 10.1006/scdb.1998.0275.

Long, A. P. *et al.* (2012) 'Lipid Droplet De Novo Formation and Fission Are Linked to the Cell Cycle in Fission Yeast', *Traffic*, 13(5), pp. 705–714. doi: 10.1111/j.1600-0854.2012.01339.x.

Lupberger, J. *et al.* (2019) 'Combined Analysis of Metabolome, Proteomes, and Transcriptomes of HCV-infected Cells and Liver to Identify Pathways Associated With Disease Development', *Gastroenterology*, 157(2), pp. 537–551. doi: 10.1053/j.gastro.2019.04.003.Combined.

Maccarrone, M., Melino, G. and Finazzi-Agrò, A. (2001) 'Lipoxygenases and their involvement in programmed cell death', *Cell Death and Differentiation*, 8(8), pp. 776–784. doi: 10.1038/sj.cdd.4400908.

Madrigal-Matute, J. and Cuervo, A. M. (2016) 'Regulation of Liver Metabolism by Autophagy', *Gastroenterology*, 150(2), pp. 328–339. doi: 10.1053/j.gastro.2015.09.042.

Magalhães, A. C. *et al.* (2016) 'Peroxisomes are platforms for cytomegalovirus' evasion from the cellular immune response', *Scientific Reports*, 6(April), pp. 1–14. doi: 10.1038/srep26028.

Marcinkiewicz, A. *et al.* (2006) 'The phosphorylation of serine 492 of perilipin A directs lipid droplet fragmentation and dispersion', *Journal of Biological Chemistry*, 281(17), pp. 11901–11909. doi: 10.1074/jbc.M600171200.

Martin-Acebes, M. A. *et al.* (2014) 'The Composition of West Nile Virus Lipid Envelope Unveils a Role of Sphingolipid Metabolism in Flavivirus Biogenesis', *Journal of Virology*, 88(20), pp. 12041–12054. doi: 10.1128/jvi.02061-14.

Masaki, T. *et al.* (2008) 'Interaction of Hepatitis C Virus Nonstructural Protein 5A with Core Protein Is Critical for the Production of Infectious Virus Particles', *Journal of Virology*, 82(16), pp. 7964–7976. doi: 10.1128/jvi.00826-08.

Masaki, T. *et al.* (2014) 'Involvement of Hepatitis C Virus NS5A Hyperphosphorylation Mediated by Casein Kinase I- in Infectious Virus Production', *Journal of Virology*, 88(13), pp. 7541–7555. doi: 10.1128/jvi.03170-13.

Van Meer, G. (2001) 'Caveolin, cholesterol, and lipid droplets?', *Journal of Cell Biology*, 152(5), pp. 29–34. doi: 10.1083/jcb.152.5.F29.

Merz, A. *et al.* (2011) 'Biochemical and morphological properties of hepatitis C virus particles and determination of their lipidome', *Journal of Biological Chemistry*, 286(4), pp. 3018–3032. doi: 10.1074/jbc.M110.175018.

Meyers, N. L. *et al.* (2016) 'Entangled in a membranous web: ER and lipid droplet reorganization during hepatitis C virus infection', *Current Opinion in Cell Biology*, 41, pp. 117–124. doi: 10.1016/j.ceb.2016.05.003.

Meylan, E. *et al.* (2005) 'Cardif is an adaptor protein in the RIG-I antiviral pathway and is targeted by hepatitis C virus', *Nature*, 437(7062), pp. 1167–1172. doi: 10.1038/nature04193.

Miura, S. *et al.* (1992) 'Carboxyl-terminal consensus Ser-Lys-Leu-related tripeptide of peroxisomal proteins functions in vitro as a minimal peroxisome-targeting signal', *Journal of Biological Chemistry*, 267(20), pp. 14405–14411. doi: 10.1016/s0021-9258(19)49726-3.

Miyanari, Y. *et al.* (2007) 'The lipid droplet is an important organelle for hepatitis C virus production', *Nature Cell Biology*, 9(9), pp. 1089–1097. doi: 10.1038/ncb1631.

Moradpour, D., Penin, F. and Rice, C. M. (2007) 'Replication of hepatitis C virus', *Nature Reviews*

Microbiology, 5(6), pp. 453–463. doi: 10.1038/nrmicro1645.

Moriishi, K. and Matsuura, Y. (2007) 'Host factors involved in the replication of hepatitis C virus', *Reviews in Medical Virology*, 17(5), pp. 343–354. doi: 10.1002/rmv.542.

Murphy, D. J. and Vance, J. (1999) 'Mechanisms of lipid-body formation', *Trends in Biochemical Sciences*, 24(3), pp. 109–115. doi: 10.1016/S0968-0004(98)01349-8.

Murphy, S., Martin, S. and Parton, R. G. (2010) 'Quantitative analysis of lipid droplet fusion: Inefficient steady state fusion but rapid stimulation by chemical fusogens', *PLoS ONE*, 5(12), p. e15030. doi: 10.1371/journal.pone.0015030.

Nagan, N. and Zoeller, R. A. (2001) *Plasmalogens: Biosynthesis and functions*, *Progress in Lipid Research*. doi: 10.1016/S0163-7827(01)00003-0.

Nagy, N. E. *et al.* (1997) 'Storage of vitamin A in extrahepatic stellate cells in normal rat', *Journal of Lipid Research*, 38(4), pp. 645–658. doi: 10.1016/s0022-2275(20)37232-1.

Nair, D. M., Purdue, P. E. and Lazarow, P. B. (2004) 'Pex7p translocates in and out of peroxisomes in Saccharomyces cerevisiae', *Journal of Cell Biology*, 167(4), pp. 599–604. doi: 10.1083/jcb.200407119.

Naldini, L. *et al.* (1996) 'In vivo gene delivery and stable transduction of nondividing cells by a lentiviral vector', *Science*, 272(5259), pp. 263–267. doi: 10.1126/science.272.5259.263.

Nasheri, N. *et al.* (2013) 'Modulation of fatty acid synthase enzyme activity and expression during hepatitis C virus replication', *Chemistry and Biology*, 20(4), pp. 570–582. doi: 10.1016/j.chembiol.2013.03.014.

Nevo-Yassaf, I. *et al.* (2012) 'Role for TBC1D20 and Rab1 in Hepatitis C Virus Replication via Interaction with Lipid Droplet-Bound Nonstructural Protein 5A', *Journal of Virology*, 86(12), pp. 6491–6502. doi: 10.1128/jvi.00496-12.

Nguyen, L. N. *et al.* (2014) 'Stearoyl Coenzyme A Desaturase 1 Is Associated with Hepatitis C Virus Replication Complex and Regulates Viral Replication', *Journal of Virology*, 88(21), pp. 12311–12325. doi: 10.1128/jvi.01678-14.

Novikoff, A. B. *et al.* (1980) 'Organelle relationships in cultured 3T3-L1 preadipocytes', *Journal of Cell Biology*, 87(1), pp. 180–196. doi: 10.1083/jcb.87.1.180.

Novikoff, A. B. and Novikoff, P. M. (1982) 'Microperoxisomes and peroxisomes in relation to lipid metabolism', *ANNALS NEW YORK ACADEMY OF SCIENCES*, 386, pp. 138–152.

Oakes, S. A. and Papa, F. R. (2015) 'The role of endoplasmic reticulum stress in human pathology', *Annual Review of Pathology: Mechanisms of Disease*, 10, pp. 173–194. doi: 10.1146/annurev-pathol-012513-104649.

Okamoto, K. *et al.* (2004) 'Intramembrane Proteolysis and Endoplasmic Reticulum Retention of Hepatitis C Virus Core Protein', *Journal of Virology*, 78(12), pp. 6370–6380. doi: 10.1128/jvi.78.12.6370-6380.2004.

Olzmann, J. A. and Carvalho, P. (2019) 'Dynamics and functions of lipid droplets', *Nature Reviews Molecular Cell Biology*, 20(3), pp. 137–155. doi: 10.1038/s41580-018-0085-z.

Olzmann, J. A., Kopito, R. R. and Christianson, J. C. (2013) 'The mammalian endoplasmic reticulum-associated degradation system', *Cold Spring Harbor Perspectives in Biology*, 5(9). doi: 10.1101/cshperspect.a013185.

Onal, G. *et al.* (2017) 'Lipid Droplets in Health and Disease', *Lipids in Health and Disease*, 16(1), pp. 1–15. doi: 10.1186/s12944-017-0521-7.

Opaliński, Ł. *et al.* (2011) 'Membrane curvature during peroxisome fission requires Pex11', *EMBO Journal*, 30(1), pp. 5–16. doi: 10.1038/emboj.2010.299.

Paar, M. *et al.* (2012) 'Remodeling of lipid droplets during lipolysis and growth in adipocytes', *Journal of Biological Chemistry*, 287(14), pp. 11164–11173. doi: 10.1074/jbc.M111.316794.

Page, A., Fusil, F. and Cosset, F.-L. (2020) 'Toward tightly tuned gene expression following lentiviral vector transduction', *Viruses*, 12(12), p. 1427. doi: 10.3390/v12121427.

Papackova, Z. and Cahova, M. (2015) 'Fatty acid signaling: The new function of intracellular lipases', *International Journal of Molecular Sciences*, 16(2), pp. 3831–3855. doi: 10.3390/ijms16023831.

Passmore, J. B. *et al.* (2020) 'Mitochondrial fission factor (MFF) is a critical regulator of peroxisome maturation', *Biochimica et Biophysica Acta - Molecular Cell Research*, 1867(7), p. 118709. doi: 10.1016/j.bbamcr.2020.118709.

Payne, S. (2017) 'Family Flaviviridae', in *Viruses: From Understanding to Investigation*, pp. 129–139. doi: 10.1016/b978-0-12-803109-4.00015-5.

Penin, F. *et al.* (2004) 'Structural Biology of Hepatitis C Virus', *Hepatology*, 39(1), pp. 5–19. doi: 10.1002/hep.20032.

Peramuna, A. and Summers, M. L. (2014) 'Composition and occurrence of lipid droplets in the cyanobacterium Nostoc punctiforme', *Archives of Microbiology*, 196(12), pp. 881–890. doi: 10.1007/s00203-014-1027-6.

Pineau, L. and Ferreira, T. (2010) 'Lipid-induced ER stress in yeast and β cells: Parallel trails to a common fate', *FEMS Yeast Research*, 10(8), pp. 1035–1045. doi: 10.1111/j.1567-1364.2010.00674.x.

Piodi, A. *et al.* (2008) 'Morphological changes in intracellular lipid droplets induced by different hepatitis C virus genotype core sequences and relationship with steatosis', *Hepatology*, 48(1), pp. 16–27. doi:

10.1002/hep.22288.

Poole, B., Leighton, F. and De Duve, C. (1969) 'The synthesis and turnover of rat liver peroxisomes', *Journal of Cell Biology*, 59(2), pp. 491–506. doi: 10.1083/jcb.59.2.491.

Popescu, C. I. *et al.* (2011) 'NS2 protein of hepatitis C virus interacts with structural and non-structural proteins towards virus assembly', *PLoS Pathogens*, 7(2). doi: 10.1371/journal.ppat.1001278.

Popescu, C. I. *et al.* (2014) 'Hepatitis C virus life cycle and lipid metabolism', *Biology*, 3(4), pp. 892–921. doi: 10.3390/biology3040892.

Poppelreuther, M. *et al.* (2012) 'The N-terminal region of acyl-CoA synthetase 3 is essential for both the localization on lipid droplets and the function in fatty acid uptake', *Journal of Lipid Research*, 53(5), pp. 888–900. doi: 10.1194/jlr.M024562.

Poulain, A. *et al.* (2017) 'Rapid protein production from stable CHO cell pools using plasmid vector and the cumate gene-switch', *Journal of Biotechnology*, 255(June), pp. 16–27. doi: 10.1016/j.jbiotec.2017.06.009.

Price, V. E. . *et al.* (1962) 'The kinetics of catalase synthesis and destruction in vivo.', *The Journal of biological chemistry*, 237(11), pp. 3468–3475. doi: 10.1016/s0021-9258(19)70841-2.

Pu, J. *et al.* (2011) 'Interactomic study on interaction between lipid droplets and mitochondria', *Protein and Cell*, 2(6), pp. 487–496. doi: 10.1007/s13238-011-1061-y.

Qiang, G. and Jhaveri, R. (2012) 'Lipid Droplet Binding of Hepatitis C Virus Core Protein Genotype 3', *ISRN Gastroenterology*, 2012, pp. 1–7. doi: 10.5402/2012/176728.

Queiroz, A. *et al.* (2019) 'Lipidomic analysis reveals serum alteration of plasmalogens in patients infected with ZIKA virus', *Frontiers in Microbiology*, 10(APR), pp. 1–10. doi: 10.3389/fmicb.2019.00753.

Ramage, H. R. *et al.* (2015) 'A combined proteomics/genomics approach links hepatitis C virus infection with nonsense-mediated mRNA decay', *Molecular Cell*, 57(2), pp. 329–340. doi: 10.1016/j.molcel.2014.12.028.

Reddy, J. K. and Hashimoto, T. (2001) 'Peroxisomal β-oxidation and peroxisome proliferator-activated receptor α: An adaptive metabolic system', *Annual Reviews*, (21), pp. 193–230. doi: 10.1002/9783527678679.dg09347.

Reue, K. (2011) 'A thematic review series: Lipid droplet storage and metabolism: From yeast to man', *Journal of Lipid Research*, 52(11), pp. 1865–1868. doi: 10.1194/jlr.E020602.

Roermund, C. W. T. *et al.* (2008) 'The human peroxisomal ABC half transporter ALDP functions as a homodimer and accepts acyl–CoA esters', *The FASEB Journal*, 22(12), pp. 4201–4208. doi: 10.1096/fj.08-110866.

Rosenthal, M. *et al.* (2020) 'Uncovering targeting priority to yeast peroxisomes using an in-cell competition assay', *Proceedings of the National Academy of Sciences of the United States of America*, 117(35), pp. 21432–21440. doi: 10.1073/pnas.1920078117.

Rottensteiner, H. *et al.* (2004) 'Peroxisomal Membrane Proteins contain common Pex19p-binding sites that are an integral part of their targeting signals', *Molecular Biology of the Cell*, 15(December), pp. 3406–3417. doi: 10.1091/mbc.E04.

Sacksteder, K. A. and Gould, S. J. (2000) 'The genetics of peroxisome biogenesis', *Annual Reviews*.

Salloum, S. *et al.* (2013) 'Rab18 Binds to Hepatitis C Virus NS5A and Promotes Interaction between Sites of Viral Replication and Lipid Droplets', *PLoS Pathogens*, 9(8). doi: 10.1371/journal.ppat.1003513.

Salmon, A. B., Richardson, A. and Pérez, V. I. (2010) 'Update on the oxidative stress theory of aging: Does oxidative stress play a role in aging or healthy aging?', *Free Radical Biology and Medicine*, 48(5), pp. 642–655. doi: 10.1016/j.freeradbiomed.2009.12.015.

Samsa, M. M. *et al.* (2009) 'Dengue virus capsid protein usurps lipid droplets for viral particle formation', *PLoS Pathogens*, 5(10). doi: 10.1371/journal.ppat.1000632.

Sandermann, H. (2003) 'Differential lipid affinity of xenobiotics and natural compounds', *FEBS Letters*, 554(1–2), pp. 165–168. doi: 10.1016/S0014-5793(03)01143-8.

Sandoz, K. M. *et al.* (2014) 'The broad-spectrum antiviral compound ST-669 restricts chlamydial inclusion development and bacterial growth and localizes to host cell lipid droplets within treated cells', *Antimicrobial Agents and Chemotherapy*, 58(7), pp. 3860–3866. doi: 10.1128/AAC.02064-13.

Scheel, T. K. H. and Rice, C. M. (2013) 'Understanding the hepatitis C virus life cycle paves the way for highly effective therapies', *Nat Med*, 19(7), pp. 837–849. doi: 10.1038/nm.3248.Understanding.

Schlager, S. *et al.* (2015) 'Adipose triglyceride lipase acts on neutrophil lipid droplets to regulate substrate availability for lipid mediator synthesis', *Journal of Leukocyte Biology*, 98(5), pp. 837–850. doi: 10.1189/jlb.3a0515-206r.

Schrader, M. (2001) 'Tubulo-reticular clusters of peroxisomes in living COS-7 cells: Dynamic behavior and association with lipid droplets', *Journal of Histochemistry and Cytochemistry*, 49(11), pp. 1421–1429. doi: 10.1177/002215540104901110.

Schrader, M. *et al.* (2013) 'Peroxisome interactions and cross-talk with other subcellular compartments in animal cells', *Subcellular Biochemistry*, 69, pp. 1–22. doi: 10.1007/978-94-007-6889-5_1.

Schrader, M., Kamoshita, M. and Islinger, M. (2019) 'Organelle interplay—peroxisome interactions in health and disease', *Journal of Inherited Metabolic Disease*, 43(1), pp. 71–89. doi: 10.1002/jimd.12083.

Schreiber, R. *et al.* (2012) 'Retinyl ester hydrolases and their roles in vitamin A homeostasis', *Biochimica et Biophysica Acta - Molecular and Cell Biology of Lipids*, 1821(1), pp. 113–123. doi: 10.1016/j.bbalip.2011.05.001.

Schreiber, R. and Zechner, R. (2015) 'Lipolysis meets inflammation: Arachidonic acid mobilization from fat', *Journal of Lipid Research*, 55(12), pp. 2447–2449. doi: 10.1194/jlr.C055673.

Schuldiner, M. and Bohnert, M. (2017) 'A different kind of love – lipid droplet contact sites', *Biochimica et Biophysica Acta - Molecular and Cell Biology of Lipids*, 1862(10), pp. 1188–1196. doi: 10.1016/j.bbalip.2017.06.005.

Schulze, R. J., Sathyanarayan, A. and Mashek, D. G. (2017) 'Breaking fat: the regulation and mechanisms of lipophagy Ryan', *Biochim Biophys Acta*, 1862(10 Pt B), pp. 1178–1187. doi: 10.1016/j.bbalip.2017.06.008.Breaking.

Seelig, J. (2004) 'Thermodynamics of lipid-peptide interactions', *Biochimica et Biophysica Acta - Biomembranes*, 1666(1–2), pp. 40–50. doi: 10.1016/j.bbamem.2004.08.004.

Senoo, H. *et al.* (2013) 'Uptake and storage of vitamin A as lipid droplets in the cytoplasm of cells in the lamina propria mucosae of the rat intestine', *Cell Biology International*, 37(11), pp. 1171–1180. doi: 10.1002/cbin.10140.

Senoo, H., Kojima, N. and Sato, M. (2007) 'Vitamin A-Storing Cells (Stellate Cells)', *Vitamins and Hormones*, 75(06), pp. 131–159. doi: 10.1016/S0083-6729(06)75006-3.

Seth, R. B. *et al.* (2005) 'Identification and characterization of MAVS, a mitochondrial antiviral signaling protein that activates NF-κB and IRF3', *Cell*, 122(5), pp. 669–682. doi: 10.1016/j.cell.2005.08.012.

Shai, N., Schuldiner, M. and Zalckvar, E. (2016) 'No peroxisome is an island - Peroxisome contact sites', *Biochimica et Biophysica Acta - Molecular Cell Research*, 1863(5), pp. 1061–1069. doi: 10.1016/j.bbamcr.2015.09.016.

Shen, W. J., Azhar, S. and Kraemer, F. B. (2016) 'Lipid droplets and steroidogenic cells', *Experimental Cell Research*, 340(2), pp. 209–214. doi: 10.1016/j.yexcr.2015.11.024.

Shi, S. T. and Lai, M. M. C. (2006) 'HCV 5' and 3'UTR: When Translation Meets Replication', *Hepatitis C Viruses: Genomes and Molecular Biology*, pp. 49–87. Available at: http://www.ncbi.nlm.nih.gov/pubmed/21250387.

Shpilka, T. *et al.* (2015) 'Lipid droplets and their component triglycerides and steryl esters regulate autophagosome biogenesis', *The EMBO Journal*, 34(16), pp. 2117–2131. doi: 10.15252/embj.201490315.

Singh, I. *et al.* (1984) 'Lignoceric acid is oxidized in the peroxisome: Implications for the Zellweger cerebro-

hepato-renal syndrome and adrenoleukodystrophy', *Proceedings of the National Academy of Sciences of the United States of America*, 81(13 I), pp. 4203–4207. doi: 10.1073/pnas.81.13.4203.

Sladitschek, H. L. and Neveu, P. A. (2015) 'MXS-chaining: A highly efficient cloning platform for imaging and flow cytometry approaches in mammalian systems', *PLoS ONE*, 10(4), pp. 1–20. doi: 10.1371/journal.pone.0124958.

Spicher, L. and Kessler, F. (2015) 'Unexpected roles of plastoglobules (plastid lipid droplets) in vitamin K1 and E metabolism', *Current Opinion in Plant Biology*, 25(Figure 1), pp. 123–129. doi: 10.1016/j.pbi.2015.05.005.

Staels, B. and Fonseca, V. A. (2009) 'Bile acids and metabolic regulation: mechanisms and clinical responses to bile acid sequestration.', *Diabetes care*, 32 Suppl 2. doi: 10.2337/dc09-s355.

Su, A. I. *et al.* (2002) 'Genomic analysis of the host response to hepatitis C virus infection', *Proceedings of the National Academy of Sciences of the United States of America*, 99(24), pp. 15669–15674. doi: 10.1073/pnas.202608199.

Su, J. *et al.* (2018) 'The N-terminal amphipathic helix of Pex11p self-interacts to induce membrane remodelling during peroxisome fission', *Biochimica et Biophysica Acta - Biomembranes*, 1860(6), pp. 1292–1300. doi: 10.1016/j.bbamem.2018.02.029.

Sugiura, A. *et al.* (2017) 'Newly born peroxisomes are a hybrid of mitochondrial and ER-derived pre-peroxisomes', *Nature*, 542(7640), pp. 251–254. doi: 10.1038/nature21375.

Suzuki, Yasutsugu and Suzuki, Youichi (2011) 'Gene Regulatable Lentiviral Vector System', in *Viral Gene Therapy*, pp. 285–308. doi: 10.5772/18155.

Tandon, N. *et al.* (2018) 'Generation of Stable Expression Mammalian Cell Lines Using Lentivirus', *Bio-Protocol*, 8(21), pp. 8–12. doi: 10.21769/bioprotoc.3073.

Tang, H. and Grisé, H. (2009) 'Cellular and molecular biology of HCV infection and hepatitis', *Clinical Science*, 117(2), pp. 49–65. doi: 10.1042/CS20080631.

Tansey, J. T. *et al.* (2001) 'Perilipin ablation results in a lean mouse with aberrant adipocyte lipolysis, enhanced leptin production, and resistance to diet-induced obesity', *Proceedings of the National Academy of Sciences of the United States of America*, 98(11), pp. 6494–6499. doi: 10.1073/pnas.101042998.

Tariq, H. *et al.* (2012) 'An overview: In vitro models of HCV replication in different cell cultures', *Infection, Genetics and Evolution*, 12(1), pp. 13–20. doi: 10.1016/j.meegid.2011.10.009.

Tews, B. A., Popescu, C. I. and Dubuisson, J. (2010) 'Last stop before exit - Hepatitis C assembly and release as antiviral drug targets', *Viruses*, 2(8), pp. 1782–1803. doi: 10.3390/v2081782.

Thiam, A. R., Farese, R. V. and Walther, T. C. (2013) 'The biophysics and cell biology of lipid droplets', *Nature Reviews Molecular Cell Biology*, 14(12), pp. 775–786. doi: 10.1038/nrm3699.

Tolbert, N. E. and Essner, E. (1981) 'Microbodies: Peroxisomes and glyoxysomes', *Journal of Cell Biology*, 91(3 II). doi: 10.1083/jcb.91.3.271s.

Traber, M. G. and Kayden, H. J. (1987) 'Tocopherol distribution and intracellular localization in human adipose tissue', *American Journal of Clinical Nutrition*, 46(3), pp. 488–495. doi: 10.1093/ajcn/46.3.488.

Vance, J. E. (1990) 'Lipoproteins secreted by cultured rat hepatocytes contain the antioxidant 1-alk-1-enyl-2-acylglycerophosphoethanolamine', *Biochimica et Biophysica Acta (BBA)/Lipids and Lipid Metabolism*, 1045(2), pp. 128–134. doi: 10.1016/0005-2760(90)90141-J.

Velázquez, A. P. *et al.* (2016) 'Lipid droplet-mediated ER homeostasis regulates autophagy and cell survival during starvation', *Journal of Cell Biology*, 212(6), pp. 621–631. doi: 10.1083/jcb.201508102.

Velázquez, A. P. and Graef, M. (2016) 'Autophagy regulation depends on ER homeostasis controlled by lipid droplets', *Autophagy*, 12(8), pp. 1409–1410. doi: 10.1080/15548627.2016.1190074.

Verbrugge, S. E. *et al.* (2016) 'Multifactorial resistance to aminopeptidase inhibitor prodrug CHR2863 in myeloid leukemia cells: Down-regulation of carboxylesterase 1, drug sequestration in lipid droplets and pro-survival activation ERK/Akt/mTOR', *Oncotarget*, 7(5), pp. 5240–5257. doi: 10.18632/oncotarget.6169.

Verhoeven, N. M. . *et al.* (1998) 'Phytanic acid and pristanic acid are oxidized by sequential peroxisomal and mitochondrial reactions in cultured fibroblasts', *Journal of Lipid Research*, 39(1), pp. 66–74. doi: 10.1016/s0022-2275(20)34204-8.

Vevea, J. D. *et al.* (2015) 'Role for Lipid Droplet Biogenesis and Microlipophagy in Adaptation to Lipid Imbalance in Yeast', *Developmental Cell*, 35(5), pp. 584–599. doi: 10.1016/j.devcel.2015.11.010.

Volmer, R. and Ron, D. (2015) 'Lipid-dependent regulation of the unfolded protein response', *Current Opinion in Cell Biology*, 33, pp. 67–73. doi: 10.1016/j.ceb.2014.12.002.

Walther, W. and Stein, U. (2000) 'Viral Vectors for Gene Transfer', *Drugs*, 60(2), pp. 249–271. doi: 10.2165/00003495-200060020-00002.

Wanders, R. J. A. *et al.* (2001) 'Peroxisomal fatty acid α- and β-oxidation in humans: enzymology, peroxisomal metabolite transporters and peroxisomal diseases', *Biochemical Society Transactions*, 29(2), pp. 250–267. doi: 10.1042/0300-5127:0290250.

Wanders, R. J. A. *et al.* (2007) 'The peroxisomal ABC transporter family', *Pflugers Archiv European Journal of Physiology*, 453(5), pp. 719–734. doi: 10.1007/s00424-006-0142-x.

Wanders, R. J. A. (2014) 'Metabolic functions of peroxisomes in health and disease', *Biochimie*, 98(1), pp.

36–44. doi: 10.1016/j.biochi.2013.08.022.

Wanders, R. J. A. and Waterham, H. R. (2006) 'Biochemistry of mammalian peroxisomes revisited', *Annual Review of Biochemistry*, 75, pp. 295–332. doi: 10.1146/annurev.biochem.74.082803.133329.

Wang, L. *et al.* (2021) 'Lipid droplets and their interactions with other organelles in liver diseases', *International Journal of Biochemistry and Cell Biology*, 133(June 2020), p. 105937. doi: 10.1016/j.biocel.2021.105937.

Waterham, H. R. *et al.* (2007) 'A Lethal Defect of Mitochondrial and Peroxisomal Fission', *New England Journal of Medicine*, 356(17), pp. 1736–1741. doi: 10.1056/nejmoa064436.

Welte, M. A. and Gould, A. P. (2017) 'Lipid droplet functions beyond energy storage', *Biochimica et Biophysica Acta - Molecular and Cell Biology of Lipids*, 1862(10), pp. 1260–1272. doi: 10.1016/j.bbalip.2017.07.006.

WHO (2021) *Hepatitis C*, *World Health Organization*. Available at: https://www.who.int/news-room/fact-sheets/detail/hepatitis-c (Accessed: 28 October 2021).

Wierzbicki, A. S. *et al.* (2002) 'Refsum's disease: A peroxisomal disorder affecting phytanic acid α-oxidation', *Journal of Neurochemistry*, 80(5), pp. 727–735. doi: 10.1046/j.0022-3042.2002.00766.x.

Williams, C. *et al.* (2015) 'The membrane remodeling protein Pex11p activates the GTPase Dnm1p during peroxisomal fission', *Proceedings of the National Academy of Sciences of the United States of America*, 112(20), pp. 6377–6382. doi: 10.1073/pnas.1418736112.

Wissing, S. *et al.* (2011) 'Endogenous APOBEC3B restricts LINE-1 retrotransposition in transformed cells and human embryonic stem cells', *Journal of Biological Chemistry*, 286(42), pp. 36427–36437. doi: 10.1074/jbc.M111.251058.

Wodrich, H., Schambach, A. and Kräusslich, H. G. (2000) 'Multiple copies of the Mason-Pfizer monkey virus constitutive RNA transport element lead to enhanced HIV-1 Gag expression in a context-dependent manner', *Nucleic Acids Research*, 28(4), pp. 901–910. doi: 10.1093/nar/28.4.901.

Wong *et al.* (2019) 'Interplay between Zika Virus and Peroxisomes during Infection', *Cells*, 8(7), p. 725. doi: 10.3390/cells8070725.

Yamaguchi, T. *et al.* (2015) 'Characterization of lipid droplets in steroidogenic MLTC-1 Leydig cells: Protein profiles and the morphological change induced by hormone stimulation', *Biochimica et Biophysica Acta - Molecular and Cell Biology of Lipids*, 1851(10), pp. 1285–1295. doi: 10.1016/j.bbalip.2015.06.007.

Yanagi, M. *et al.* (1997) 'Transcripts from a single full-length cDNA clone of hepatitis C virus are infectious when directly transfected into the liver of a chimpanzee', *Proceedings of the National Academy of Sciences*

of the United States of America, 94(16), pp. 8738–8743. doi: 10.1073/pnas.94.16.8738.

Yang, P. L. *et al.* (2016) 'Lipid droplets maintain lipid homeostasis during anaphase for efficient cell separation in budding yeast', *Molecular Biology of the Cell*, 27(15), pp. 2368–2380. doi: 10.1091/mbc.E16-02-0106.

Yang, W. *et al.* (2009) 'Fatty Acid Synthase Is Upregulated during HCV Infection and Regulates HCV Entry and Production', *Hepatology*, 48(5), pp. 1396–1403. doi: 10.1002/hep.22508.Fatty.

Yi, M. and Lemon, S. M. (2003) '3' Nontranslated RNA Signals Required for Replication of Hepatitis C Virus RNA', *Journal of Virology*, 77(6), pp. 3557–3568. doi: 10.1128/jvi.77.6.3557-3568.2003.

Yoshida, Y. *et al.* (2015) 'Pex11mediates peroxisomal proliferation by promoting deformation of the lipid membrane', *Biology Open*, 4(6), pp. 710–721. doi: 10.1242/bio.201410801.

You, J. *et al.* (2015) 'Flavivirus Infection Impairs Peroxisome Biogenesis and Early Antiviral Signaling', *Journal of Virology*, 89(24), pp. 12349–12361. doi: 10.1128/jvi.01365-15.

Zehmer, J. K. *et al.* (2009) 'A role for lipid droplets in inter-membrane lipid traffic', *Proteomics*, 9(4), pp. 914–921. doi: 10.1002/pmic.200800584.

Zhang, J., Lan, Y. and Sanyal, S. (2017) 'Modulation of lipid droplet metabolism-A potential target for therapeutic intervention in Flaviviridae Infections', *Frontiers in Microbiology*, 8(NOV). doi: 10.3389/fmicb.2017.02286.

Zheng, C. and Su, C. (2017) 'Herpes simplex virus 1 infection dampens the immediate early antiviral innate immunity signaling from peroxisomes by tegument protein VP16', *Virology Journal*, 14(1), pp. 1–8. doi: 10.1186/s12985-017-0709-5.

Zhong, J. *et al.* (2005) 'Robust hepatitis C virus infection in vitro', *Proceedings of the National Academy of Sciences of the United States of America*, 102(26), pp. 9294–9299. doi: 10.1073/pnas.0503596102.

Zhu, Y. Z. *et al.* (2014) 'How hepatitis C virus invades hepatocytes: The mystery of viral entry', *World Journal of Gastroenterology*, 20(13), pp. 3457–3467. doi: 10.3748/wjg.v20.i13.3457.

Zufferey, R. *et al.* (1999) 'Woodchuck Hepatitis Virus posttranscriptional regulatory element enhances expression of transgenes delivered by retroviral vectors', *Journal of Virology*, 73(4), pp. 2886–2892.